SISSA, International School for Advanced Studies

PhD course in Statistical Physics

Academic Year 2011/2012

Universal properties of two-dimensional percolation

Thesis submitted for the degree of

Doctor Philosophiae

Advisor:
Prof. Gesualdo Delfino

Candidate:
Jacopo Viti

17th September 2012

Contents

Summary

Percolation was stated as a mathematical problem by Broadbendt and Hammersley [1] back in the fifties and is considered by mathematicians [2, 3] a branch of probability theory. Due to the large amount of its applications, percolation is a popular subject of research also within the physicist community.[1]

In its simplest version one takes a regular lattice $\mathcal{L}$ and draws bonds connecting neighboring sites with probability p. Connected sites form clusters of different sizes. For p larger than a threshold value p_c typical configurations contain a cluster with an infinite number of sites, the so-called infinite cluster, which eventually for $p = 1$ coincides with $\mathcal{L}$ itself. The occurrence of the infinite cluster separates two different phases, the subcritical phase ($p < p_c$) in which all the clusters are finite from the supercritical phase ($p > p_c$) in which one is infinite. The phase transition is continuous and can be described applying concepts like scaling and renormalization [4, 5], well known to theoretical physicists from the study of critical phenomena. Percolation theory [6] studies the properties of clusters, their average number, their average size and the way in which sites can be distributed among them (connectivities). It is relevant in the context of complex network [7], polymer gelation [8], diffusion of a liquid in porous media, earthquakes and damage spreading [9]. Percolation has also been applied in cosmology to model star and galaxy formation [10] and in condensed matter problems like the celebrated quantum Hall effect [11] where the transition is related to the localization of the electronic wavefunction.

[1] It is interesting to note that one of the purposes leading Broadbendt and Hammersley to the introduction of percolation was to test the performance of the computers available at the time. Nowdays numerical simulations are probably the most efficient way to investigate percolation from a physicist point of view.

The peculiarity of the percolative phase transition is the absence of any symmetry breaking mechanism, a circumstance that prevents physicists from writing an effective action for the relevant degrees of freedom in the spirit of Landau and Ginzburg. It is however interesting to observe that also the paradigmatic example of Landau-Ginzburg phase transition, i.e. the spontaneous magnetization of a ferromagnet, can be cast in the language of percolation, if one focuses on clusters of equally magnetized spins.

In this thesis we will study the percolative transition in two dimensions, concentrating on those aspects of the process which do not depend on the specific lattice realization and are therefore termed universal. Universality is a consequence of renormalization group theory. Near criticality, in a system with infinitely many degrees of freedom, fluctuations of macroscopic observables are strongly interacting and correlated on a dynamical length scale, the correlation length, larger than the typical microscopic scale or cut-off. The large distance behavior of the observables depends on the correlation length and is then unaffected by the cut-off. At the critical point, where the correlation length diverges, conformal invariance emerges and the critical behavior of a statistical mechanics model is then described by a conformally invariant field theory.

In two dimensions [12, 13] conformal field theory (CFT) has been proved extremely useful in providing the classification of the various types of critical behaviors occurring in Nature, but even away from criticality the field theory resulting from the perturbation of a CFT by a relevant operator may have remarkable features. In particular it can possess an infinite number of conservation laws which strongly constrain the particle dynamics and allow the exact solution of the scattering problem. Such field theories are called integrable [14, 15].

In this thesis we show how conformal invariance and integrability [2] allow to improve our understanding of the percolative phase transition and in particular

[2] During the days in which this thesis was written the 2011 ICTP Dirac medal has been awarded to E. Brezin, J. Cardy and A. Zamolodchikov "for recognition of their independent pioneering work on field theoretical methods to the study of critical phenomena and phase transitions; in particular for their significant contributions to conformal field theories and integrable systems. Their research and the physical implications of their formal developments have had important consequences in classical and quantum condensed matter systems and in string theory."

to derive exact or extremely accurate results, which have been tested by high-precision numerical simulations. The material presented in this thesis is based on the research articles

- *Potts q-color field theory and the scaling random cluster model* [16];
- *On the three-point connectivity in two-dimensional percolation* [17];
- *Universal amplitude ratios of two-dimensional percolation from field theory* [18];
- *Crossing probability and number of crossing clusters in off-critical percolation* [19];
- *Phase separation and interface structure in two dimensions from field theory* [20];
- *Universal properties of Ising clusters and droplets near criticality* [21].

In the first chapter we will introduce the q-color Potts model [22, 23], a generalization of the well known Ising model invariant under color permutations. After a brief overview of percolation theory, we describe how the percolative phase transition can be studied formally analyzing the ferromagnetic phase transition of the Potts model in the limit $q \to 1$. We will also recall some basic elements of CFT and will give the definition of percolative interface, a concept that mathematicians [24] use to rigorously formulate the physicist notion of scaling limit and conformal invariance.

The connection between percolation and the Potts model is based on the Fortuin and Kasteleyn representation of the partition function [25], which provides an analytic continuation of the Potts partition function to arbitrary real q, known as the random cluster model[3] [26]. The random cluster model (RCM) undergoes a percolative transition for q less than a dimensionality dependent value q_c and the second chapter is devoted to investigate how its scaling limit can be described by a field theory, which we call Potts field theory [16]. In particular we will find

[3]The random cluster model is a percolation model in which bonds are not independent random variables.

a systematic way to express connectivities in the RCM as spin correlation functions in the Potts field theory. Focusing on the bidimensional case we will also introduce the concept of kink field: kinks are the lightest excitations interpolating between vacua of different colors in the ordered ferromagnetic phase. The chapter ends with the solution of Chim and Zamolodchikov [27] for the scattering problem and with a brief discussion of how correlation functions can be computed out of criticality through the form factor approach.

Chapter 3 is devoted to the three-point connectivity at criticality. In the language of conformal field theory, percolation is a logarithmic theory, i.e. a theory with vanishing central charge in which correlation functions may have logarithmic singularities [28, 29]. We will argue how a formal use of permutational symmetry allows to keep track of the right multiplicities of the kink fields as $q \to 1$ and to determine their operator product expansion (OPE). At criticality the bulk three-point connectivity factorizes into the product of a constant R and of two-point connectivities. The constant R is exactly the structure constant arising in the OPE of the kink fields. We determined R exactly [17] also exploiting Al. Zamolodchikov [30] analytic continuation of the structure constants of the conformal minimal models. Our theoretical result has been confirmed by a numerical simulation [31].

In chapter 4 we present the computation based on the form factor approach of all the independent universal amplitude ratios of percolation [18]. In particular we obtain the ratio between the average size of finite clusters below and above the percolation threshold p_c. The numerical estimations for this quantity had been controversial for thirty years.

The study of percolation on a finite domain of the plane has also an interesting history, started by the observation of Langlands et al. [32] of the universality of the vertical crossing probability in the scaling limit on a rectangular geometry and further developed by the exact computation by Cardy at the critical point [33]. In chapter 5 we recall Cardy derivation of the crossing probability and present an off-critical extension valid in the limit in which both sides of the rectangle are large compared to the correlation length [19]. Our asymptotic formula agrees with the numerical data of [34].

In chapter 6 we discuss the density profile of the spanning cluster starting

from the more general perspective of phase separation [20].

As we observed at the beginning of this introduction a ferromagnetic transition is naturally associated to a percolative transition. Naively one would expect that the existence of a spontaneous magnetization implies the presence of an infinite cluster of equally magnetized spins and viceversa. The relation between magnetic and geometric degrees of freedom in a ferromagnet is however more subtle and it is the subject of the final chapter of the thesis where universal properties of correlated percolation in the Ising model are analyzed [21].

Chapter 1

Potts model and percolation

In this chapter we introduce the q-color Potts model on arbitrary graphs $\mathcal{G}$, discussing the Fortuin-Kasteleyn and domain wall representations of the partition function. After a brief overview of conformal field theories in two dimensions, we introduce basic notions of percolation theory and state the connection with the $q \to 1$ limit of the Potts model.

1.1 Potts model: FK and domain wall expansions

Consider a planar connected graph $\mathcal{L} \equiv (V, E)$ of vertex set V and edge set E and associate to any vertex $x \in V$ a color variable $s(x) = 1, \ldots, q \in \mathbb{N}$. Two vertices x, y are nearest neighbors if they are connected by an edge and a pair of nearest neighboring vertices is denoted by $\langle x, y \rangle$. The Potts model Hamiltonian [22, 23] is defined on $\mathcal{L}$ by

$$H_{\text{Potts}} = -J \sum_{\langle x,y \rangle} \delta_{s(x),s(y)} \tag{1.1}$$

where $\delta_{s(x),s(y)}$ is the usual Kronecker symbol. The Hamiltonian (1.1) is invariant under global permutations $\sigma \in S_q$, the symmetric group of q elements, acting on the graph variables. The partition function is the sum

$$Z_{\text{Potts}}(J, q) = \sum_{\{s(x)\}} \mathrm{e}^{-H_{\text{Potts}}}. \tag{1.2}$$

For J positive the model is ferromagnetic, antiferromagnetic otherwise.

We discuss two convenient ways of rewriting the Boltzmann weight in (1.2), leading to different graph expansions for the partition function. Take

$$\mathrm{e}^{J\delta_{s(x),s(y)}} = \begin{cases} \left[e^J - 1\right]\delta_{s(x),s(y)} + 1 \\ \left[1 - \delta_{s(x),s(y)}\right] + \mathrm{e}^J\delta_{s(x),s(y)}. \end{cases} \tag{1.3}$$

In both cases the partition function is a product of $2^{|E(\mathcal{L})|}$ terms, where $|E(\mathcal{L})|$ is the number of edges in $\mathcal{L}$. Consider the first case and define $p = 1 - \mathrm{e}^{-J}$, $v = \mathrm{e}^J$. To any term in the product we associate a graph $\mathcal{G} \subseteq \mathcal{L}$, the edges of $\mathcal{G}$ coincide with the edges $\langle x, y\rangle$ for which the term containing $\delta_{s(x),s(y)}$ has been selected in the expansion, we have

$$Z_{\mathrm{Potts}}(J, q) = v^{|E(\mathcal{L})|} \sum_{\{s(x)\}} \sum_{\mathcal{G}\subseteq\mathcal{L}} p^{|E(\mathcal{G})|}(1-p)^{|E(\mathcal{L})|-|E(\mathcal{G})|}, \tag{1.4}$$

where, due to the Kronecker delta, the variables $s(x)$ are constrained to be equal in any connected component[1] (cluster) of $\mathcal{G}$. Denoting with $|C(\mathcal{G})|$ the number of such connected components we obtain

$$Z_{\mathrm{Potts}}(J, q) = v^{|E(\mathcal{L})|} \sum_{\mathcal{G}\subseteq\mathcal{L}} p^{|E(\mathcal{G})|}(1-p)^{|E(\mathcal{L})|-|E(\mathcal{G})|} q^{|C(\mathcal{G})|}, \tag{1.5}$$

which is called the high temperature or Fortuin-Kasteleyn (FK) graph expansion [25]. The FK expansion provides an analytic continuation of the Potts partition function for $q \in \mathbb{R}$; the statistical mechanics model defined by the (1.5) for $q > 0$ is the random cluster model. The graphs entering the FK representation are the FK graphs; notice that two different FK clusters separated by a single edge can have equal color. Such situation is forbidden by the second choice of rewriting the Boltzmann weight in (1.3), which in turns leads to the domain wall expansion.

First define the dual graph $\mathcal{L}^* = (V^*, E^*)$ of $\mathcal{L}$. The vertices of $\mathcal{L}^*$ are the centers of the faces (planar regions) of $\mathcal{L}$ and edges of $\mathcal{L}^*$ cross the edges of $\mathcal{L}$, see Fig. 1.1. If the term $\left[1-\delta_{s(x),s(y)}\right]$ is chosen, the variables $s(x)$ and $s(y)$ must have different colors and we draw an edge in the dual graph $\mathcal{L}^*$, intersecting the edge $\langle x, y\rangle \in \mathcal{L}$, see Fig. 1.1. To any graph variable configurations is then associated

[1] Isolated vertices count as single connected components.

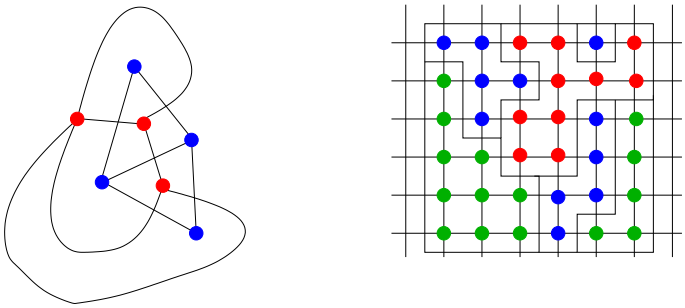

Figure 1.1: *Left.* A graph $\mathcal{L}$ and its dual $\mathcal{L}^*$. The vertices of $\mathcal{L}$ are the blue dots, the vertices of $\mathcal{L}^*$ are the red circles. *Right.* A domain wall configuration on the dual lattice $\mathcal{L}^*$ of a square lattice. The graph $\mathcal{H}^*$ contains domain walls enclosing the clusters of equally colored lattice variables.

a graph $\mathcal{H}^*$, the faces of $\mathcal{H}^*$ are clusters of equally colored graph variables. The sum over $s(x)$ gives the chromatic polynomial[2] $\pi_{\mathcal{H}}(q)$ of $\mathcal{H}$ the dual graph of $\mathcal{H}^*$ and we obtain the domain wall representation of the Potts model [35]

$$Z_{\text{Potts}}(J,q) = v^{|E(\mathcal{L})|} \sum_{\mathcal{H}^*} \pi_{\mathcal{H}}(q) v^{-\text{length}(\mathcal{H}^*)}, \tag{1.6}$$

where length($\mathcal{H}^*$) is the total length of $\mathcal{H}^*$ domain walls.

Assume $J > 0$. When $v \gg 1$ the formation of domain walls is suppressed in (1.6) and typical configurations have uniform colorations. On the other hand for $v \ll 1$ and $p \to 0$ (1.5) shows that FK clusters with few sites are more probable. The sum over their possible colors produces typically a permutational invariant configuration. Let $|V(\mathcal{L})|$ the number of vertices of $\mathcal{L}$. In the thermodynamic limit $|V(\mathcal{L})| \to \infty$ one expects the existence of a graph dependent, and then non-universal, value J_c such that for q smaller than a dimensionality dependent value $q_c(d)$ the model has a continuous (second order) phase transition [23] and the free energy

$$F_{\text{Potts}}(J,q) = -\log Z_{\text{Potts}}(J,q), \tag{1.7}$$

[2]The chromatic polynomial of a graph is the number of possible colorations of the vertices of the graph such that each vertex may have q different colors and adjacent vertices have different colors.

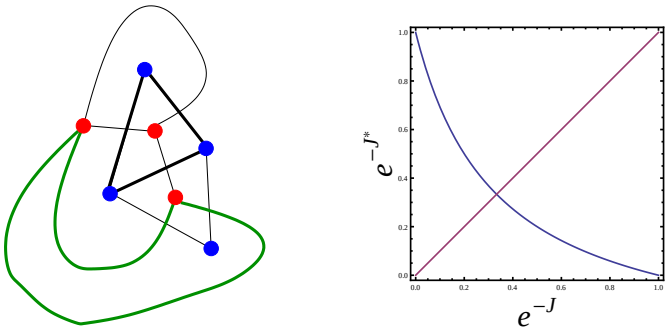

Figure 1.2: *Left.* The graph $\mathcal{G} \subset \mathcal{L}$ and its complementary graph $\mathcal{G}' \subset \mathcal{L}^*$, the edges of which are colored in green. *Right.* The duality transformation for the four color Potts model. The intersection with the diagonal of the square $[0,1] \times [0,1]$ identifies the critical value of the coupling J_c on a self-dual graph. Notice that $J^*(J^*(J)) = J$.

is singular. The value J_c separates the order phase ($J > J_c$) with spontaneously broken S_q symmetry from the disordered phase ($J < J_c$).

We conclude this section discussing the duality transformation of the Potts partition function [23]; duality provides a simple way to locate J_c. Consider the FK expansion (1.5) and recall the Euler relation for a planar graph $\mathcal{G}$ of $|C(\mathcal{G})|$ connected components

$$|C(\mathcal{G})| = |V(\mathcal{G})| - |E(\mathcal{G})| + |L(\mathcal{G})|, \tag{1.8}$$

where $|V(\mathcal{G})| = |V(\mathcal{L})|$ is the number of vertices in $\mathcal{G}$ and $|L(\mathcal{G})|$ is the number of independent closed circuits. To any FK graph $\mathcal{G}$ with edge set E associate a new graph $\mathcal{G}'$ on the dual graph $\mathcal{L}^*$. The edges of $\mathcal{G}'$ are all the edges of $\mathcal{L}^*$ that do not intersect edges of $\mathcal{G}$, see Fig. 2. We have

$$|L(\mathcal{G})| = |C(\mathcal{G}')| - 1 \tag{1.9}$$

$$|E(\mathcal{G})| + |E(\mathcal{G}')| = |E(\mathcal{L})|. \tag{1.10}$$

Defining v^* through the relation $(v^* - 1)(v - 1) = q$ the FK partition function

(1.5) is[3]

$$Z_{\rm Potts}(J,q) = (v-1)^{|E(\mathcal{L})|} q^{1-|V(\mathcal{L}^*)|} \sum_{\mathcal{G}' \subseteq \mathcal{L}^*} (v^*-1)^{|E(\mathcal{G}')|} q^{|C(\mathcal{G}')|}. \qquad (1.11)$$

Apart from a prefactor the partition function $Z_{\rm Potts}(J,q)$ on the graph $\mathcal{L}$ coincides with the partition function $Z_{\rm Potts}(J^*,q)$ on the dual graph $\mathcal{L}^*$. The duality transformation $J^*(J)$ is shown in Fig. 1.2 and maps the partition function on $\mathcal{L}$ at small coupling $J \ll 1$ into the partition function on $\mathcal{L}^*$ at large coupling $J^* \gg 1$. If now $\mathcal{L}$ is a self-dual graph, for example a bidimensional square lattice, the fixed point of the duality map $J^*(J_c) = J_c$ is the value of the coupling for which the model is critical. For $q < q_c$, approaching J_c the variables $s(x)$ become correlated on larger and larger length scales and their fluctuations do not depend on the lattice details. This feature, termed universality[4], is a consequence of the renormalization group on which we will come back in the next section and chapters of the thesis.

1.2 Basic elements of conformal field theory

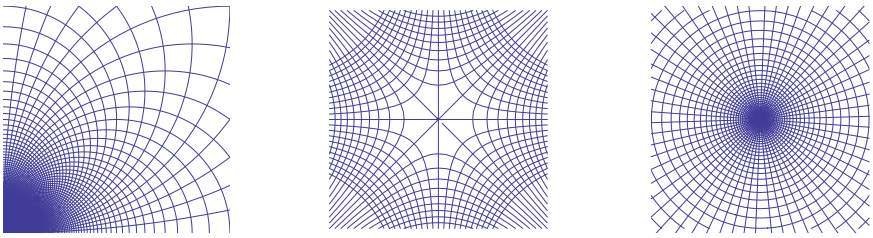

Figure 1.3: Three examples of conformal transformations in the complex plane. From left to right are drawn in the z plane the curves $\mathrm{Re}(w) = const$ and $\mathrm{Im}(w) = const$ for the mappings $w(z) = \frac{1}{z}, \sqrt{z}$ and $\log z$.

We recall some basic results of conformal field theory in two dimensions. Let $\mathcal{L}$ be a regular lattice with lattice spacing a and $H\big(\{s(x)\},\{J\}\big)$ the Hamiltonian of

[3] We used $|L(\mathcal{L})| = |V(\mathcal{L}^*)| - 1$ and $|C(\mathcal{L})| = 1$.

[4] More precisely, different statistical mechanics models share the same properties at large distances on the critical surface identified by the irrelevant directions of the renormalization group transformation.

a statistical mechanics model formulated in terms of variables $s(x)$ and coupling set $\{J\}$. The two-point correlation function is the average

$$\langle s(x)s(0)\rangle = \frac{1}{Z}\sum_{\{s(x)\}} \mathrm{e}^{-H} s(x)s(0). \tag{1.12}$$

Near the critical point the behavior of (1.12)

$$\langle s(x)s(0)\rangle = \xi^{-2X_s} F\big(|x|/\xi\big) \tag{1.13}$$

defines the correlation length ξ, the typical length scale of the fluctuations and X_s the scaling dimension[5] of $s(x)$. ξ diverges at criticality and the region of validity of (1.13) is the scaling region. In the scaling region the functional form (1.13) is not affected[6] by the specific details of the lattice $\mathcal{L}$ and we can identify renormalized local densities (scaling fields), for example $\phi(x) \sim a^{-X_s} s(x)$, whose conjugated couplings transform multiplicatively under the linearized renormalization group transformation [4, 5]. In the continuum limit $a \to 0$ the dynamics of the densities is described by an Euclidean two-dimensional quantum field theory

$$\langle \phi(x)\phi(0)\rangle_S = \frac{1}{Z}\int \mathcal{D}\phi\ \mathrm{e}^{-S[\phi]}\phi(x)\phi(0), \tag{1.14}$$

with action S specified by the requirement that for $|x| \gg a$

$$\langle s(x)s(0)\rangle = K\langle \phi(x)\phi(0)\rangle_S, \tag{1.15}$$

where K is an a-dependent normalization constant. The mass of the quantum field theory m is the inverse of ξ. At the fixed point of the renormalization group transformation $\xi = \infty$ and the densities $\phi_i(x)$ with scaling dimension X_{ϕ_i} obey global scale invariance under $x \to bx$

$$\phi_i(bx) = b^{-X_{\phi_i}}\phi(x). \tag{1.16}$$

The corresponding quantum field theory has action S^* and it is massless, with two-point function

$$\langle \phi_i(x)\phi_i(0)\rangle_{S^*} = \frac{1}{|x|^{2X_{\phi_i}}}, \tag{1.17}$$

[5] In d dimensions for a scalar order parameter $2X_s = d - 2 + \eta$ with η the usual anomalous dimension.

[6] $F(t) \to \mathrm{e}^{-t} + \text{const.}$ in the infrared limit $|x| \gg \xi$ and $F(t) \to t^{-2X\phi}$ in the ultraviolet limit $|x| \ll \xi$.

which is a power-law. In writing (1.17) we also assumed rotational and translational invariance; if we further require the invariance of S^* under local scale transformations $x \to b(x)x$ the full group of symmetry is the conformal group and S^* is conformal invariant [36].

Restrict from now on to two dimensions [12]. Conformal transformations of coordinates maintain local angles between vectors in the plane, see Fig. 1.3. For convenience we introduce complex coordinates $z = x_1 + ix_2$ and $\bar{z} = x_1 - ix_2$, the Euclidean metric $g = \frac{1}{2}\left[dz \otimes d\bar{z} + d\bar{z} \otimes dz\right]$ is off-diagonal in the coordinates $(z, \bar{z})$ and therefore the tangent vectors $\partial \equiv \frac{d}{dz}$ and $\bar{\partial} \equiv \frac{d}{d\bar{z}}$ have zero norm. The transformation of coordinates $w(z, \bar{z})$ preserves the angles if

$$\langle \partial_w, \partial_w \rangle = \langle \bar{\partial}_w, \bar{\partial}_w \rangle = 0, \tag{1.18}$$

$$\langle \partial_w, \bar{\partial}_w \rangle = \frac{1}{2}\Omega(w, \bar{w}), \tag{1.19}$$

where $\partial_w \equiv \frac{d}{dw}$, $\bar{\partial}_w \equiv \frac{d}{d\bar{w}}$ and the inner product $\langle a, b \rangle$ between two vectors a, b is $g(a, b)$. It is simple to prove that (1.18) and (1.19) are satisfied by the isogonal mappings $w(z, \bar{z}) = w(z)$ and $w(z, \bar{z}) = w(\bar{z})$ giving $\Omega(w, \bar{w}) = \left|\frac{dz}{dw}\right|^2$. However only analytic functions preserve the local angle orientation and define a conformal mapping.

The scaling fields for which the requirement of conformal covariance analogous to (1.19) naturally translates into

$$\phi_i(w, \bar{w}) = \left|\frac{dz}{dw}\right|^{X_{\phi_i}} \phi_i(z, \bar{z}) \tag{1.20}$$

are the primary fields of the conformal field theory. Conformal transformations are analytic functions and it is useful to regard z and $\bar{z}$ as independent variables defining two different scaling dimensions h_{ϕ_i}, $\bar{h}_{\phi_i}$ such that $X_{\phi_i} = h_{\phi_i} + \bar{h}_{\phi_i}$. Under $z \to w(z)$, $\bar{z} \to \bar{w}(\bar{z})$ a primary field transforms as

$$\phi_i(w, \bar{w}) = \left(\frac{dz}{dw}\right)^{h_{\phi_i}} \left(\frac{d\bar{z}}{d\bar{w}}\right)^{\bar{h}_{\phi_i}} \phi_i(z, \bar{z}). \tag{1.21}$$

The real numbers h_{ϕ_i} and $\bar{h}_{\phi_i}$ are equal for a scalar field and are called conformal dimensions. An infinitesimal conformal transformation $w(z) = z + \varepsilon(z)$ is generated by the stress energy tensor $T_{\mu\nu}(x)$, which is symmetric, traceless and

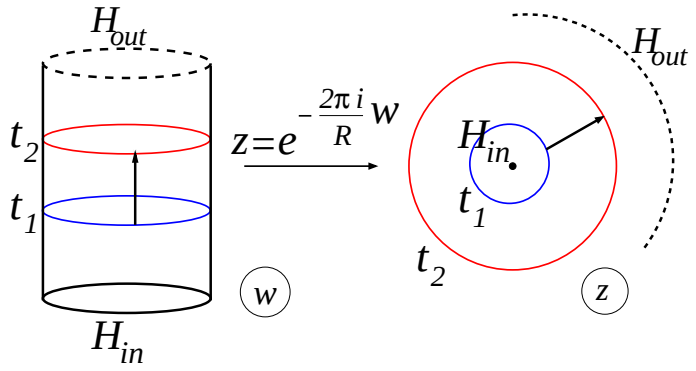

Figure 1.4: Radial quantization of a conformal field theory on the z plane is obtained from the conformal mapping $z = \mathrm{e}^{-\frac{2\pi i w}{R}}$, where $w = x + iy$ is the Euclidean coordinate on the cylinder. The asymptotic Hilbert spaces of massless particles are denoted by H_{in} and H_{out}.

conserved. In complex coordinates $T_{\mu\nu}$ has only two independent components $T_{zz} = T_{11} - 2iT_{12} - T_{22} \equiv T(z)$ and $T_{\bar{z}\bar{z}} = T_{11} + 2iT_{12} - T_{22} \equiv \bar{T}(\bar{z})$, which are purely analytic and antianalytic as a consequence of the conservation law $\partial^\mu T_{\mu\nu} = 0$.

To quantize a conformal field theory we introduce light-cone coordinates $w_\pm = x \pm t$ and think the Minkowsky space-time as a cylinder of circumference[7] R. The asymptotic Hilbert spaces H_{in} and H_{out} are defined on the cylinder at time $t = \pm\infty$. Operators of the quantum theory $\Phi(x,t)$ are of the factorized form $\Phi_+(w_+)\Phi_-(w_-)$ and inside correlation functions time-ordering $\mathcal{T}$ is understood

$$\langle \Phi_1(x_1,t_1)\dots\Phi_n(x_n,t_n)\rangle \equiv \langle \mathcal{T}\{\Phi_1(x_1,t_1)\dots\Phi_n(x_n,t_n)\}\rangle, \tag{1.22}$$

$\mathcal{T}\{\Phi_1(x_1,t_1)\dots\Phi_n(x_n,t_n)\} = \sum_{\sigma\in S_n}\prod_{i=1}^{n-1}\theta(t_{\sigma(i)} - t_{\sigma(i+1)})\Phi_{\sigma(1)}\dots\Phi_{\sigma(n)}$. After the analytic continuation $t = iy$ to Euclidean space let $w = x + iy$. The quantization prescription (radial quantization) on the complex plane of z is obtained exploiting conformal covariance through the mapping $z = \mathrm{e}^{-\frac{2i\pi}{R}w}$, see Fig. 1.4. For example, suppose to compute on the z plane the equal times commutator

[7] This is necessary because a massless field theory on the line has not well defined asymptotic states.

between two operators $A(\zeta)$, $B(z)$. Time ordering on the cylinder translates into radial ordering on the plane and we find

$$[A(\zeta), B(z)] = \lim_{|\zeta|\to|z|} \theta\big(|\zeta| - |z|\big) A(\zeta)B(z) - \theta\big(|z| - |\zeta|\big) B(z)A(\zeta). \tag{1.23}$$

If the operator A is expressed as a contour integral of some operator density $Q(w)$ at constant time $|w| = |\zeta|$

$$A = \oint_{|w|=|\zeta|} \frac{dw}{2\pi i}\, Q(w), \tag{1.24}$$

the commutator reads

$$[A, B(z)] = \oint_{C_z} \frac{dw}{2\pi i}\, Q(w)B(z), \tag{1.25}$$

where C_z is a contour encircling the point z. To evaluate (1.23) it is necessary to know the singularities arising from the short distance expansion $\lim_{w\to z} Q(w)B(z)$ which are ruled by the Operator Product Expansion (OPE). Let us consider the stress energy tensor $T(z)$. By dimensional analysis

$$\lim_{w\to z} T(w)T(z) = \frac{c/2}{(w-z)^4} + \frac{2T(z)}{(w-z)^2} + \frac{\partial T(z)}{z-w} + \text{regular terms}, \tag{1.26}$$

the real parameter c is the central charge of the conformal field theory. As operators A and B of the form (1.24) we take the Laurent modes defined as

$$L_n = \frac{1}{2\pi i} \oint_{C_O} dz\; z^{n+1} T(z), \tag{1.27}$$

with C_O a contour encircling the origin O. The combined use of (1.26) and (1.23) gives the commutation rule

$$[L_n, L_m] = (n-m)L_{n+m} + \frac{c}{12}\, \delta_{n+m,0}\; n(n^2-1), \tag{1.28}$$

which defines the Virasoro algebra. Consider now a primary field[8] $\phi_h(z)$ with conformal dimension h. Assuming the OPE

$$\lim_{w\to z} T(w)\phi_h(z) = \frac{h\phi_h(z)}{(w-z)^2} + \frac{\partial\phi_h(z)}{w-z} + \text{regular terms} \tag{1.29}$$

[8] We only focus on the dependence from the coordinate z.

from (1.23) the commutation relations with the Laurent modes

$$[L_n, \phi_h(z)] = h(n+1)z^n\phi_h(z) + z^{n+1}\partial\phi(z) \tag{1.30}$$

follow. The study of the representation theory of the Virasoro algebra (1.28) is equivalent to the characterization of the Hilbert space H_{in} and we summarize the basic results [4, 13].

- The Hilbert space H_{in} is the vector space of an infinite dimensional representation of the Virasoro algebra. Highest weights $|h\rangle$ are eigenvector of L_0 defined by the action of the primary $\phi_h(0)$ on the conformal invariant vacuum $|\Omega\rangle$. Form (1.30)

  $$L_0|h\rangle = h|h\rangle. \tag{1.31}$$

  The vacuum $|\Omega\rangle$ is the only highest weight with conformal weight $h = 0$.

- Descendant states of $|h\rangle$ are obtained applying the modes L_{-n}, $n > 0$, to $|h\rangle$. The descendant state $L_{-n_1} \dots L_{-n_k}|h\rangle$ has L_0 eigenvalue $h + N$, $N = \sum_{i=1}^{k} n_i$. N is the level of the descendant and the number of descendant states of $|h\rangle$ at level N is $P(N)$, the number of partitions of N into positive, not necessarily distinct, integers. The set of states resulting from the application of the L_{-n}'s to the highest weight $|h\rangle$ is the Verma module of $|h\rangle$. The Hilbert space H_{in} is a direct sum of Verma modules.

- The $P(N) \times P(N)$ matrix resulting from the scalar products of the descendant states of $|h\rangle$ at level N is the Grahm matrix $G(h, c, N)$. Virasoro algebra representations are unitary if all the elements of $G(h, c, N)$ are non-negative and irreducible if they are non-vanishing. The classification of the Virasoro algebra representations is based on the exact formula, found by Kac, for the determinant of $G(h, c, N)$. We summarize the conclusions.

  - For $c < 0$ there are no unitary representations.
  - For $c > 1$ all the representations are unitary and irreducible for every value of h.
  - For $c = 1$ there are infinite values of h for which the representations are reducible but all of them are unitary.

– For $0 < c < 1$ unitary representations are obtained for

$$c = 1 - \frac{6}{t(t+1)}, \quad h_{m,n} = \frac{[(t+1)m - tn]^2 - 1}{4t(t+1)}, \tag{1.32}$$

where t, m and n are integers with $t > 2$ and $m = 1, \ldots, t-1$ $n = 1, \ldots, m$. The representations are reducible and irreducible representations are obtained subtracting all the vectors with vanishing norm (null vectors) from the Verma module. For a given t, the conformal field theory defined by (1.32) is called the minimal model $\mathcal{M}_t$[9]. In a minimal model the null norm condition for a vector generates a differential equation for the primary correlation functions, which can be solved exactly. The primary fields with conformal dimensions (1.32) are also the generators of the OPE algebra.

1.3 Critical q-color Potts model

The critical Potts model for arbitrary values of q is described by a conformal field theory[10]. The parameter t in (1.32) relates to q as [37, 38]

$$\sqrt{q} = 2 \sin \frac{\pi(t-1)}{2(t+1)}. \tag{1.33}$$

The theory is minimal only for integer $q < 4$. The value $q = 4$ corresponds to $c = 1$ and for $q > 4$ the Potts phase transition is first order ($q_c(2) = 4$). The maximum number of colors allowing the existence of a second order phase transition in two dimensions can be found by simple group theoretic considerations, as we will show in sections 2.3 and 2.7. The conformal dimensions h_ε and h_s for the Potts thermal and spin fields can be conjectured for arbitrary q [37, 38]

$$h_\varepsilon = h_{2,1} = \frac{t+3}{4t}, \tag{1.34}$$

$$h_s = h_{\frac{t+1}{2}, \frac{t+1}{2}} = \frac{(t+3)(t-1)}{16t(t+1)}. \tag{1.35}$$

[9] For $c < 0$ also exist representations which are minimal, i.e. they contain a finite number of primaries, but not unitary. The simplest example is the Lee-Yang model.

[10] When q is not integer we are referring to the random cluster model representation of the partition function.

We observe from (1.32) that for $q \neq 2, 3$ the Verma module of the Potts spin field s does not contain null vectors and no differential equations are known to be satisfied by its correlation functions.

As an example of conformal minimal model we discuss the critical three-color Potts model. The Hamiltonian is

$$H = -J \sum_{\langle x,y \rangle} \frac{2}{3}\Big[\cos\big(\varphi(x) - \varphi(y)\big) + \frac{1}{2}\Big], \tag{1.36}$$

where $\varphi(x) = \frac{2\pi}{3} s(x)$ and $s(x) = 1, 2, 3$. It is useful to consider the complex spin variables $\sigma(x) = \mathrm{e}^{i\varphi(x)}$ and $\bar{\sigma}(x) = \mathrm{e}^{-i\varphi(x)}$, in terms of which the Hamiltonian (1.36) shows an explicit $S_3 = \mathbb{Z}_3 \rtimes \mathbb{Z}_2$ symmetry[11], the $\mathbb{Z}_2$ factor is associated to the symmetry $\sigma \to \bar{\sigma}$. In the scaling limit the most relevant fields of the continuum theory are the spin field $s(x) = \sigma(x) + \bar{\sigma}(x)$ and the energy field $\varepsilon(x)$. As discussed in section 1.1 the model is critical on a square lattice for $J_c = \log(1 + \sqrt{3})$. A comparison with the critical exponents of the exact lattice solution due to Baxter [39] allows to identify the critical quantum theory as the minimal model $\mathcal{M}_5$ with central charge $4/5$. The primary fields of the $\mathcal{M}_5$ theory are collected with their conformal weights in the Kac table.

$n = 4$				$\frac{1}{8}$
3			$\frac{1}{15}$	$\frac{2}{3}$
2		$\frac{1}{40}$	$\frac{21}{40}$	$\frac{13}{8}$
1	0	$\frac{2}{5}$	$\frac{7}{5}$	3
m	1	2	3	4

Table 1.1: The Kac table for the minimal model $\mathcal{M}_5$. The conformal dimensions $h_{m,n}$ are indicated.

The spin field corresponds to $\phi_{3,3}$ and the energy field to $\phi_{2,1}$. The conformal dimensions in the second row of the table do not have an interpretation in the lattice solution and the corresponding fields decouple from the OPE algebra. The

[11] The presence of the semi-direct product $\rtimes$ is due to the fact that $\mathbb{Z}_2$ is not a normal subgroup of S_3.

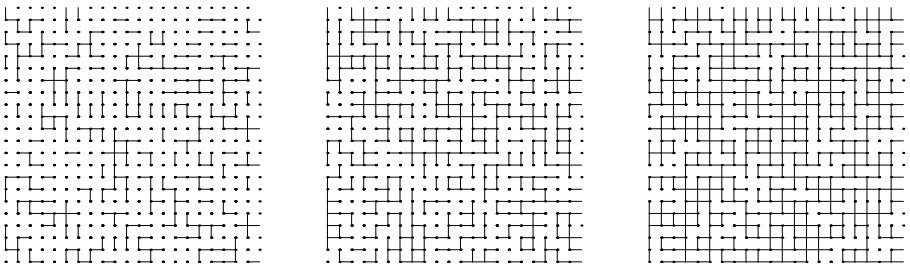

Figure 1.5: Typical configurations in a bond percolation problem on a square lattice. The bond occupation probabilities are 0.3, 0.5 and 0.7.

explanation of the decoupling involves the construction of the modular invariant partition function on the torus [40, 41].

1.4 A short introduction to percolation

Consider the planar connected graph $\mathcal{L}$ defined in section 1.1. Bond percolation on $\mathcal{L}$ is the random process[12] in which the edges of $\mathcal{L}$ can be occupied with probability $p \in [0,1]$. The set of occupied edges defines a graph $\mathcal{G} \subseteq \mathcal{L}$, see Fig. 1.5, with probability measure $\Lambda(\mathcal{G})$

$$\Lambda(\mathcal{G}) = p^{|E(\mathcal{G})|}(1-p)^{|E(\mathcal{L})|-|E(\mathcal{G})|}. \tag{1.37}$$

The connected components of $\mathcal{G}$ are the percolative clusters. Two vertices $x, y \in V$ are connected in the graph $\mathcal{G}$ if there exists a path of occupied edges starting from x and ending at y. Connected vertices belong to the same cluster. The probability $P_{aa}(x,y)$ that the vertices x and y belong to the same cluster a[13]

$$P_{aa}(x,y) = \sum_{\mathcal{G}\subseteq\mathcal{L}} \Lambda(\mathcal{G})\theta(x,y|\mathcal{G}), \tag{1.38}$$

is the two-point connectivity in percolation. In (1.38) the function $\theta(x,y|\mathcal{G}) = 1$ if x and y are connected and zero otherwise. In general, if the letters $a_1, \ldots, a_n$ denote particular clusters we can define the n-point connectivity $P_{a_1\ldots a_n}(x_1, \ldots, x_n)$

[12] We focus on bond percolation, but a site percolation problem can be also considered. Universal results in the scaling limit are identical for bond and site percolation.

[13] We used $\sum_{\mathcal{G}\subseteq\mathcal{L}} \Lambda(\mathcal{G}) = 1$.

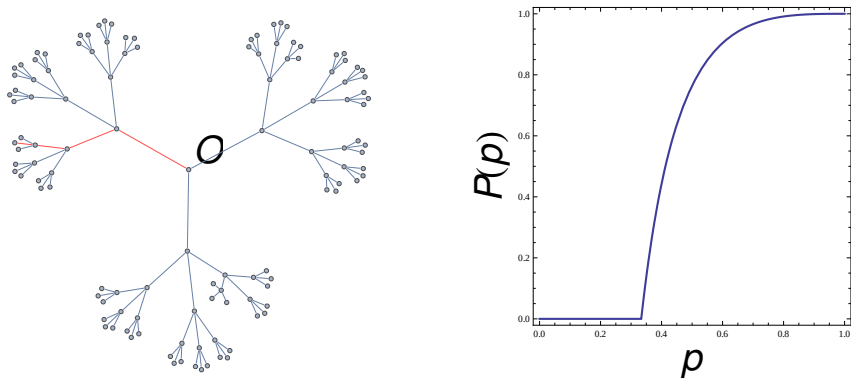

Figure 1.6: *Left.* Percolation problem on a Cayley tree with coordination number $\sigma = 3$. A path of occupied edges connecting the origin O to the boundary of the tree is colored in red. *Right.* The function $P(p)$ obtained solving (1.40) for $\sigma = 3$.

as the probability that the vertex x_i belongs to the cluster a_i. The number of n-point connectivities is the number of partitions of a set of n elements, the Bell number B_n. Connectivities in the random cluster model will be analyzed in the next chapter.

We introduce the percolative phase transition with an example. Take $\mathcal{L}$ a Cayley tree with coordination number σ and N sites (vertices), Fig. 1.6, and consider in the limit $N \to \infty$ the probability $P(p)$ that the origin O is connected to a point on the boundary. We have

$$P = \sum_{k=1}^{\sigma} \binom{\sigma}{k} p^k (1-p)^{\sigma-k} (1 - Q^k), \tag{1.39}$$

with $P + Q = 1$. The probability P satisfies the algebraic equation

$$P = 1 - (1 - pP)^{\sigma}, \tag{1.40}$$

which can be solved graphically. For $p \leq p_c \equiv 1/\sigma$ the only solution is $P = 0$ and a unique non-vanishing solution is obtained when $p > p_c$. The threshold value p_c separates the subcritical phase ($p < p_c$) from the supercritical phase ($p > p_c$). The critical exponent β is defined by

$$P(p) \sim B(p - p_c)^{\beta}, \quad p \to p_c^+, \tag{1.41}$$

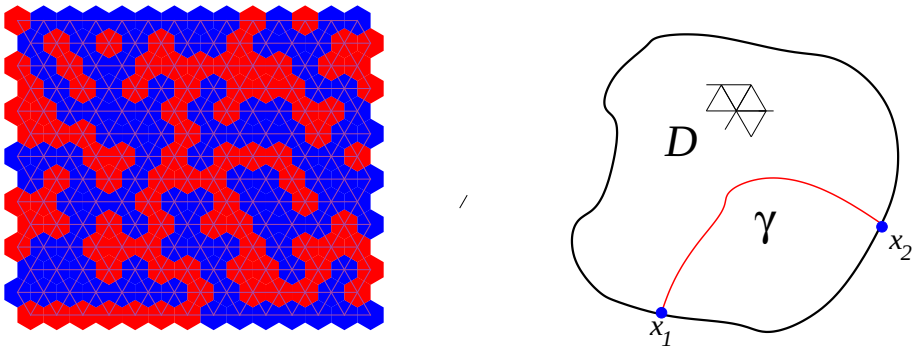

Figure 1.7: *Left.* Site percolation problem on a triangular lattice T at $p_c = 1/2$. The percolation interface ends on the right on the lattice. *Right.* The definition of the interface γ with end points x_1 and x_2 in the continuum limit $a \to 0$ on a simply connected domain $D \subset \mathbb{H}$.

and $\beta = 1$ in a Cayley tree, see Fig. 1.6. In the supercritical phase the cluster containing the origin also contains an infinite number of sites in the thermodynamic limit $N \to \infty$ and it is called the infinite cluster. $P(p)$ can be also characterized as the average fraction of sites belonging to it. The average size of finite[14] clusters containing the origin $S = \sum_{x \in \mathcal{L}} P_{aa}(x, 0)$ is another classical observable in percolation theory. S diverges at p_c and the critical exponent γ is defined as

$$S \sim \Gamma^{\pm} |p - p_c|^{-\gamma}. \tag{1.42}$$

The superscript $\pm$ on the critical amplitude $\Gamma^{\pm}$ refers to p_c being approached from below or above. In a Cayley tree $\gamma = 1$. The percolative transition on a Cayley tree is actually an artifact due to the effective infinite dimensionality of the graph. Connectivities are exponentially decaying with the distance also at p_c.

On the hypercubic lattice $\mathcal{L} = \mathbb{Z}^d$ ($d \geq 2$) with lattice spacing a, the transition is also signaled by the divergence of the correlation length ξ

$$\xi \sim f^{\pm} |p - p_c|^{-\nu}, \tag{1.43}$$

[14] In the supercritical phase all the clusters except the infinite one.

defined from the behavior of the two-point connectivity in the scaling limit $\xi \gg a$ near p_c

$$P_{aa}(x,y) = \xi^{2-d-\eta} F\big(|x-y|/\xi\big). \tag{1.44}$$

A critical exponent α is finally introduced for the singular part of the mean number of clusters $\langle N_c \rangle$ with

$$\frac{\langle N_c \rangle}{N} \sim A^{\pm} |p - p_c|^{2-\alpha}, \tag{1.45}$$

N being the total number of sites of $\mathcal{L}$. Critical exponents α, β, γ and ν are expected to be universal as well as suitable critical amplitude ratios[15].

In two dimensions a rigorous definition of the scaling region for percolation is possible and requires the notion of percolation interface γ. Mathematically the percolation interface is defined starting from the critical ($p_c = 1/2$) site percolation problem on a triangular lattice T as follows. Consider the dual hexagonal lattice H and color its faces in red or blue, see Fig. 1.7, according to the site in the center being occupied or empty. Boundary conditions are chosen in such a way that the sites on the bottom of T are half empty and half occupied. The point in which boundary conditions change is O. The random curve γ is drawn on the edges of H starting from O and separates a red colored region on its left from a blue colored region on its right. It can be shown that in the limit in which the lattice spacing $a \to 0$, the random curve γ defines a random process on a simply connected domain D of the upper half plane $\mathbb{H}$ which is known as Schramm Lowener Evolution (SLE) [42, 43, 44]. If the end points of γ are fixed on the boundary of D, see Fig. 1.7, a measure $\mu(\gamma; x_1, x_2, D)$ for the curves γ can be defined[16] directly in the continuum limit. The measure satisfies two properties

- *Markov property.* Divide the curve γ in two parts γ_1 from x_1 to x and γ_2 from x to x_2, then the conditional measure

$$\mu(\gamma_2|\gamma_1; x_1, x_2, D) = \mu(\gamma_2; x, x_2, D\backslash\gamma_1). \tag{1.46}$$

[15] Universality in percolation and the existence of the scaling limit have been tested for many years in numerical simulations and taken for granted by physicists.

[16] In the example of site percolation of Fig. (1.7) the probability to obtain the interface γ is just $2^{-\text{length}(\gamma)}$

- *Conformal Invariance.* Consider a conformal mapping Φ which maps the interior of D into the interior of a new domain D'. The points x_1 and x_2 on the boundary are mapped into the points x_1' and x_2' on the boundary of D'. The map Φ induces a new probability measure for the transformed curve $\Phi(\gamma)$, $\Phi * \mu$ and it is required

$$\Phi * \mu(\gamma; x_1, x_2, D) = \mu(\Phi(\gamma), x_1', x_2', D'). \tag{1.47}$$

  The formalism of SLE allows a rigorous derivation[17] of the critical exponents for two-dimensional percolation that confirm the exact value obtained by physicists through arguments that we recall in the next section.

1.5 Percolation as the $q \to 1$ limit of the Potts model

Apart from an inessential prefactor the probability measure for a graph $\mathcal{G}$ in the FK representation (1.5) coincides at $q = 1$ with (1.37). This simple observation identifies the FK clusters in the random cluster model at $q = 1$ with the percolative clusters[18]. The geometric phase transition of percolation is mapped onto the formal ferromagnetic phase transition of the Potts model with discrete symmetry group S_q in the limit $q \to 1$. To be more explicit, define at integer q the Potts order parameter

$$\sigma_\alpha(x) = q\delta_{s(x),\alpha} - 1, \tag{1.48}$$

where $\alpha = 1, \ldots, q$ and $\sum_{\alpha=1}^{q} \sigma_\alpha = 0$. Take a finite simply connected domain[19] $D \subset \mathbb{R}^d$ and fix $s(x) = \alpha$ on the boundary of D. Correlation functions computed with such a choice of boundary conditions are denoted with the subscript α. In the FK representation $\langle \sigma_\alpha(x) \rangle_\alpha$ does not receive any contribution from graphs in which the point x belongs to clusters which do not touch the boundary. If instead x belongs to a cluster touching the boundary we simply obtain a factor

[17] On a triangular lattice, but universality is expected to hold.

[18] The connection is with bond percolation. We will not emphasize any more distinctions between site and bond percolation since we will be interested in studying universal properties in the scaling limit.

[19] These considerations directly apply in the continuum limit.

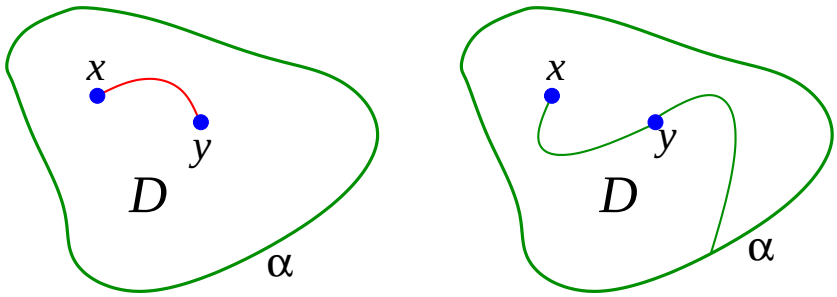

Figure 1.8: Graphical representation of the FK expansion for the two-point function of the Potts order parameter σ_α. The boundary spins have fixed value α.

$q-1$. It follows

$$\langle \sigma_\alpha \rangle_\alpha = (q-1) P_q(x), \tag{1.49}$$

where $P_q(x)$ is the probability that x is connected to the boundary of D, computed with the random cluster model measure (1.5). In the thermodynamic limit in which D covers the whole plane $\mathbb{R}^2$ the expectation value $\langle \sigma_\alpha \rangle_\alpha$ is a constant. It vanishes in the phase of unbroken S_q symmetry and defines the Potts spontaneous magnetization[20] in the broken phase with color α. The probability $P_q(x)$ is expected to be an analytic function of q and the limit

$$P \equiv \lim_{q \to 1} \frac{\langle \sigma_\alpha \rangle_\alpha}{q-1} \tag{1.50}$$

is expected to exist and define the order parameter of percolation, introduced in the previous section. Consider now the FK representation of the connected two-point correlation function

$$G_{\alpha\alpha}(x,y) = \langle \sigma_\alpha(x) \sigma_\alpha(y) \rangle_\alpha - \langle \sigma_\alpha \rangle_\alpha^2, \tag{1.51}$$

computed in the thermodynamic limit with boundary conditions α. The correlation function (1.51) has non-vanishing contributions from graphs $\mathcal{G}$ in which the two points are connected[21] or in which the two points are connected to the

[20] Notice that the presence of an infinite FK cluster implies the presence of an infinite cluster of α magnetized Potts spins (spin cluster). The viceversa is false.

[21] If the points are not connected to each other or are not connected to the boundary the sum over the spin color $\sum_\alpha \sigma_\alpha$ factorizes and gives a vanishing result.

boundary, see Fig. 1.8. In the thermodynamic limit in the broken phase of color α the probability that the two points are connected to the boundary coincides with the probability that both points belong to the infinite cluster $P_i(x,y)$. We obtain[22]

$$G_{\alpha\alpha}(x,y) = \frac{q-1}{q} P_{aa}(x,y) + (q-1)^2 (P_i(x,y) - P^2) \tag{1.52}$$

and the average size of finite clusters in percolation is

$$S = \lim_{q\to 1} \frac{\int d^2x \; G_{\alpha\alpha}(x,y)}{q-1}. \tag{1.53}$$

The dependence on y in (1.53) can be eliminated by translational invariance. Finally we observe that the singular part of the mean cluster number per site in percolation can be computed directly from (1.5) as

$$\frac{\langle N_c \rangle}{N} = \lim_{q\to 1} \frac{f_q^{\rm sing}}{q-1}, \tag{1.54}$$

where $f_q^{\rm sing}$ is the singular part of the q-color Potts free energy density and we have taken into account that $f_1 = 0$. The validity of the relations (1.50), (1.53) and (1.54) relies on the possibility to analytically continue the Potts partition function for arbitrary q. Critical exponents of two-dimensional percolation are then obtained from the basic scaling relations

$$\alpha = 2 - 2\nu, \quad \nu = \frac{1}{2 - X_\varepsilon}, \quad \beta = \nu X_s, \quad \gamma = 2\nu(1 - X_s), \tag{1.55}$$

where X_ε and X_s are twice the conformal dimensions h_ε and h_s in (1.34), computed at $t = 2$. Their values are

$$\alpha = -\frac{2}{3}, \quad \beta = \frac{5}{36}, \quad \gamma = \frac{43}{18}, \quad \nu = \frac{4}{3}. \tag{1.56}$$

[22] Of course (1.52) is valid also in the unbroken phase.

Chapter 2

Potts q-color field theory and the scaling random cluster model

In this chapter we study structural properties of the q-color Potts field theory as a field theory able to capture for positive real q the scaling limit of the random cluster model. The OPE of the spin fields and kink fields is analyzed, as well as the duality transformation between their correlators in the two-dimensional case. At the end of the chapter we briefly introduce the concept of integrable field theory in $1+1$ dimensions, discussing the peculiar features of factorized scattering matrices. We present the specific example of the two-dimensional S_q invariant Potts field theory perturbed away from criticality by the relevant energy density field.

2.1 Introduction and general remarks

In chapter 1 we introduced the FK representation of the Potts model

$$Z_{\text{Potts}}(J,q) = v^{|E(\mathcal{L})|} \sum_{\mathcal{G}\subseteq\mathcal{L}} p^{|E(\mathcal{G})|}(1-p)^{|E(\mathcal{L})|-|E(\mathcal{G})|} q^{|C(\mathcal{G})|} \tag{2.1}$$

and commented that for non-integer values of q the partition function (2.1) defines a generalized percolative problem which is called the random cluster model. In the thermodynamic limit the random cluster model undergoes, for q continuous, a percolative phase transition associated to the appearance, for p larger than a q-dependent critical value p_c, of a non-zero probability of finding an infinite cluster. The transition is first order for q larger than a dimensionality-dependent value q_c, and second order otherwise; in particular, the limit $q \to 1$, which eliminates the factor $q^{|C(\mathcal{G})|}$ in (2.1), describes ordinary percolation as we discussed in section 1.5 When q is an integer larger than 1, the percolative transition of the random cluster model contains, in a sense to be clarified below, the ferromagnetic transition of the Potts model. For $q \leq q_c$, when a scaling limit exists, the problem admits a field theoretical formulation. There must be a field theory, which we call Potts field theory, that describes the scaling limit of the random cluster model for q real, as well as that of the Potts ferromagnet for q integer[1]. This theory has the Potts spin fields as fundamental fields (the FK mapping relates Potts spin correlators and connectivities for the FK clusters) and is characterized by S_q-invariance. The obvious question of the meaning of S_q symmetry for q non-integer arose at least since the ϵ expansion treatment of [45], and appears to admit a general answer: although one starts from expressions which are formally defined only for q integer, formal use of the symmetry unambiguously leads to final expressions containing q as a parameter which can be taken continuous.

The two-dimensional case allows for the most advanced, non-perturbative results. The Potts field theory is integrable and the underlying scattering theory was exactly solved in [27] for continuous $q \leq q_c = 4$. We will present some basic features of integrable field theories in section 2.6.

In the next sections we will investigate instead, for q continuous, some structural properties of the Potts field theory as a theory characterized by S_q invariance under color permutations and able to describe the scaling limit of the random cluster model. We first of all observe that the issue of the content of the theory is better addressed, in any dimension, focusing on linearly independent correlation functions rather than on field multiplicities. For this purpose one needs to have in mind the relation of spin correlators with cluster connectivities for q real,

[1]Potts field theory is described by the action (2.100) in two dimensions.

rather than with magnetic properties for q integer. Just to make an example already considered[2] in [17], the correlator of three spin fields with the same color is proportional to the probability that three points are in the same FK cluster. This probability is well defined and non-vanishing for continuous values of q in the random cluster model, in particular for the case $q = 2$ in which the spin correlator has a zero enforcing Ising spin reversal symmetry; stripped of a trivial factor $q - 2$, this spin correlator enters the description of cluster connectivity at $q = 2$ as for generic real values of q. Similarly, a number $n_c \leq n$ of different colors enters the generic n-point spin correlator: a correlator with $n_c > q$ has no role in the description of the Potts ferromagnet, but enters the determination of cluster connectivities in the random cluster model.

One then realizes that the dimensionality F_n of the space of linearly independent n-point spin correlators for real values of q is actually q-independent and must coincide with that of the space of linearly independent n-point connectivities. We show that this is indeed the case and that F_n coincides with the number[3] of partitions of a set of n elements into subsets each containing more than one element; the relation between spin correlators and cluster connectivities is also given and written down explicitly up to $n = 4$. Only a number $M_n(q)$, smaller than F_n for n large enough, of independent spin correlators enters the determination of the magnetic properties at q integer, making clear that the magnetic theory is embedded into the larger percolative theory[4]. Once the relevant correlation functions have been identified, an essential tool for their study is the OPE of the spin fields. Again, the existence of such an object for real values of q is made a priori not obvious by the badly defined multiplicity of the fields. We show, however, that its structure can be very naturally identified (equations (2.47) and (2.48) below). The additional property we will study, duality, is specific of the two-dimensional case. It is well known [22, 23] that spin correlators computed in the symmetric phase of the square lattice Potts model coincide with disorder correlators computed in the spontaneously broken phase. Here we study duality directly in the continuum, for real values of q, and with the main purpose of clari-

[2] See chapter 3 of this thesis.

[3] We consider the symmetric phase, i.e. the case $p \leq p_c$.

[4] See [46] and [21] for detailed studies of this fact in the Ising model.

fying the role of kink fields. These are the fields that in any two-dimensional field theory with a discrete internal symmetry create the kink excitations interpolating between two degenerate vacua of the spontaneously broken phase; in general, they are linearly related to the usual disorder fields, which are mirror images of the spin fields, in the sense that they carry the same representation of the symmetry. In the Potts field theory, however, it appears that in many respects the use of kink fields provides a simpler way of dealing with the symmetry for real values of q. The duality between spin and kink field n-point correlators is a non-trivial problem that we study in detail up to $n = 4$, both for bulk and boundary correlations. The problem of correlation functions for points located on the boundary of a simply connected domain is simplified by topological constraints which, in the limit in which the boundary is moved to infinity, also account for non-trivial relations among kink scattering amplitudes. In the next section we investigate cluster connectivities and Potts spin correlators, their multiplicity and the relation between them. In section 2.3 we analyze OPE's and obtain in particular that for the Potts spin fields for real values of q. Duality between spin and kink field correlators in two dimensions is studied in general in section 2.4 and specialized to boundary correlations in section 2.5. Some technical remarks and details are contained in the final appendices.

2.2 Counting correlation functions

2.2.1 Cluster connectivities

Correlations within the random cluster model (2.1) are expressed by the connectivity functions giving the probability that n points $x_1, \ldots, x_n$ fall into a given FK cluster configuration. In order to define the connectivities we associate to a point x_i a label a_i, with the convention that two points x_i and x_j belong to the same cluster if $a_i = a_j$, and to different clusters otherwise. We then use the notation $P_{a_1 \ldots a_n}(x_1, ..., x_n)$ for the generic n-point connectivity function, within the phase in which there is no infinite cluster, i.e. for $p \leq p_c$. The total number of functions $P_{a_1 \ldots a_n}(x_1, \ldots, x_n)$ is the number B_n of possible partitions (clusteri-

zations) of the n points[5]; these B_n functions sum to one and form a set that we call $\mathcal{C}^{(n)}$.

It is not difficult to realize that the elements of $\mathcal{C}^{(n)}$ can be rewritten as linear combinations of "basic" k-point connectivities, with $k = 2, \ldots, n$; we call F_k the number of basic k-point connectivities, and $\mathcal{P}^{(k)} \subset \mathcal{C}^{(k)}$ the set they form. There is a simple procedure to build $\mathcal{P}^{(n)}$ given the $\mathcal{P}^{(k)}$'s for $k = 2, \ldots, n-1$. Let us start with $n = 2$: $\mathcal{C}^{(2)} = \{P_{aa}, P_{ab}\}$, but $P_{aa} + P_{ab} = 1$ implies $F_2 = 1$ and we can choose $\mathcal{P}^{(2)} = \{P_{aa}\}$. Consider now $n = 3$: $\mathcal{C}^{(3)} = \{P_{aaa}, P_{aab}, P_{aba}, P_{baa}, P_{abc}\}$, however starting from P_{aaa} and summing over the nonequivalent configurations of the last point we have $P_{aaa} + P_{aab} = P_{aa0}$, where $P_{aa0} \equiv P_{aa}(x_1, x_2)$ belongs, we chose it on purpose, to $\mathcal{P}^{(2)}$. We observe that only one linear combination of connectivities in $\mathcal{C}^{(3)}$ reproduces, taking into account the coordinate dependence, the two-point connectivity in $\mathcal{P}^{(2)}$; we obtain then the sum rules

$$P_{aaa} + P_{aab} = P_{aa0} \equiv P_{aa}(x_1, x_2), \tag{2.2}$$

$$P_{aaa} + P_{aba} = P_{a0a} \equiv P_{aa}(x_1, x_3), \tag{2.3}$$

$$P_{aaa} + P_{baa} = P_{0aa} \equiv P_{aa}(x_2, x_3), \tag{2.4}$$

$$P_{aaa} + P_{aab} + P_{aba} + P_{baa} + P_{abc} = 1. \tag{2.5}$$

This system of equations exhausts all the possible linear relations among the elements of $\mathcal{C}^{(3)}$; a reduction to a non-basic two-point connectivity (i.e. not belonging to $\mathcal{P}^{(2)}$, for example P_{ab0}) will indeed produce an equation which is a linear combination of those above. It follows, in particular, that the five elements of $\mathcal{C}^{(3)}$ can be written in terms of $P_{aaa}, P_{aa0}, P_{0aa}, P_{a0a}$, so that $F_3 = 1$ and we can choose $\mathcal{P}^{(3)} = \{P_{aaa}\}$.

In general, suppose we have chosen the F_k basic connectivities in $\mathcal{P}^{(k)}$ for $k = 2 \ldots n-1$. Given $P_{a_1 \ldots a_n} \in \mathcal{C}^{(n)}$, we can fix k of its n indices according to an element of $\mathcal{P}^{(k)}$; summing over the nonequivalent configurations of the remaining $n-k$ indices we obtain a linear relation for the connectivities of $\mathcal{C}^{(n)}$. We can do this for each of the F_k elements in $\mathcal{P}^{(k)}$ and for $\binom{n}{k}$ choices of k indices among n indices. The number of independent sum rules for the elements of $\mathcal{C}^{(n)}$ is then

$$E_n = \binom{n}{n-1} F_{n-1} + \binom{n}{n-2} F_{n-2} + \ldots + \binom{n}{2} F_2 + 1\,, \tag{2.6}$$

[5]The B_n's are known as Bell numbers and are discussed in Appendix A.

n	1	2	3	4	5	6	7	8	9	10
B_n	1	2	5	15	52	203	877	4140	21147	115975
F_n	0	1	1	4	11	41	162	715	3425	17722
$M_n(2)$	0	1	0	1	0	1	0	1	0	1
$M_n(3)$	0	1	1	3	5	11	21	43	85	171
$M_n(4)$	0	1	1	4	10	31	91	274	820	2461

Table 2.1: The Bell numbers B_n give the number of partitions of n points. The number F_n of linearly independent n-point spin correlators (2.11) coincides with the number of partitions on n points into subsets containing at least two points. A number $M_n(q)$ of these correlators determines the n-point magnetic correlations in the q-color Potts ferromagnet.

with the last term accounting for the fact that the n-point connectivities sum to one. The number F_n of elements of $\mathcal{P}^{(n)}$ is the minimum number of connectivities in $\mathcal{C}^{(n)}$ needed to solve the linear system of E_n equations in B_n unknowns, i.e.

$$F_n = B_n - \binom{n}{n-1} F_{n-1} - \binom{n}{n-2} F_{n-2} - ... - \binom{n}{2} F_2 - 1\,. \tag{2.7}$$

Defining $F_0 \equiv 1$ and knowing that $F_1 = 0$, we rewrite (2.7) as

$$B_n = \sum_{k=0}^{n} \binom{n}{k} F_k\,, \quad \forall n \geq 0. \tag{2.8}$$

We show in Appendix A that (2.8) implies that F_n is the number of partitions of a set of n points into subsets containing at least two points. We list in Table 2.1 the first few B_n and F_n. The combinatorial interpretation of the F_n's suggests that a natural choice for the set $\mathcal{P}^{(n)}$ of linearly independent n-points connectivities is to consider clusterizations with no isolated points, i.e. $\mathcal{P}^{(2)} = \{P_{aa}\}$, $\mathcal{P}^{(3)} = \{P_{aaa}\}$, $\mathcal{P}^{(4)} = \{P_{aaaa}, P_{aabb}, P_{abab}, P_{abba}\}$, and so on.

2.2.2 Spin correlators

As we will see in a moment, it follows from the FK mapping that the Potts spin correlators can be expressed as linear combinations of the cluster connectivities.

Consistency of this statement requires that the number of linearly independent spin correlators coincides with the number of linearly independent cluster connectivities. The spin variables of the Potts model were defined in (1.48) as

$$\sigma_\alpha(x) = q\delta_{s(x),\alpha} - 1\,, \qquad \alpha = 1, \ldots, q\,, \tag{2.9}$$

where $s(x)$ is the color variable appearing in (1.1), and satisfy

$$\sum_{\alpha=1}^{q} \sigma_\alpha(x) = 0\,. \tag{2.10}$$

The expectation value $\langle\sigma_\alpha\rangle$ is the order parameter of the Potts transition, since it differs from zero only in the spontaneously broken phase. More generally we denote by

$$G_{\alpha_1\ldots\alpha_n}(x_1, \ldots, x_n) = \langle\sigma_{\alpha_1}(x_1)\ldots\sigma_{\alpha_n}(x_n)\rangle_{J\leq J_c} \tag{2.11}$$

the n-point spin correlators in the symmetric phase. We now show that, for q real parameter, the number of linearly independent functions (2.11) coincides with F_n.

Let the string $(\alpha_1\ldots\alpha_n)$ identify the correlator (2.11), and suppose that α_k is isolated within this string, i.e. it is not fixed to coincide with any other index within the string. We can then use (2.10) to sum over α_k and obtain, exploiting permutational symmetry, a linear relation among correlators involving a string similar to the original one together with strings without isolated indices. The simplest example,

$$0 = \sum_\beta G_{\alpha\beta} = G_{\alpha\alpha} + (q-1)G_{\alpha\gamma}\,, \qquad \gamma \neq \alpha\,, \tag{2.12}$$

is sufficient to understand that (2.10) produces meaningful equations also if q is non-integer, the only consequence being that some multiplicity factors in front of the correlators become non-integer; also, the requirement $\gamma \neq \alpha$ should imply $q \geq 2$, but in the sense of analytic continuation to real values of q (2.12) is equally valid for $q < 2$. Similarly, starting with a string with m isolated indices $\alpha_{k_1}, \ldots, \alpha_{k_m}$, summing over α_{k_1} and using permutational symmetry we generate a linear relation involving the original string with the m isolated indices $\alpha_{k_1}, \ldots, \alpha_{k_m}$ together with strings in which α_{k_1} is no more isolated, i.e. with at

most[6] $m-1$ isolated indices. Iterating this procedure, any correlation function (2.11) with isolated indices can be written as linear combination of correlation functions without isolated indices. Recalling the meaning of F_n in terms of set partitions, we then see that there are at most F_n S_q-nonequivalent, linearly independent correlation functions (2.11), i.e. those without isolated indices. On the other hand, the constraint (2.10) does not generate any new linear relation if we start with a string which does not contain any isolated index. The number of linearly independent functions (2.11) is then exactly F_n.

Let us now detail the linear relation between cluster connectivities and spin correlators. The latter admit the FK clusters expansion,

$$G_{\alpha_1\dots\alpha_n}(x_1,\dots,x_n)=\frac{v^{|E(\mathcal{L})|}}{Z_{Potts}}{\sum_{\{s(x)\}}}'\sum_{\mathcal{G}\subseteq\mathcal{L}}p^{|E(\mathcal{G})|}(1-p)^{|E(\mathcal{L})-E(\mathcal{G})|}\prod_{i=1}^{n}\left(q\delta_{s(x_i),\alpha_i}-1\right), \tag{2.13}$$

where the prime on the first sum means that sites belonging to the same FK cluster are forced to have the same color s. Notice that, if one of the points x_i is isolated from the others in a cluster of a given graph $\mathcal{G}$, then the sum over its colors gives zero due to (2.10); hence, consistently with our previous analysis, (2.13) receives a contribution only from partitions of the sites x_i's into clusters containing at least two of these sites. If $P_{a_1\dots a_n}(x_1,\dots,x_n)$ is the probability of such a partition, then the number of distinct clusters will be $m<n$, and to any pair (x_i,α_i) we can associate one of the distinct letters $c_1,\dots,c_m$ chosen among the a_i's. The coefficient of $P_{a_1\dots a_n}$ in the expansion (2.13) is then[7]

$$\frac{1}{q^m}\sum_{s_1=1}^{q}\prod_{x_i\subset c_1}\left(q\delta_{s_1,\alpha_i}-1\right)\cdots\sum_{s_m=1}^{q}\prod_{x_i\subset c_m}\left(q\delta_{s_m,\alpha_i}-1\right); \tag{2.14}$$

the notation $x_i\subset c$ means that to the point x_i is associated the letter c (x belongs to the cluster c). For $n=2,3$ the dimensionality of correlation spaces is $F_2=F_3=1$ and (2.14) gives

$$G_{\alpha\alpha} = q_1\,P_{aa}\,, \tag{2.15}$$

$$G_{\alpha\alpha\alpha} = q_1q_2\,P_{aaa}\,, \tag{2.16}$$

[6]We can have strings with $m-1$ or $m-2$ isolated indices.

[7]The prefactor $1/q^m$ ensures the correct probability measure for the graph $\mathcal{G}$.

where we introduced the notation

$$q_k \equiv q - k\,. \tag{2.17}$$

The first relation with a matrix form appears at the four-point level ($F_4 = 4$), for which (2.14) leads to

$$G_{\alpha\alpha\alpha\alpha} = q_1(q^2 - 3q + 3)P_{aaaa} + q_1^2(P_{aabb} + P_{abba} + P_{abab}), \tag{2.18}$$

$$G_{\alpha\alpha\beta\beta} = (2q - 3)P_{aaaa} + q_1^2 P_{aabb} + P_{abba} + P_{abab}, \tag{2.19}$$

$$G_{\alpha\beta\beta\alpha} = (2q - 3)P_{aaaa} + P_{aabb} + q_1^2 P_{abba} + P_{abab}, \tag{2.20}$$

$$G_{\alpha\beta\alpha\beta} = (2q - 3)P_{aaaa} + P_{aabb} + P_{abba} + q_1^2 P_{abab}. \tag{2.21}$$

The last set of equations, as well as those one obtains for $n > 4$, can be inverted to express the connectivities in terms of the spin correlators, making clear that all the F_n nonequivalent and independent spin correlators are necessary to determine the connectivities of the random cluster model. On the other hand, a number $M_n(q) \leq F_n$ of these spin correlators determine the magnetic correlations in the Potts model at q integer. This is due to the fact that the spin correlators are themselves the magnetic observables, and that for q integer some of them vanish (e.g. $G_{\alpha\alpha\ldots\alpha}(x_1, \ldots, x_n)$ at $q = 2$, n odd, see (2.16)), those involving more than q colors are meaningless in the magnetic context, and additional linear relations may hold at specific values[8] of q. The numerical sequences $M_n(q)$ are determined in Appendix B for $q = 2, 3, 4$ (the case $q = 2$ is of course trivial); the first few values are given in Table 2.1 and plots are shown in Fig. 2.1. It is interesting, in

[8] For example the relation $3G_{\alpha\alpha\alpha\alpha} = 2(G_{\alpha\beta\beta\alpha} + G_{\alpha\beta\alpha\beta} + G_{\alpha\alpha\beta\beta})$ holds specifically at $q = 3$ and the system of equations (19)–(22) is no longer invertible. More generally, we expect that the $F_n \times F_n$ matrix $T_n(q)$ giving the spin correlators in terms of the "basic" connectivities (given explicitly by (2.15), (2.16) and (2.18)–(2.21) for $n = 2, 3, 4$) has determinant

$$\det(T_n) = q^{a_n}(q-1)\prod_{k=2}^{n-1}(q-k)^{d_n(k)}\,, \tag{2.22}$$

with $d_n(k) = \sum_{j=1}^{k}\tilde{S}(n,j) - M_n(k)$, $\tilde{S}(n,j)$ being the generalized Stirling numbers discussed in Appendix A, and a_n determined by the requirement that the total degree of the polynomial (2.22) is $D_n = \sum_{k=1}^{n}(n-k)\tilde{S}(n,k)$, as follows examining (2.14). $d_n(k)$ is the difference between the number of magnetically meaningful correlators at $q = k$ and the number $M_n(k)$ of those which are linearly independent; it follows from (2.126) and (2.139) that $d_n(k) = 0$ for $k \geq n$. We checked (2.22) up to $n = 5$.

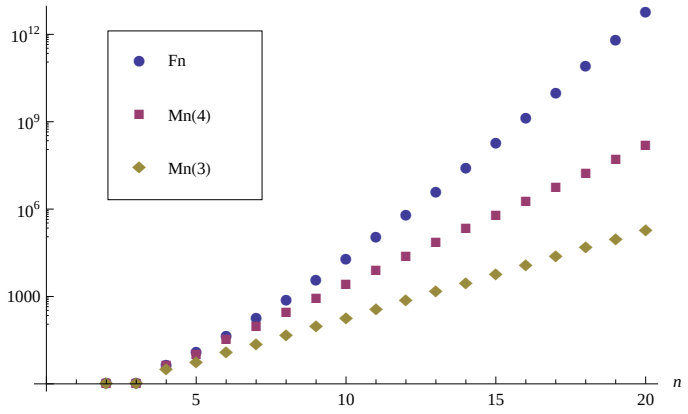

Figure 2.1: Plots of the first 20 values of the sequences F_n (number of independent n-point spin correlators for q real) and $M_n(q)$ (number of independent n-point spin correlators in the magnetic sector) for $q = 3, 4$.

particular, to compare the large n behavior of the dimensionalities of the magnetic and percolative correlation spaces. Defining

$$M_n(q) \overset{n\gg 1}{\sim} \mathrm{e}^{n s_q(n)}, \tag{2.23}$$

(2.133) and (2.138) give $s_q(n) = \log(q-1)$, a result which can be consistently interpreted as a kind of entropy for the Potts spin σ_α and is expected to hold for any integer $q > 1$. F_n exhibits instead the super-exponential growth [47]

$$F_n \overset{n\gg 1}{\sim} \mathrm{e}^{n s(n)}, \tag{2.24}$$

$$s(n) = \log n - \log\log n - 1 + \frac{\log\log n}{\log n} + O\left(\frac{1}{\log n}\right). \tag{2.25}$$

2.2.3 Scaling limit and correlators of kink fields

For $q \leq q_c$, i.e. when the phase transition is continuous, the Potts field theory describes the scaling limit $J \to J_c$ of the Potts model, with the spin variables $\sigma_\alpha(x)$ playing the role of fundamental fields (x is now a point in Euclidean space). In particular, the q degenerate ferromagnetic ground states which the Potts model possesses above J_c correspond in the scaling limit to degenerate vacua of the

Potts field theory. In the two-dimensional case the kinks interpolating between a vacuum with color α and one with color β are topologically stable and provide the elementary excitations of the spontaneously broken phase[9]; they are created by the kink fields $\mu_{\alpha\beta}(x)$, which are non-local with respect to the spin fields σ_α. The products of kink fields are subject to the adjacency condition $\mu_{\alpha\beta}(x)\mu_{\beta\gamma}(y)$. Duality relates, in a way to be investigated in the next sections, the kink field correlators in the broken phase

$$\tilde{G}_{\beta_1\dots\beta_n}(x_1,\dots,x_n) = \langle \mu_{\beta_1\beta_2}(x_1)\mu_{\beta_2\beta_3}(x_2)\dots\mu_{\beta_n\beta_1}(x_n)\rangle_{J\geq J_c} \tag{2.26}$$

to the spin correlators in the symmetric phase (2.11). Consistency of the duality relation requires that the number of S_q-nonequivalent correlators (2.26) coincides again with F_n. We now show that this is indeed the case.

Consider to start with the string of kink fields $\mu_{\beta_1\beta_2}\mu_{\beta_2\beta_3}\dots\mu_{\beta_n\beta_{n+1}}$ and associate to it $n+1$ points P_i, $i=1,\dots,n+1$, on a line. Each point P_i has a color β_i which must differ from those of the adjacent points. Let us show first of all that the number C_{n+1} of S_q-nonequivalent colorations of the points P_i coincides with the Bell number B_n. If the adjacency condition is relaxed, the number of nonequivalent colorations of the $n+1$ points is B_{n+1}. The string will consist of $k+1$ substrings, each with a definite color different from those of the adjacent substrings, that we can think to separate by placing k domain walls between them; this can be done in $\binom{n}{k}$ ways. The $k+1$ substrings can be colored in C_{k+1} S_q-nonequivalent ways and we have

$$B_{n+1} = \sum_{k=0}^{n}\binom{n}{k}C_{k+1} \quad \forall n\geq 0. \tag{2.27}$$

Since $C_1 = 1$, the result $C_{n+1} = B_n$ then follows from (2.119) by induction.

The case we just discussed includes L_{n+1} nonequivalent colorations in which $\beta_1 = \beta_{n+1}$ (the case (2.26) we are actually interested in) and O_{n+1} nonequivalent colorations in which $\beta_1 \neq \beta_{n+1}$, i.e. $L_{n+1} + O_{n+1} = C_{n+1}$. On the other hand, if we start with n points having $\beta_1 \neq \beta_n$ and we add P_{n+1} with $\beta_{n+1} = \beta_1$, the number of nonequivalent colorations does not change, i.e. $L_{n+1} = O_n$. We then see that

$$L_{n+1} + L_{n+2} = C_{n+1} = B_n\,, \qquad \forall n\geq 0\,. \tag{2.28}$$

[9] See [48] for a lattice study of Potts kinks.

This relation, together with the initial condition $L_1 = 1$, can be used to generate the L_n's from the B_n's. Of course L_{n+1} is the number of nonequivalent correlators (2.26) we were looking for. Comparison of (2.28) with (2.124) then leads to the final identification $L_{n+1} = F_n$.

2.3 Operator product expansions

Generically the OPE of scalar fields $A_i(x)$ with scaling dimension X_i takes the form

$$\lim_{x_1 \to x_2} A_i(x_1) A_j(x_2) = \sum_m C_{ij}^m \frac{A_m(x_2)}{x_{12}^{X_i + X_j - X_m}} , \tag{2.29}$$

where we include for simplicity only scalar fields in the r.h.s. and use the notation $x_{ij} \equiv |x_i - x_j|$; in the following we will replace (2.29) by the symbolic notation

$$A_i \cdot A_j = \sum_m C_{ij}^m A_m . \tag{2.30}$$

The nature of the fields $\mu_{\alpha\beta}(x)$ naturally leads to the two-channel OPE [17]

$$\mu_{\alpha\beta} \cdot \mu_{\beta\gamma} = \delta_{\alpha\gamma} \tilde{I} + (1 - \delta_{\alpha\gamma})(C_\mu \mu_{\alpha\gamma} + \ldots) , \tag{2.31}$$

where the neutral channel $\alpha = \gamma$ contains the expansion $\tilde{I} = I + C_\varepsilon \varepsilon + \ldots$ over S_q-invariant fields (identity I, energy ε, and so on), and the charged channel $\alpha \neq \gamma$ the expansion over $\mu_{\alpha\gamma}$ and less relevant kink fields; C_ε and C_μ are simplified notations for the OPE coefficients, for which exact expressions for continuous q have been given in [17].

The fields $\mu_{\alpha\beta}(x)$ are expected to be related to the disorder fields $\mu_\alpha(x)$ by the linear transformation

$$\mu_\alpha(x) = \sum_\sigma C_\alpha^{\rho\sigma} \mu_{\rho\sigma}(x) , \tag{2.32}$$

where $C_\alpha^{\rho\sigma} \in \mathbb{C}$ are coefficients[10] to be investigated below, and ρ-independence is a consequence of permutational symmetry. The field μ_α carries the same representation of permutational symmetry as σ_α (in particular, $\sum_{\alpha=1}^q \mu_\alpha = 0$) but,

[10] No confusion should arise with the OPE coefficients C_{ij}^m of (2.29).

as $\mu_{\alpha\beta}$, it is non-local with respect to σ_α. In other words, σ_α and μ_α are identical (dual) fields living in mutually non-local sectors of the theory; in particular they share the same scaling dimension and the same OPE. Mutual non-locality reflects in the fact that, while $\langle\sigma_\alpha\rangle \neq 0$ for $J > J_c$, $\langle\mu_\alpha\rangle \neq 0$ for $J < J_c$. More precisely, in view of the coinciding scaling dimension, it is sufficient to adopt the same normalization of the fields to ensure that $\langle\sigma_\alpha\rangle_J = \langle\mu_\alpha\rangle_{J^*}$, where J^* is the dual[11] of J. The duality extends to multi-point functions, in such a way that the spin correlators (2.11) can also be written as

$$G_{\alpha_1\dots\alpha_n}(x_1,\dots,x_n) = \langle\mu_{\alpha_1}(x_1)\dots\mu_{\alpha_n}(x_n)\rangle_{J^*\geq J_c}\,. \tag{2.33}$$

The rest of this section is devoted to investigate the relation (2.32) and to determine the structure of the OPE $\mu_\alpha\cdot\mu_\beta$ (or, equivalently, $\sigma_\alpha\cdot\sigma_\beta$).

The q degenerate vacua of the Potts model above J_c can be associated to the vertices of an hypertetrahedron in $q-1$ dimensions whose $q(q-1)$ oriented sides are associated to the kink fields $\mu_{\alpha\beta}$. Permutational symmetry of the vacua allows to group these fields into classes $\tilde{\mu}_i$, $i = 1,\dots,q-1$, each containing q kink fields starting from different vacua, in such a way that choosing a vacuum amounts to select $q-1$ kink fields, one from each class, starting from that vacuum and arriving at the other vacua (Fig. 2.2). Ignoring structure constants, the OPE (31) has the form of a multiplication between elements of a finite group. Independence from the choice of the starting vacuum of the kinks ensures that the elements of this finite group are the classes $\tilde{\mu}_i$, $i = 1,\dots,q-1$, together with the topologically neutral class $\tilde{I}$. We denote then by K_q their fusion table as prescribed by (31), as well as the finite group of order q it defines. The symmetry also ensures that all the rows of the matrix C_α can be obtained from the first by regular permutations[12]. The relation (2.32) (which we could equivalently write as $\mu_\alpha = \sum_\rho C_\alpha^{\rho\sigma}\mu_{\rho\sigma}$) is effectively a sum over the $q-1$ classes $\tilde{\mu}_i$, as we now illustrate separately discussing the cases $q = 2, 3, 4$.

[11] In the scaling limit we consider, J and J^* are the points where the elementary excitations of the symmetric phase and those of the spontaneously broken phase have the same mass m; $m = 0$ at the self-dual point J_c.

[12] Permutations which do not leave any element invariant. It is not difficult to realize that such permutations are elements of K_q.

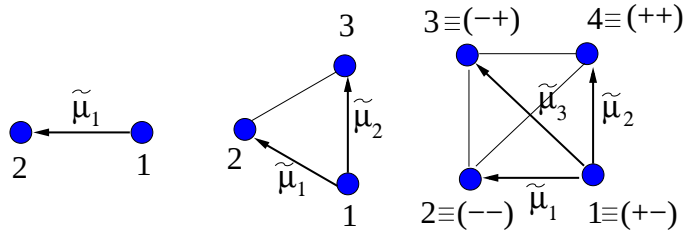

Figure 2.2: The vacua of the Potts field theory for $q = 2, 3, 4$ are labeled by $\alpha = 1, \ldots, q$ and denoted by dots (for $q = 4$ we use the Ashkin-Teller notation $\boldsymbol{\alpha} \equiv (\alpha_1, \alpha_2)$). Fixing a specific vacuum (1 in this case) amounts to choose a representative kink field within each class $\tilde{\mu}_i$ (see the text).

q=2. Permutational symmetry $S_2 = \mathbb{Z}_2$ implies the equivalence of the two kink fields μ_{12} and μ_{21}, which we collect in the class $\tilde{\mu}_1$; from (2.31) we derive $K_2 = \mathbb{Z}_2$ (see Fig. 2.3). We can choose

$$\mu_\alpha = \omega_2^\alpha \tilde{\mu}_1, \quad C_\alpha = \begin{pmatrix} 0 & \omega_2^\alpha \\ \omega_2^\alpha & 0 \end{pmatrix}, \quad \alpha = 1, 2\,, \tag{2.34}$$

with $\omega_q = \mathrm{e}^{2\pi i/q}$, in order to fulfill $\sum_\alpha \mu_\alpha = 0$ and consistently derive

$$\mu_\alpha \cdot \mu_\alpha = \tilde{I}, \tag{2.35}$$

$$\mu_\alpha \cdot \mu_\beta = -\tilde{I}\,, \qquad \alpha \neq \beta\,. \tag{2.36}$$

q=3. The OPE of the kink fields $\mu_{\alpha\beta}$ is equivalent to the fusion table of the classes $\tilde{\mu}_1, \tilde{\mu}_2$ and $\tilde{I}$. Being $\mathbb{Z}_3$ the only discrete group of order three, full consistency requires $K_3 = \mathbb{Z}_3$, together with the identifications $\tilde{\mu}_1 = \{\mu_{12}, \mu_{23}, \mu_{31}\}$, $\tilde{\mu}_2 = \{\mu_{13}, \mu_{21}, \mu_{32}\}$. Notice that $\mathrm{Aut}(\mathbb{Z}_3) = \mathbb{Z}_2$, and the non-trivial automorphism[13] corresponds to the charge conjugation operator $\mathcal{C}$, with $\mathcal{C}\tilde{\mu}_1 = \tilde{\mu}_2$. Using $\mu_\alpha(x) = 3\delta_{\tilde{s}(x),\alpha} - 1$, the charge conjugated operators realizing the $\mathbb{Z}_3$ OPE are identified with[14] $\tilde{\mu}_1 = \mathrm{e}^{2\pi i \tilde{s}(x)/3}$ and $\tilde{\mu}_2 = \mathrm{e}^{-2\pi i \tilde{s}(x)/3}$, where $\tilde{s}(x)$ is the dual color variable;

[13] Given a group G, $\phi : G \to G$ is an automorphism if $\phi(ab) = \phi(a)\phi(b), \forall a, b \in G$. The set of all the automorphisms with natural composition as a product form a group called $\mathrm{Aut}(G)$.

[14] The basis $\tilde{\mu}_1$, $\tilde{\mu}_2$ is that used in [49].

$\cdot$	$\tilde{I}$	$\tilde{\mu}_1$
$\tilde{I}$	$\tilde{I}$	$\tilde{\mu}_1$
$\tilde{\mu}_1$	$\tilde{\mu}_1$	$\tilde{I}$

$\cdot$	$\tilde{I}$	$\tilde{\mu}_1$	$\tilde{\mu}_2$
$\tilde{I}$	$\tilde{I}$	$\tilde{\mu}_1$	$\tilde{\mu}_2$
$\tilde{\mu}_1$	$\tilde{\mu}_1$	$\tilde{\mu}_2$	$\tilde{I}$
$\tilde{\mu}_2$	$\tilde{\mu}_2$	$\tilde{I}$	$\tilde{\mu}_1$

$\cdot$	$\tilde{I}$	$\tilde{\mu}_1$	$\tilde{\mu}_2$	$\tilde{\mu}_3$
$\tilde{I}$	$\tilde{I}$	$\tilde{\mu}_1$	$\tilde{\mu}_2$	$\tilde{\mu}_3$
$\tilde{\mu}_1$	$\tilde{\mu}_1$	$\tilde{I}$	$\tilde{\mu}_3$	$\tilde{\mu}_2$
$\tilde{\mu}_2$	$\tilde{\mu}_2$	$\tilde{\mu}_3$	$\tilde{I}$	$\tilde{\mu}_1$
$\tilde{\mu}_3$	$\tilde{\mu}_3$	$\tilde{\mu}_2$	$\tilde{\mu}_1$	$\tilde{I}$

Figure 2.3: Fusion tables K_q at $q = 2, 3, 4$. They correspond to the groups $\mathbb{Z}_2$, $\mathbb{Z}_3$ and D_2, respectively.

using also $\delta_{\tilde{s},\alpha} = \frac{1}{3}\sum_{\beta=1}^{3} \mathrm{e}^{\frac{2\pi i}{3}(\tilde{s}-\alpha)\beta}$ one obtains

$$\mu_\alpha = \omega_3^{-\alpha}\tilde{\mu}_1 + \omega_3^{\alpha}\tilde{\mu}_2, \quad C_\alpha = \begin{pmatrix} 0 & \omega_3^{-\alpha} & \omega_3^{\alpha} \\ \omega_3^{\alpha} & 0 & \omega_3^{-\alpha} \\ \omega_3^{-\alpha} & \omega_3^{\alpha} & 0 \end{pmatrix}, \quad \alpha = 1, 2, 3\,, \tag{2.37}$$

and then

$$\mu_\alpha \cdot \mu_\alpha = 2\tilde{I} + C_\mu\, \mu_\alpha + \dots, \tag{2.38}$$

$$\mu_\alpha \cdot \mu_\beta = -\tilde{I} - C_\mu(\mu_\alpha + \mu_\beta) + \dots\,, \qquad \alpha \neq \beta\,; \tag{2.39}$$

the relation $\omega_3^{\alpha} + \omega_3^{\beta} + \omega_3^{-(\alpha+\beta)} = 0$, $\alpha \neq \beta$, is used.

q=4. The four-state Potts model can be seen as the case $J = J_4$ of the Ashkin-Teller model defined by the Hamiltonian

$$\mathcal{H}_{AT} = -\sum_{\langle x,y\rangle}\{J[\tau_1(x)\tau_1(y) + \tau_2(x)\tau_2(y)] + J_4\,\tau_1(x)\tau_1(y)\tau_2(x)\tau_2(y)\}, \tag{2.40}$$

where $\tau_i = \pm 1$, $i = 1, 2$, are Ising variables. Defining $\boldsymbol{s} = (\tau_1, \tau_2)$, $\boldsymbol{\alpha} = (\alpha_1, \alpha_2)$, with $\alpha_i = \pm 1$, and $\delta_{\boldsymbol{s},\boldsymbol{\alpha}} = \delta_{\tau_1,\alpha_1}\delta_{\tau_2,\alpha_2}$, the Potts spin (2.9) can be written as

$$\sigma_{\boldsymbol{\alpha}} = 4\delta_{\boldsymbol{s},\boldsymbol{\alpha}} - 1 = \alpha_1\tau_1 + \alpha_2\tau_2 + \alpha_1\alpha_2\tau_1\tau_2. \tag{2.41}$$

The kink fields $\mu_{\boldsymbol{\alpha\beta}}$ interpolate between the four degenerate vacua of the two coupled Ising models (see e.g. [50]); the classes $\tilde{\mu}_1 = \{\mu_{12}, \mu_{21}, \mu_{34}, \mu_{43}\}$ and $\tilde{\mu}_2 = \{\mu_{14}, \mu_{41}, \mu_{23}, \mu_{32}\}$ are constructed in analogy to the case $q = 2$, the fields in $\tilde{\mu}_3 = \{\mu_{13}, \mu_{31}, \mu_{24}, \mu_{42}\}$ are instead obtained taking the OPE according to

(2.31) (see also Fig. 2.2). We derive $K_4 = D_2 = \mathbb{Z}_2 \times \mathbb{Z}_2$, see Fig. 2.3; notice that $\mathrm{Aut}(D_2) = S_3$. We can also take

$$\mu_{\boldsymbol{\alpha}} = \alpha_1\tilde{\mu}_1 + \alpha_2\tilde{\mu}_2 + \alpha_1\alpha_2\tilde{\mu}_3\,, \qquad C_{\boldsymbol{\alpha}} = \begin{pmatrix} 0 & \alpha_1 & \alpha_1\alpha_2 & \alpha_2 \\ \alpha_1 & 0 & \alpha_2 & \alpha_1\alpha_2 \\ \alpha_1\alpha_2 & \alpha_2 & 0 & \alpha_1 \\ \alpha_2 & \alpha_1\alpha_2 & \alpha_1 & 0 \end{pmatrix}, \tag{2.42}$$

from which we obtain

$$\mu_{\boldsymbol{\alpha}} \cdot \mu_{\boldsymbol{\alpha}} = 3\tilde{I} + 2C_\mu\, \mu_{\boldsymbol{\alpha}} + \dots\,, \tag{2.43}$$

$$\mu_{\boldsymbol{\alpha}} \cdot \mu_{\boldsymbol{\beta}} = -\tilde{I} - C_\mu(\mu_{\boldsymbol{\alpha}} + \mu_{\boldsymbol{\beta}}) + \dots\,, \qquad \alpha \neq \beta\,. \tag{2.44}$$

It is interesting to remark some formal properties emerging from this analysis. We see that, by construction, K_q at $q = 2, 3, 4$ is a finite abelian group of order q, i.e. by Cayley theorem a regular abelian subgroup[15] of S_q. K_q must also be invariant under permutations of the $q-1$ classes $\tilde{\mu}_i$, an operation which corresponds to fix one vacuum and permute the remaining $q-1$. Formally this amounts to write $\mathrm{Aut}(K_q) = S_{q-1}$, and we expect the full symmetry group of the theory to be realized as[16]

$$S_q = K_q \rtimes S_{q-1}\,. \tag{2.45}$$

This in turn implies the possibility of writing S_q as a semidirect product of abelian subgroups of the form

$$S_q = K_q \rtimes K_{q-1} \rtimes \dots K_2, \quad K_2 = \mathbb{Z}_2, \tag{2.46}$$

a property which is equivalent to the solvability of the permutational group. More precisely[17], the solvability of S_q would imply the existence of the factorization (2.46), as indeed remarkably happens at $q = 2, 3, 4$, with $K_2 = \mathbb{Z}_2$, $K_3 = \mathbb{Z}_3$, $K_4 = D_2$ and $\mathrm{Aut}(\mathbb{Z}_3) = \mathbb{Z}_2$, $\mathrm{Aut}(D_2) = S_3$. It is well known [52], however,

[15] The classes $\tilde{\mu}_i$ are associated to the regular permutations π_i, $i = 1, \dots, q-1$, of S_q as $\tilde{\mu}_i = \{\mu_{1\pi_i(1)}, \dots, \mu_{q\pi_i(q)}\}$. Without loss of generality one can assume $\pi_i(1) = i + 1$.

[16] The presence of the semidirect product $\rtimes$ is due to the fact that S_{q-1} is not a normal subgroup of S_q.

[17] We thank C. Casolo for this observation. Interesting remarks about solvable groups and lattice duality can be found in [51].

that for $q > 4$ S_q possesses no abelian normal subgroup, making impossible in particular to realize the condition (2.45). Then S_q is not solvable for any $q > 4$, a circumstance which is interesting to compare with the fact that $q_c = 4$ is also the upper bound for the existence of the Potts field theory in the two-dimensional case, i.e. the only case for which kink fields exist and the above construction is possible.

A remarkable feature appearing from (2.36), (2.39) and (2.44) is that $\mu_\alpha \cdot \mu_{\beta\neq\alpha}$ is identical at $q = 2, 3, 4$ (recall that $\mu_1 + \mu_2 = 0$ at $q = 2$). It is then absolutely natural to assume that this form actually holds unchanged for continuous values of q, and to write

$$\sigma_\alpha \cdot \sigma_\beta = -I - C_\mu(\sigma_\alpha + \sigma_\beta) + \dots , \qquad \alpha \neq \beta, \tag{2.47}$$

where the dots correspond to less relevant fields and we switched to the equivalent expression in terms of the spin fields for a reason to be made immediately clear. On the other hand, the complementary relation

$$\sigma_\alpha \cdot \sigma_\alpha = q_1\, I + q_2 C_\mu\, \sigma_\alpha + \cdots \tag{2.48}$$

follows observing that (2.10) and (2.47) give

$$\begin{aligned} 0 = \sigma_\alpha \cdot \sum_\beta \sigma_\beta &= \sigma_\alpha \cdot \sigma_\alpha + \sum_{\beta\neq\alpha} \sigma_\alpha \cdot \sigma_\beta \\ &= \sigma_\alpha \cdot \sigma_\alpha + \sum_{\beta\neq\alpha} [-I - C_\mu(\sigma_\alpha + \sigma_\beta) + \dots] \; ; \end{aligned}$$

(2.48) is of course consistent with (2.35), (2.38) and (2.43). While the disorder fields $\mu_\alpha(x)$ are specific of the two-dimensional case, the spin fields $\sigma_\alpha(x)$ are well defined in any dimension. It is then quite obvious to expect that (2.47) and (2.48) hold for real values of $q \leq q_c$ in any dimension.

The linear relation (2.10) among the spin fields induces a relation less direct than usual between the OPE coefficients and the structure constants appearing in the three-point functions. In general, the structure constants C_{ijk} are defined by the critical correlators

$$\langle A_i(x_1) A_j(x_2) A_k(x_3) \rangle = \frac{C_{ijk}}{x_{12}^{X_i+X_j-X_k}\, x_{13}^{X_i+X_k-X_j}\, x_{23}^{X_j+X_k-X_i}} \; ; \tag{2.49}$$

taking the limits $x_{12} \to 0$ and $x_{23} \to 0$ and using (2.29), C_{ijk} is expressed in term of the OPE coefficients as

$$C_{ijk} = \sum_{X_m = X_k} C_{ij}^m C_{mk}^I \,. \tag{2.50}$$

We then find

$$C_{\sigma_\alpha \sigma_\alpha \sigma_\alpha} = q_2 q_1 C_\mu, \tag{2.51}$$

$$C_{\sigma_\alpha \sigma_\alpha \sigma_\beta} = C_{\sigma_\alpha \sigma_\beta \sigma_\alpha} = C_{\sigma_\beta \sigma_\alpha \sigma_\alpha} = -q_2 C_\mu, \tag{2.52}$$

$$C_{\sigma_\alpha \sigma_\beta \sigma_\gamma} = 2 C_\mu \,, \tag{2.53}$$

with different indices denoting different colors.

2.4 Duality relations

Equations (2.32) and (2.33) imply a linear relation between the spin correlators (2.11) in the symmetric phase and the correlators (2.26) of kink fields in the broken phase. This duality takes the form

$$\begin{aligned} G_{\alpha_1 \dots \alpha_n}(x_1, \dots, x_n) &= \sum_{\beta_1, \dots, \beta_n} \tilde{D}^{\beta_1 \dots \beta_n}_{\alpha_1 \dots \alpha_n} \tilde{G}_{\beta_1 \dots \beta_n}(x_1, \dots, x_n) \\ &= \sum_{\beta_1, \dots, \beta_n}{}' \Big(\prod_{i=1}^{n_c(\boldsymbol{\beta})-1} q_i \Big) \, D^{\beta_1 \dots \beta_n}_{\alpha_1 \dots \alpha_n} \tilde{G}_{\beta_1 \dots \beta_n}(x_1, \dots, x_n) \,, \end{aligned} \tag{2.54}$$

where the primed sum runs over all choices of $\boldsymbol{\beta} = \{\beta_1, \dots, \beta_n\}$ which are nonequivalent under permutations, $n_c(\boldsymbol{\beta})$ is the number of different colors in $\boldsymbol{\beta}$, and the factors q_i have been extracted for later convenience. The task is that of determining the coefficients $D^{\beta_1 \dots \beta_n}_{\alpha_1 \dots \alpha_n}$, for continuous values of q; of course it is sufficient to consider a set of F_n linearly independent spin correlators. We will discuss explicitly this problem up to the first case with $F_n > 1$, i.e. $n = 4$.

n=1. The trivial identity $\langle \sigma_\alpha \rangle = \langle \mu_{\alpha\beta} \rangle = 0$ simply reflects the fact that we consider spin correlators in the symmetric phase[18], and that $\mu_{\alpha\beta}$ is a kink field.

[18]Since this is understood, here and in the following we omit the subscripts $J \leq J_c$ for spin correlators and $J \geq J_c$ for kink field correlators.

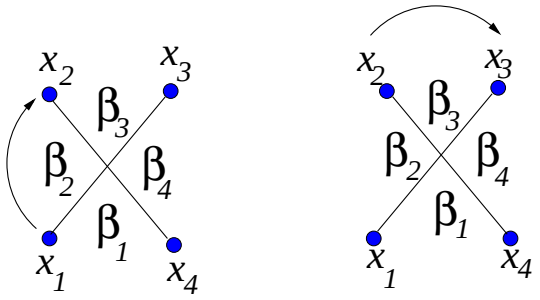

Figure 2.4: Pictorial representation of the four-point correlation functions of kink fields $\tilde{G}_{\beta_1\beta_2\beta_3\beta_4}(x_1,\ldots,x_4)$. The two pinchings $x_1 \to x_2$ and $x_2 \to x_3$ used for the study of the duality relation (2.57) are indicated.

n=2. $F_2 = 1$ and we consider

$$\langle \sigma_\alpha(x_1)\sigma_\alpha(x_2)\rangle = q_1 D^{\alpha\beta}_{\alpha\alpha}\ \langle \mu_{\alpha\beta}(x_1)\mu_{\beta\alpha}(x_2)\rangle\,. \tag{2.55}$$

We can take the limit $x_{12} \to 0$ on both sides and equate the coefficients of the leading singularity $x_{12}^{-2X_\sigma}$, which are obtained using (2.48) and (2.31). This immediately yields $D^{\alpha\beta}_{\alpha\alpha} = 1$.

n=3. $F_3 = 1$ and we consider

$$\langle \sigma_\alpha(x_1)\sigma_\alpha(x_2)\sigma_\alpha(x_3)\rangle = q_1 q_2 D^{\alpha\beta\gamma}_{\alpha\alpha\alpha}\ \langle \mu_{\alpha\beta}(x_1)\mu_{\beta\gamma}(x_2)\mu_{\gamma\alpha}(x_3)\rangle\,. \tag{2.56}$$

We can again use the OPE's to take the limit $x_{12} \to 0$ on both sides and reduce[19] to (2.55); this leads to $D^{\alpha\beta\gamma}_{\alpha\alpha\alpha} = 1$.

n=4. We will consider the $F_4 = 4$ linearly independent spin correlators (2.18–

[19] Notice that the OPE on the l.h.s. apparently produces singularities from the S_q-invariant operators $\mathcal{O}_k$ in $\tilde{I}$ which do not arise in the r.h.s., where $\alpha \neq \gamma$. Everything is consistent, however, since $\langle \mathcal{O}_k \sigma_\alpha\rangle = 0$ by symmetry.

2.21), which expand as

$$\begin{aligned}\langle\sigma_{\alpha_1}(x_1)\sigma_{\alpha_2}(x_2)\sigma_{\alpha_3}(x_3)\sigma_{\alpha_4}(x_4)\rangle = q_1q_2q_3D^{\alpha\beta\gamma\delta}_{\alpha_1\alpha_2\alpha_3\alpha_4}\langle\mu_{\alpha\beta}(x_1)\mu_{\beta\gamma}(x_2)\mu_{\gamma\delta}(x_3)\mu_{\delta\alpha}(x_4)\rangle \\ +q_1q_2D^{\alpha\beta\gamma\beta}_{\alpha_1\alpha_2\alpha_3\alpha_4}\ \langle\mu_{\alpha\beta}(x_1)\mu_{\beta\gamma}(x_2)\mu_{\gamma\beta}(x_3)\mu_{\beta\alpha}(x_4)\rangle \\ +q_1q_2D^{\alpha\beta\alpha\gamma}_{\alpha_1\alpha_2\alpha_3\alpha_4}\ \langle\mu_{\alpha\beta}(x_1)\mu_{\beta\alpha}(x_2)\mu_{\alpha\gamma}(x_3)\mu_{\gamma\alpha}(x_4)\rangle \\ +q_1D^{\alpha\beta\alpha\beta}_{\alpha_1\alpha_2\alpha_3\alpha_4}\ \langle\mu_{\alpha\beta}(x_1)\mu_{\beta\alpha}(x_2)\mu_{\alpha\beta}(x_3)\mu_{\beta\alpha}(x_4)\rangle\,.\end{aligned} \tag{2.57}$$

We start again equating the coefficients of the short distance singularities on the two sides. However, an important difference with the cases $n < 4$ now appears. Indeed, while the OPE in the l.h.s. can be taken for any pair of points x_i and x_j, the kink nature of the fields on the r.h.s. allows us to use (2.31) only for adjacent fields. In other words, we can compare only the singularities arising for $x_{12} \to 0$ and $x_{23} \to 0$ (see Fig. 2.4; $x_{34} \to 0$ and $x_{14} \to 0$ add nothing new). Equating the coefficients of the singularities in the "neutral" and "charged" channels, and using the duality relations already obtained for $n = 2, 3$, leads to the following sets of equations

$$\begin{cases} D^{\alpha\beta\alpha\gamma}_{\alpha\alpha\alpha\alpha} = D^{\alpha\beta\gamma\beta}_{\alpha\alpha\alpha\alpha} \\ q_2 = q_3D^{\alpha\beta\gamma\delta}_{\alpha\alpha\alpha\alpha} + D^{\alpha\beta\gamma\beta}_{\alpha\alpha\alpha\alpha} \\ q_1 = q_2D^{\alpha\beta\gamma\beta}_{\alpha\alpha\alpha\alpha} + D^{\alpha\beta\alpha\beta}_{\alpha\alpha\alpha\alpha} \end{cases} \qquad \begin{cases} D^{\alpha\beta\alpha\gamma}_{\alpha\beta\alpha\beta} = D^{\alpha\beta\gamma\beta}_{\alpha\beta\alpha\beta} \\ 2 = q_1q_3D^{\alpha\beta\gamma\delta}_{\alpha\beta\alpha\beta} + q_1D^{\alpha\beta\gamma\beta}_{\alpha\beta\alpha\beta} \\ 1 = q_1q_2D^{\alpha\beta\gamma\beta}_{\alpha\beta\alpha\beta} + q_1D^{\alpha\beta\alpha\beta}_{\alpha\beta\alpha\beta} \end{cases} \tag{2.58}$$

$$\begin{cases} 1 = q_1q_2D^{\alpha\beta\gamma\beta}_{\alpha\alpha\beta\beta} + q_1D^{\alpha\beta\alpha\beta}_{\alpha\alpha\beta\beta} \\ 2 = q_1q_3D^{\alpha\beta\gamma\delta}_{\alpha\alpha\beta\beta} + q_1D^{\alpha\beta\alpha\gamma}_{\alpha\alpha\beta\beta} \\ q_1 = q_2D^{\alpha\beta\alpha\gamma}_{\alpha\alpha\beta\beta} + D^{\alpha\beta\alpha\beta}_{\alpha\alpha\beta\beta} \end{cases} \qquad \begin{cases} 1 = q_1q_2D^{\alpha\beta\alpha\gamma}_{\alpha\beta\beta\alpha} + q_1D^{\alpha\beta\alpha\beta}_{\alpha\beta\beta\alpha} \\ 2 = q_1q_3D^{\alpha\beta\gamma\delta}_{\alpha\beta\beta\alpha} + q_1D^{\alpha\beta\gamma\beta}_{\alpha\beta\beta\alpha} \\ q_1 = q_2D^{\alpha\beta\gamma\beta}_{\alpha\beta\beta\alpha} + D^{\alpha\beta\alpha\beta}_{\alpha\beta\beta\alpha} \end{cases} \tag{2.59}$$

where different indices denote different colors. Notice that the method produces four equations for each correlation function (two per pinching and per channel), but only three turn out to be independent. Since each duality relation (2.57) involves four coefficients, the above equations are not sufficient to fix everything. We now show how the duality for the correlators $G_{\alpha\alpha\alpha\alpha}$, $G_{\alpha\alpha\beta\beta}$, $G_{\alpha\beta\beta\alpha}$ can be completely determined exploiting also the relations (2.32), (2.33).

The matrices C_α defined in (2.32) are Hermitian, due to the presence of the antilinear charge conjugation operator $\mathcal{C}$, with $\mathcal{C}^2 = I$, $\mathcal{C}\mu_{\rho\sigma}\mathcal{C} = \mu_{\sigma\rho}$, $\mathcal{C}\mu_\alpha\mathcal{C} = \mu_\alpha$ and $\mathcal{C}C_\alpha^{\rho\sigma}\mathcal{C} = (C_\alpha^{\rho\sigma})^*$. They also satisfy $C_\alpha^{\rho\rho} = 0$, $\rho = 1, \ldots, q$, and $\sum_\alpha C_\alpha = 0$. Other properties follow requiring the consistency of the OPE's for the kink fields and for the dual spin μ_α. For example,

$$\mu_\alpha \cdot \mu_\alpha = \sum_{\sigma,\omega} C_\alpha^{\rho\sigma} C_\alpha^{\sigma\omega} \mu_{\rho\sigma} \cdot \mu_{\sigma\omega} \tag{2.60}$$

$$= \Big(\sum_{\sigma\neq\rho} C_\alpha^{\rho\sigma} C_\alpha^{\sigma\rho} \Big) \tilde{I} + \sum_{\omega\neq\rho} \Big(\sum_{\sigma\neq\rho,\omega} C_\alpha^{\rho\sigma} C_\alpha^{\sigma\omega} \Big) \big[C_\mu \mu_{\rho\omega} + \ldots \big] \,; \tag{2.61}$$

comparing with (2.48) we obtain the matrix relation

$$C_\alpha^2 = q_1 I + q_2 C_\alpha \,. \tag{2.62}$$

Analogously, from (2.47) we derive

$$C_\alpha C_\beta = -I - (C_\alpha + C_\beta) \,, \qquad \alpha \neq \beta \,, \tag{2.63}$$

which implies in particular $[C_\alpha, C_\beta] = 0$. Hence, the set of q Hermitian matrices C_α can be simultaneously diagonalized by a unitary transformation U and put in the form

$$C_\alpha^{\rho\sigma}|_{\rm diag} = (q\delta_{\alpha\rho} - 1)\delta_{\rho\sigma} \,, \tag{2.64}$$

which follows from the observation that the C_α's are traceless, sum to zero and, due to (2.62), have -1 and q_1 as only eigenvalues. It is also simple to check that

$$\langle \mu_\alpha \mu_\alpha \rangle = \frac{1}{q} {\rm Tr}\, C_\alpha^2 \; \langle \mu_{\alpha\beta} \mu_{\beta\alpha} \rangle = q_1 \langle \mu_{\alpha\beta} \mu_{\beta\alpha} \rangle \,, \tag{2.65}$$

$$\langle \mu_\alpha \mu_\alpha \mu_\alpha \rangle = \frac{1}{q} {\rm Tr}\, C_\alpha^3 \; \langle \mu_{\alpha\beta} \mu_{\beta\gamma} \mu_{\gamma\alpha} \rangle = q_2 q_1 \langle \mu_{\alpha\beta} \mu_{\beta\gamma} \mu_{\gamma\alpha} \rangle \,, \tag{2.66}$$

in agreement with (2.55), (2.56). Starting from the diagonal form (2.64) and the existence of the unitary matrix U it is possible to show (see Appendix C) that

$$C_\alpha^{\rho\sigma} = {\rm e}^{i(\varphi_{\alpha\sigma} - \varphi_{\alpha\rho})} - \delta_{\rho\sigma}, \tag{2.67}$$

where the phases $\varphi_{\alpha\rho}$ must satisfy the equation[20]

$$\frac{1}{q}\sum_{\rho=1}^{q} \mathrm{e}^{i(\varphi_{\alpha\rho}-\varphi_{\beta\rho})} = \delta_{\alpha\beta}\,. \tag{2.68}$$

We can now notice that (2.32), (2.33) and (2.54) imply

$$q_1 D^{\alpha\beta\alpha\beta}_{\alpha_1\alpha_2\alpha_3\alpha_4} = \frac{1}{q}\sum_{\rho,\sigma} C^{\rho\sigma}_{\alpha_1} C^{\sigma\rho}_{\alpha_2} C^{\rho\sigma}_{\alpha_3} C^{\sigma\rho}_{\alpha_4}\,; \tag{2.69}$$

using $|C^{\rho\sigma}_{\alpha}| = 1-\delta_{\rho\sigma}$ and hermiticity $C^{\sigma\rho}_{\alpha} = (C^{\rho\sigma}_{\alpha})^*$ we obtain $D^{\alpha\beta\alpha\beta}_{\alpha\alpha\alpha\alpha} = D^{\alpha\beta\alpha\beta}_{\alpha\alpha\beta\beta} = D^{\alpha\beta\alpha\beta}_{\alpha\beta\beta\alpha} = 1$, independently of the phases $\varphi_{\alpha\beta}$. With this information, (2.58) and (2.59) determine the remaining coefficients, giving

$$G_{\alpha\alpha\alpha\alpha} = q_1q_2q_3\,\tilde{G}_{\alpha\beta\gamma\delta} + q_1q_2\,\left(G_{\alpha\beta\gamma\beta} + \tilde{G}_{\alpha\beta\alpha\gamma}\right) + q_1\,\tilde{G}_{\alpha\beta\alpha\beta}, \tag{2.70}$$

$$G_{\alpha\alpha\beta\beta} = -q_2q_3\,\tilde{G}_{\alpha\beta\gamma\delta} - q_2\,\tilde{G}_{\alpha\beta\gamma\beta} + q_1q_2\,\tilde{G}_{\alpha\beta\alpha\gamma} + q_1\,\tilde{G}_{\alpha\beta\alpha\beta}, \tag{2.71}$$

$$G_{\alpha\beta\beta\alpha} = -q_2q_3\,\tilde{G}_{\alpha\beta\gamma\delta} + q_1q_2\,\tilde{G}_{\alpha\beta\gamma\beta} - q_2\,\tilde{G}_{\alpha\beta\alpha\gamma} + q_1\,\tilde{G}_{\alpha\beta\alpha\beta}, \tag{2.72}$$

with different indices denoting different colors.

The problem with the remaining correlator $G_{\alpha\beta\alpha\beta}$ is that (2.69) does not help, because the phases do not cancel, and we are left with the three equations coming from the OPE for four unknowns.

2.5 The boundary case

Since the OPE's for the kink and spin fields reflect local properties of the field theory, the duality relations obtained in the previous section hold true also in the case in which the points $x_1,\ldots,x_n$ in (2.54), instead of being located on the infinite plane, lie inside a simply connected domain $L \subset \mathbb{R}^2$. Actually, the duality relations continue to hold also in the case the points $x_1,\ldots,x_n$ are located on the boundary of L, simply because the OPE's (2.31), (2.47) and (2.48), whose structure is completely determined by the symmetry, can be used also for points

[20]The properties of matrices C_α we obtain in this section do not refer to any specific value of q. Of course they are satisfied by the matrices that we already determined in the previous section for $q = 2, 3, 4$.

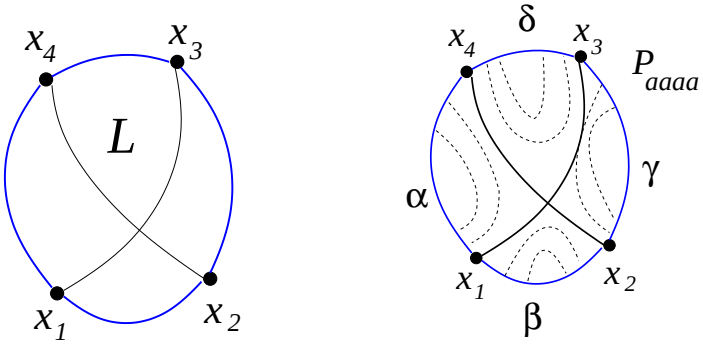

Figure 2.5: Four-point boundary correlations on a simply connected domain L. *Left.* Clusters connecting x_1 to x_3 and x_2 to x_4 necessarily cross and cannot be distinct. *Right.* Dashed lines represent allowed clusters in the FK representation on the dual lattice $\mathcal{L}^*$; continuous lines correspond to clusters on $\mathcal{L}$ connecting all the four points. In the continuum limit $\mathcal{L}$, $\mathcal{L}^*$ and L coincide.

on the boundary, provided bulk OPE coefficients and scaling dimensions are replaced by boundary OPE coefficients and scaling dimensions. It is not difficult to see, however, that having the points on the boundary rather than in the bulk may reduce the number of linearly independent correlation functions. The first interesting case, that we now discuss, arises for $n = 4$.

Let us order the points $x_1, \ldots, x_4$ on the boundary as shown in Fig. 2.5. Since in this boundary case a cluster containing x_1 and x_3 must necessarily cross a cluster containing x_2 and x_4, the probability $P_{abab}(x_1, x_2, x_3, x_4)$ that these two pairs of points belong to two different clusters necessarily vanishes. This topological constraint reduces to three the number of linearly independent boundary spin correlators (we denote them with a superscript B); indeed, inverting (2.18)–(2.21) and setting $P_{abab} = 0$ gives[21]

$$q_1(q^2 - 3q + 1)G^B_{\alpha\beta\alpha\beta} - (2q - 3)G^B_{\alpha\alpha\alpha\alpha} + q_1(G^B_{\alpha\alpha\beta\beta} + G^B_{\alpha\beta\beta\alpha}) = 0\,. \qquad (2.73)$$

Using the duality relations (2.70), (2.71), (2.72) and the OPE equations (2.58)

[21] Different greek indices in eqs. (2.73–2.81) denote different colors.

for $G_{\alpha\beta\alpha\beta}$, (2.73) can be rewritten as

$$\left[1+q_1(q^2-3q+1)D^{\alpha\beta\alpha\beta}_{\alpha\beta\alpha\beta}\right]\left(\tilde{G}^B_{\alpha\beta\alpha\beta}+\tilde{G}^B_{\alpha\beta\gamma\delta}-\tilde{G}^B_{\alpha\beta\alpha\gamma}-\tilde{G}^B_{\alpha\beta\gamma\beta}\right)=0\,, \qquad (2.74)$$

or, in view of the reduction in the number of independent correlators , as the linear relation[22]

$$\tilde{G}^B_{\alpha\beta\alpha\beta}+\tilde{G}^B_{\alpha\beta\gamma\delta}=\tilde{G}^B_{\alpha\beta\alpha\gamma}+\tilde{G}^B_{\alpha\beta\gamma\beta}. \qquad (2.75)$$

Using this equation to eliminate $\tilde{G}^B_{\alpha\beta\alpha\beta}$ in (2.70), (2.71) and (2.72), the duality for boundary correlators is fully determined as

$$G^B_{\alpha\alpha\alpha\alpha}=q_1(q_2q_3-1)\tilde{G}^B_{\alpha\beta\gamma\delta}+q_1^2(\tilde{G}^B_{\alpha\beta\gamma\beta}+\tilde{G}^B_{\alpha\beta\alpha\gamma}), \qquad (2.76)$$

$$G^B_{\alpha\alpha\beta\beta}=(2q_2-q_1^2)\tilde{G}^B_{\alpha\beta\gamma\delta}+\tilde{G}^B_{\alpha\beta\gamma\beta}+q_1^2\tilde{G}^B_{\alpha\beta\alpha\gamma}, \qquad (2.77)$$

$$G^B_{\alpha\beta\beta\alpha}=(2q_2-q_1^2)\tilde{G}^B_{\alpha\beta\gamma\delta}+q_1^2\tilde{G}^B_{\alpha\beta\gamma\beta}+\tilde{G}^B_{\alpha\beta\alpha\gamma}. \qquad (2.78)$$

Substituting in (2.18)–(2.21) with $P_{abab}=0$ one also obtains for the boundary connectivities the simple relations

$$P^B_{aaaa}=\tilde{G}^B_{\alpha\beta\gamma\delta}, \qquad (2.79)$$

$$P^B_{aabb}=\tilde{G}^B_{\alpha\beta\alpha\gamma}-\tilde{G}^B_{\alpha\beta\gamma\delta}, \qquad (2.80)$$

$$P^B_{abba}=\tilde{G}^B_{\alpha\beta\gamma\beta}-\tilde{G}^B_{\alpha\beta\gamma\delta}. \qquad (2.81)$$

Equation (2.79) can be interpreted as follows in the language of lattice duality. If we interpret the insertion of a kink field on the boundary as creating a domain wall along the boundary of the dual lattice $\mathcal{L}^*$, the correlator $\tilde{G}^B_{\alpha\beta\gamma\delta}$ corresponds to a partition of the boundary into four regions with different colors and will receive contributions only from graphs on $\mathcal{L}^*$ without FK clusters connecting different regions. Equation (2.79) then means that these graphs are in one-to-one correspondence with the graphs on $\mathcal{L}$ in which the four boundary points all belong to the same FK cluster (see Fig. 2.5)). Similar reasoning can be used for (2.80) and (2.81).

[22]Duality for boundary correlators of the q-color Potts model on the lattice was studied in [53, 54, 55], where dual partition functions with domain wall boundary conditions correspond to our kink field boundary correlators $\tilde{G}^B_{\alpha_1\alpha_2,\ldots}$; with this identification, the relation (2.75) is contained in [55]. Potts partition functions on a non-simply connected domain have been studied in [56]. An early investigation of Potts correlation functions is in [57].

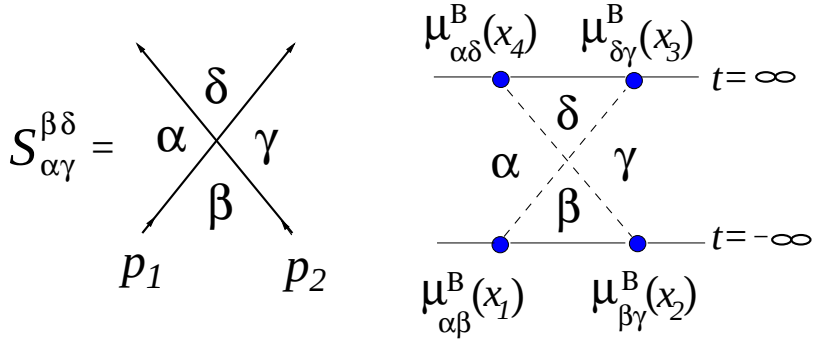

Figure 2.6: The elastic kink-kink scattering amplitudes $S^{\beta\delta}_{\alpha\gamma}(s)$ (left) are related by the LSZ formalism to the four-point correlation functions $\tilde{G}^B_{\alpha\beta\gamma\delta}$ of the asymptotic fields $\mu^B_{\alpha\beta}(x)$ (right).

We conclude this section observing that (2.75) leads to a linear relation among the elastic kink-kink scattering amplitudes in the $(1+1)$-dimensional field theory associated by Wick rotation to the Euclidean theory on the plane. In this case, indeed, the boundary fields $\mu^B_{\alpha\beta}(x)$ entering (2.75) can be interpreted as the asymptotic fields which create a kink excitation $K_{\alpha\beta}$ at time $t \to \pm\infty$ (Fig. 2.6). The kink-kink elastic amplitudes

$$S^{\beta\delta}_{\alpha\gamma}(s) = {}_{\rm out}\langle K_{\alpha\delta}(p_4)K_{\delta\gamma}(p_3)|K_{\alpha\beta}(p_1)K_{\beta\gamma}(p_2)\rangle_{\rm in}\,, \tag{2.82}$$

where the square of the center of mass energy $s = (p_1+p_2)^2_\mu$ is the only relativistic invariant for this $(1+1)$-dimensional process[23], can be written within the LSZ formalism (see e.g. [58]) as

$$\begin{aligned} S^{\beta\delta}_{\alpha\gamma}(s) = \lim_{t_1,t_2\to-\infty}\ \lim_{t_3,t_4\to+\infty} \int {\rm d}x_1 \ldots \int {\rm d}x_4\ {\rm e}^{ip_4\cdot x_4}{\rm e}^{ip_3\cdot x_3}{\rm e}^{-ip_1\cdot x_1}{\rm e}^{-ip_2\cdot x_2} \\ \overleftrightarrow{\partial_{t_4}}\,\overleftrightarrow{\partial_{t_3}}\,\overleftrightarrow{\partial_{t_2}}\,\overleftrightarrow{\partial_{t_1}}\,\langle \mu^B_{\alpha\beta}(x_1,t_1)\mu^B_{\beta\gamma}(x_2,t_2)\mu^B_{\gamma\delta}(x_3,t_3)\mu^B_{\delta\alpha}(x_4,t_4)\rangle\,, \end{aligned} \tag{2.83}$$

where the integrals are taken along the one-dimensional space coordinate and $\overleftrightarrow{\partial_t}$ is defined by $A\overleftrightarrow{\partial_t}B = A(\partial_t B) - (\partial_t A)B$. Equation (2.75) then leads to

$$S^{\beta\delta}_{\alpha\gamma}(s) + S^{\beta\beta}_{\alpha\alpha}(s) = S^{\beta\beta}_{\alpha\gamma}(s) + S^{\beta\gamma}_{\alpha\alpha}(s)\,, \tag{2.84}$$

[23]The relativistic invariant s can be written as $2m^2(1+\cosh(\theta_1-\theta_2))$ where θ_i, $i=1,2$ are the rapidities we will introduce in section 2.6.

where different indices denote different colors. This relation was already found in [27] as a byproduct of the Yang-Baxter equations, i.e. of the integrability of the scaling limit of the q-color Potts model. Here integrability, which is the subject of the final sections of this chapter, does not appear to play a role, and then (2.84) should hold also for non-minimal, non-integrable realizations of the symmetry, if they exist. Ultimately, the vanishing of the probability that the trajectories of two particles do not cross in the $(1+1)$-dimensional space-time relates amplitudes which would be independent on the basis of color symmetry alone.

2.6 Integrable field theories in $1+1$ dimensions

Consider the $1+1$ dimensional Minkowsky space-time with coordinate (t, x) and diagonal metric $\mathrm{diag}(1, -1)$. The proper Lorentz group $\mathcal{L}_+$ consists of boosts along the x axis. A generic boost is an hyperbolic rotation $\Lambda(\eta)$ with rapidity[24] η. Since $\mathcal{L}_+$ is abelian its irreducible representations, labeled by an index s, are one-dimensional. The characters[25] $\chi_s(\eta)$ then coincide with the matrices of the representation and must satisfy $\chi_s(\eta)\chi_s(\theta) = \chi_s(\eta+\theta)$, from which $\chi_s(\eta) = \mathrm{e}^{s\eta}$. We require s rational to obtain only multi-valued[26] representations of the rotational group in two dimensions after the analytic continuation $\eta \to i\phi$. A field $\Phi_s(x,t)$ transforming according to the s irreducible representation under the boost $\Lambda(\eta)$

$$\Phi'_s(x',t') = \mathrm{e}^{s\eta}\Phi_s(x,t) \tag{2.85}$$

is a Lorentz tensor with spin s. For example the light cone momenta $P_\pm = E \pm p$ are Lorentz tensors with spin ± 1 respectively and the components T_{++}, T_{--}, T_{+-} and T_{-+} of the stress energy tensor are Lorentz tensors with spin 2, -2 and zero. Introduce the Euclidean time $t = iy$ and the complex coordinates $z = x + iy$,

[24] For example for a particle at rest with two-momentum $P = (m, 0)$, $\Lambda(\eta)P = (m\cosh\eta, m\sinh\eta)$.

[25] $\chi_s(\eta)$ is a shorthand notation for $\chi_s(\Lambda(\eta))$.

[26] Irrational Lorentz spins would give infinite-valued representations of the two-dimensional rotational group under the analytic continuation $\eta \to i\phi$.

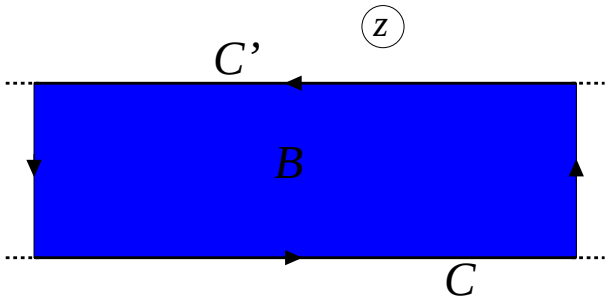

Figure 2.7: If we call B the area of the rectangle then by Stokes theorem $\int_C A_\mu dx^\mu + \int_{C'} A_\mu dx^\mu = \int_B d^2x\ \varepsilon^{\mu\nu}\partial_\mu A_\nu$. Where we have assumed that the field A^μ is vanishing at $x = \pm\infty$. Using complex coordinates and the conservation law (2.86) one can show that the line integral in (2.87) is a constant.

$\bar{z} = x - iy$. Given the classical conservation law[27]

$$\bar{\partial} T_{s-1} = \partial \Theta_{s+1}, \tag{2.86}$$

a classical conserved charge Q_s of spin s is obtained as the line integral see Fig. 2.7

$$Q_s = \int_C dz\ T_{s-1} + \int_C d\bar{z}\ \Theta_{s+1}. \tag{2.87}$$

We will call a quantum field theory integrable [14, 15] if it possesses an infinite number of conserved charges (operators on an Hilbert space) Q_s which are local and in involution, i.e. $[Q_s, Q'_{s'}] = 0$. Locality is encoded in the fact that charges act diagonally on the one-particle states of the field theory. One-particle states $|\theta\rangle_a$ are labeled by their rapidity[28] θ and by their internal quantum numbers a.

[27] In complex coordinate let $A^z = A^x + iA^y$ and $A^{\bar{z}} = A^x - iA^y$ be the components with spin $s = 1$ and -1 of an irrotational current $\partial_\mu \varepsilon^{\mu\nu} A_\nu = 0$. Notice that the dual field $\tilde{A}^\mu = \varepsilon^{\mu\nu} A_\nu$ has zero divergence. The irrotationality condition reads $\partial A^z = \bar{\partial} A^{\bar{z}}$. Lowering the indices we define $A \equiv A_z = g_{z\bar{z}} A^{\bar{z}}$, $\bar{A} \equiv A_{\bar{z}} = g_{\bar{z}z} A^z$, with the off-diagonal matrix of section 1.2. The expression (2.87) then follows from the application of Stokes theorem.

[28] The energy and momentum of a particle of mass m and rapidity θ are $(E, p) = (m\cosh\theta, m\sinh\theta)$

The states are normalized as

$$ {}_b\langle\theta'|\theta\rangle_a = 2\pi\delta_{ab}\delta(\theta-\theta'). \tag{2.88}$$

Lorentz invariance[29] fixes also

$$ Q_s|\theta\rangle_a = \mathrm{e}^{s\theta}\rho_s^a|\theta\rangle_a, \tag{2.89}$$

with ρ_s^a a constant. For example $\rho_{\pm 1}^a = m_a$, the mass of the particle a for $Q_{\pm 1} = P_{\pm}$. A massive[30] quantum field theory is defined by its asymptotic Hilbert spaces H_{in} and H_{out}. The asymptotic n-particle *in* states are collections of non-interacting particles at $t = -\infty$ of the form

$$ |\theta_1\theta_2\ldots\theta_n\rangle^{in}_{a_1\ldots a_n}, \quad \theta_1 > \theta_2 \cdots > \theta_n. \tag{2.90}$$

The asymptotic n-particle *out* states are collections of non-interacting particles at $t = \infty$ of the form

$$ |\theta_1\theta_2\ldots\theta_n\rangle^{out}_{a_1\ldots a_n}, \quad \theta_1 < \theta_2 \cdots < \theta_n. \tag{2.91}$$

The n-particle asymptotic states are eigenvectors of the quantum field theory conserved charges Q_s

$$ Q_s|\theta_1\theta_2\ldots\theta_n\rangle^{in,out}_{a_1\ldots a_n} = \Big(\sum_{i=1}^{n}\mathrm{e}^{s\theta_i}\rho_s^{a_i}\Big)|\theta_1\theta_2\ldots\theta_n\rangle^{in,out}_{a_1\ldots a_n}. \tag{2.92}$$

The linear operator mapping the Hilbert space H_{out} into the Hilbert space H_{in} is the S matrix

$$ S : H_{out} \to H_{in}. \tag{2.93}$$

The S matrix is a Lorentz scalar. In an integrable quantum field theory (IQFT) the dynamics of the scattering processes must conserve the additive charges Q_s. In particular

[29] Let U_η be the unitary operator representing the boost $\Lambda(\eta)$ on the Hilbert space. Then $U_\eta Q_s U_\eta^{-1} = \mathrm{e}^{-s\eta}Q_s$. If we assume $Q_s|\theta\rangle = f_s(\theta)|\theta\rangle$, then $f_s(\theta+\eta)\mathrm{e}^{-s\eta} = f_s(\theta)$ and the result follows taking $\theta = 0$.

[30] We avoid complications in the definition of the asymptotic Hilbert spaces for massless field theories.

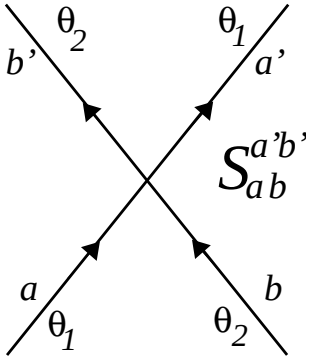

Figure 2.8: Pictorial representation of the two-particle S matrix element $S_{ab}^{a'b'}(\theta_{12})$. Time is flowing in the direction of the arrows.

- The number of particles in the *in* state before the scattering coincides with the number of particles in the *out* state after the scattering. No particles production is possible.
- The set of rapidities in the *in* state before the scattering coincides with the set of rapidities in the *out* state after the scattering. Internal quantum numbers between *in* and *out* states can be different.
- The scattering is factorized and multi-particle scattering processes can be expressed as sequences of two-particle scattering processes.

In an IQFT, the solution of the scattering problem is reduced to the computation of the two-particle S matrix elements, see Fig. 2.8

$$|\theta_1\theta_2\rangle_{ab}^{in} = \sum_{a',b'} S_{ab}^{a'b'}(\theta_1 - \theta_2)|\theta_2\theta_1\rangle_{b'a'}^{out}. \tag{2.94}$$

The two-particle S matrix element is a meromorphic function of the rapidity difference $\theta_{12} = \theta_1 - \theta_2$ and satisfies the requirements of

- *Unitarity*

$$\sum_{a',b'} S_{ab}^{a'b'}(\theta_{12}) S_{a'b'}^{a''b''}(-\theta_{12}) = \delta_a^{a''}\delta_b^{b''}. \tag{2.95}$$

- *Crossing symmetry*

$$S_{ab}^{a'b'}(\theta_{12}) = S_{\bar{b}'a}^{\bar{b}a'}(i\pi - \theta), \tag{2.96}$$

  where $\bar{b}$ is a set of quantum numbers obtained from the set b, applying the charge conjugation operator $\mathcal{C}$.

The S matrix is also invariant under parity $S_{ab}^{a'b'}(\theta_{12}) = S_{ba}^{b'a'}(\theta_{12})$ and time-reverse $S_{ab}^{a'b'}(\theta_{12}) = S_{a'b'}^{ab}(\theta_{12})$. Factorization of the scattering processes is encoded in the Yang-Baxter relations

$$\sum_{a',b',c'} S_{ab}^{a'b'}(\theta_{12}) S_{a'c}^{a''c'}(\theta_{13}) S_{b'c'}^{b''c''}(\theta_{23}) = \sum_{a',b',c'} S_{bc}^{b'c'}(\theta_{23}) S_{ac'}^{a'c''}(\theta_{13}) S_{a'b'}^{a''b''}(\theta_{12}). \tag{2.97}$$

If the two-particle S matrix element $S_{ab}^{a'b'}(\theta_{12})$ has poles on the imaginary rapidity axis, they are interpreted as bound states arising in the scattering of the a particle with the b particle. Suppose

$$S_{ab}^{a'b'}(\theta_{12}) \sim \frac{i\big(\Gamma_{ab}^{c}\big)^2}{\theta_{12} - iu_{ab}^{c}}, \quad \Gamma_{ab}^{c} \in \mathbb{R} \tag{2.98}$$

for $\theta_{12} \to iu_{ab}^{c}$ and $u_{ab}^{c} \in \mathbb{R}$. The particle c has mass fixed by the conservation of the two-momentum and given by $m_c^2 = m_a^2 + m_b^2 - 2m_a m_b \cos \bar{u}_{ab}^{c}$, with the angle[31] $\bar{u}_{ab}^{c} = \pi - u_{ab}^{c}$. The unitarity and crossing relations must then be supplemented by the bootstrap equation

$$\Gamma_{ab}^{c}\ S_{dc}^{ef}(\theta) = \sum_{i,j,h} \Gamma_{hj}^{f}\ S_{da}^{ih}(\theta - i\bar{u}_{a\bar{c}}^{\bar{b}}) S_{ib}^{ej}(\theta + i\bar{u}_{b\bar{c}}^{\bar{a}}). \tag{2.99}$$

2.7 Exact solution of the Potts q-color field theory in two dimensions

The Euclidean action describing fluctuations of Potts observables out of criticality in the scaling limit is

$$\mathcal{A}_{scaling} = \mathcal{A}_{CFT} + \tau \int d^2x\ \varepsilon(x), \tag{2.100}$$

[31] The masses m_a, m_b and m_c can be visualized as sides of a triangle of external angles u_{ab}^{c}, u_{ac}^{b} and u_{bc}^{a}.

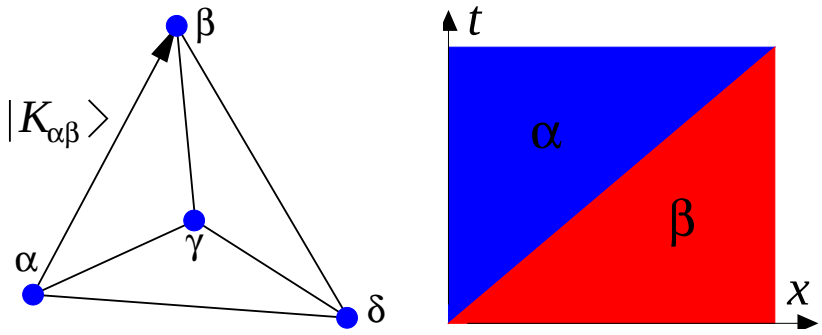

Figure 2.9: *Left.* In the phase of broken S_q symmetry the different vacua can be visualized as the vertices of an hypertetrahedron in $q-1$ dimensions. Kinks correspond to the sides of the hypertetrahedron. *Right.* A pictorial representation of the kink $|K_{\alpha\beta}\rangle$ interpolating between the vacuum $|\Omega_\beta\rangle$ with color β and the vacuum $|\Omega_\alpha\rangle$ with color α.

where $\mathcal{A}_{CFT}$ is the conformal invariant Potts action and $\tau \sim \frac{J-J_c}{J_c}$. The scaling action (2.100) describes the renormalization group trajectories generated by the most relevant field invariant under S_q transformations, i.e. the energy density $\varepsilon(x)$. We will assume $\tau > 0$ and consider the phase in which S_q symmetry is spontaneously broken. The quantum field theory is massive and associated to a finite correlation length. The field $\varepsilon(x)$ is the field $\phi_{2,1}$ in the Kac notation of chapter 1 and, as shown by Zamoldchikov counting argument [59], (2.100) is integrable.

In the phase of broken S_q symmetry the field theory vacua set $\{|\Omega_\alpha\rangle\}$, $\alpha = 1,\dots,q$ can be associated to the set of vertices of an hypertetrahedron in $q-1$ dimensions, see Fig. 2.9. Lowest mass excitations[32] are kinks $|K_{\alpha\beta}\rangle$ interpolating between the vacua $|\Omega_\alpha\rangle$ and $|\Omega_\beta\rangle$ and they correspond to the oriented sides of the hypertetrahedron. The kink $|K_{\alpha\beta}\rangle$ describes the propagation of a domain wall in the statistical mechanics model separating the ferromagnetic phases[33] α and β.

[32] It is understood that when discussing the scattering theory we work in the $1+1$ dimensional Minkowsky space-time.

[33] The phase α is the phase in which the symmetry is broken in the direction α. For $J > J_c$ the phase α is obtained fixing the boundary spins $s(x) = \alpha$ and then taking the thermodynamic

Multiparticle asymptotic kink states are subject to adjacency rules. For example an *in* n-kink state is of the form

$$|K_{\alpha_1\alpha_2}(\theta_1)K_{\alpha_2\alpha_2}(\theta_2)\dots K_{\alpha_n\alpha_{n+1}}(\theta_n)\rangle \tag{2.101}$$

with the rapidities ordered in decreasing order and $\alpha_i \neq \alpha_{i+1}$. Kinks $|K_{\alpha\beta}\rangle$ are interpolated by the kink fields $\mu_{\alpha\beta}(x,t)$ and the one-kink form factor

$$F^{\mu_{\alpha\beta}}_{\beta\alpha} = \langle\Omega_\alpha|\mu_{\alpha\beta}(0,0)|K_{\beta\alpha}(\theta)\rangle \tag{2.102}$$

is non-zero[34].

We will come back later on the properties of the two-kink form factors of a neutral[35] operator $\Phi(x,t)$. Before discussing the scattering theory of the action (2.100) it is interesting to note that the existence of kink fields in two dimensions is connected with the presence of invariant (normal) subgroups of the symmetry group G of the field theory[36]. In the broken phase the group G acts on the set of vacua $V = \{v_1, v_2, \dots, v_n\}$ through its permutation representation. The number[37] of disorder fields is the number of elements of the orbit[38] of a vacuum v_i, $|G(v_i)|$, and we can assume the action transitive i.e. $G(v_i) = V$. Kink fields are associated, in principle not uniquely, to some group elements h^i_α such that G can be decomposed into the left cosets[39]

$$G = G_{v_i} \cup h^i_1\, G_{v_i} \cup \dots \cup h^i_{n-1}\, G_{v_i} \quad \forall i = 1 \dots n, \tag{2.103}$$

limit.

[34]By Lorentz invariance (2.102) does not depend on θ.

[35]An operator is neutral if it does not carry a topological charge. In this case it couples with n-kink states such that the color of the initial and final vacua are equal.

[36]This completes the discussion in section 2.3 of the previous chapter where we argued that the symmetry group S_q acting on the vacua of the q-color Potts model in the broken phase factorizes in presence of kink fields as $K_q \rtimes S_{q-1}$. The finite group of q elements K_q corresponds to the invariant group H, describing the composition rules of the kinks and S_{q-1} is the stabilizer of a given vacuum.

[37]The idea of associating kink (disorder) fields in two dimensions to elements of the symmetry group G is also present in [49] .

[38]The orbit $G(v_i)$ is the set of elements of V which can be obtained from v_i applying transformations $g \in G$.

[39]This is the content of the orbit-stabilizer theorem [52] and the elements h^i_α are elements of G such that $h^i_\alpha(v_i) = v_{i'}$, $i \neq i'$.

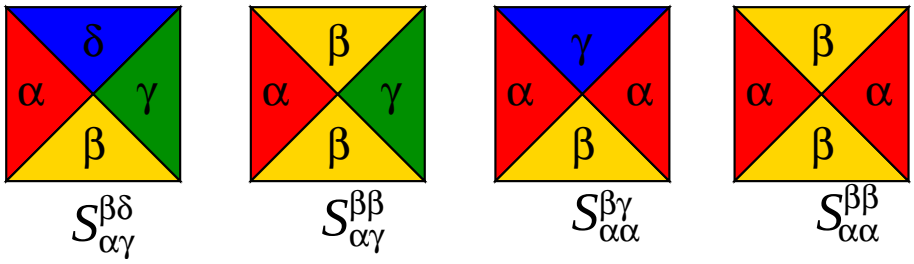

Figure 2.10: The four permutational nonequivalent two-kink S matrix amplitudes.

where G_{v_i} is the stabilizer[40] of v_i under the action of G. Since there exists $g \in G$ such that $G_{v_j} = g^{-1}\ G_{v_i}\ g$ we also have

$$g^{-1}\ G\ g = G_{v_j} \cup (g^{-1} h_1^i\ g) G_{v_j} \cup \cdots \cup (g^{-1}\ h_{n-1}^i\ g)\ G_{v_j}. \tag{2.104}$$

Requiring independence of the h_α^i from the vacuum indices in (2.103) and (2.104), amounts to the condition $g^{-1} h_\alpha^i\ g = h_\beta^j$. This is satisfied in particular if all the elements h_α^i can be chosen in an invariant subgroup $H \subset G$ of n elements including the identity.

Coming back to the discussion of the scattering theory, S_q symmetry restricts to four the number of independent two-kink S matrix amplitudes defined as

$$|K_{\alpha\beta}(\theta_1) K_{\beta\gamma}(\theta_2)\rangle_{in} = \sum_\delta S^{\beta\delta}_{\alpha\gamma}(\theta_1 - \theta_2) |K_{\alpha\delta}(\theta_2) K_{\delta\gamma}(\theta_1)\rangle_{out}. \tag{2.105}$$

They are shown in Fig. 2.10. Below we reproduce their analytic form, found by Chim and Zamoldchikov [27] solving the unitarity, crossing and boostrap constraints. Let q be parameterized as $\sqrt{q} = 2 \sin \frac{\pi\lambda}{3}$ and introduce

$$\Pi\Big(\frac{\lambda\theta}{i\pi}\Big) = \frac{\sin\lambda(\theta + i\pi/3)}{\sin\lambda(\theta - i\pi)} \mathrm{e}^{\mathcal{A}(\theta)}, \tag{2.106}$$

with the integral representation for $\mathcal{A}(\theta)$

$$\mathcal{A}(\theta) = \int_0^\infty \frac{dx}{x}\ \frac{\sinh\frac{x}{2}\big(1 - \frac{1}{\lambda}\big) - \sinh\frac{x}{2}\big(\frac{1}{\lambda} - \frac{5}{3}\big)}{\sinh\frac{x}{2\lambda}\cosh\frac{x}{2}}. \tag{2.107}$$

[40] The stabilizer of v_i $G_{v_i} = \{g \in G \text{ s.t. } g(v_i) = v_i\}$.

The four two-kink S matrix amplitudes are given by[41]

$$S^{\beta\delta}_{\alpha\gamma}(\theta) = \frac{\sinh\lambda\theta\sinh\lambda(\theta-i\pi)}{\sinh\lambda\big(\theta-\frac{2\pi i}{3}\big)\sinh\lambda\big(\theta-\frac{i\pi}{3}\big)}\;\Pi\Big(\frac{\lambda\theta}{i\pi}\Big) \tag{2.108}$$

$$S^{\beta\beta}_{\alpha\gamma}(\theta) = \frac{\sin\frac{2\pi\lambda}{3}\sinh\lambda(\theta-i\pi)}{\sin\frac{\pi\lambda}{3}\sinh\lambda\big(\theta-\frac{2\pi i}{3}\big)}\;\Pi\Big(\frac{\lambda\theta}{i\pi}\Big) \tag{2.109}$$

$$S^{\beta\gamma}_{\alpha\alpha}(\theta) = \frac{\sin\frac{2\pi\lambda}{3}\sinh\lambda\theta}{\sin\frac{\pi\lambda}{3}\sin\lambda\big(\theta-\frac{i\pi}{3}\big)}\;\Pi\Big(\frac{\lambda\theta}{i\pi}\Big) \tag{2.110}$$

$$S^{\beta\beta}_{\alpha\alpha}(\theta) = \frac{\sin\pi\lambda}{\sin\frac{\pi\lambda}{3}}\;\Pi\Big(\frac{\lambda\theta}{i\pi}\Big). \tag{2.111}$$

The final part of this section is a brief review of the properties of the two-kink form factors

$$\langle\Omega_\alpha|\Phi(0,0)|K_{\alpha\beta}(\theta_1)K_{\beta\gamma}(\theta_2)\rangle \equiv F^\Phi_{\alpha\beta\gamma}(\theta_2-\theta_1). \tag{2.112}$$

Form factors [60, 61] arise in the Kallen-Lehmann spectral representation of correlation functions in field theory. The two-point function of the neutral operator Φ in the q-color Potts field theory decomposes as

$$\langle\Omega_\alpha|\Phi(x,t)\Phi(0,0)|\Omega_\alpha\rangle = \tag{2.113}$$

$$\sum_{n=0}^{\infty}\sum_{\alpha_1,\ldots,\alpha_{n-1}}\int_{\theta_1>\theta_2>\cdots>\theta_n}\frac{d\theta_1}{2\pi}\cdots\frac{d\theta_n}{2\pi}\;\mathrm{e}^{mit\sum_{j=0}^n\cosh\theta_j - mix\sum_{j=0}^n\sinh\theta_j}|F^\Phi_{\alpha\ldots\alpha_{n-1}\alpha}|^2, \tag{2.114}$$

where

$$F^\Phi_{\alpha\ldots\alpha_{n-1}\alpha}(\theta_1,\ldots,\theta_n) = \langle\Omega_\alpha|\Phi(0,0)|K_{\alpha\alpha_1}(\theta_1)\ldots K_{\alpha_{n-1}\alpha}(\theta_n)\rangle. \tag{2.115}$$

The two-kink form factors of a neutral operator Φ satisfy the functional relations [62]

$$F^\Phi_{\alpha\beta\alpha}(\theta) = \sum_\gamma S^{\beta\gamma}_{\alpha\alpha}(\theta)F^\Phi_{\alpha\gamma\beta}(-\theta) \tag{2.116}$$

$$F^\Phi_{\alpha\beta\alpha}(\theta) = F^\Phi_{\beta\alpha\beta}(2i\pi-\theta) \tag{2.117}$$

[41] Different indices denote different vacua.

supplemented by the normalization condition of the residue

$$\mathrm{Res}_{\theta=i\pi} F^{\Phi}_{\alpha\beta\alpha}(\theta) = i\big(\langle\Phi\rangle_\alpha - \langle\Phi\rangle_\beta\big). \tag{2.118}$$

Two-kink form factors are known at arbitrary $q \in (0,4]$ for the thermal operator ε and for integer $q = 1,2,3,4$ for the order parameter σ_α in (1.48), see [62] and [18].

Appendix A

Given a set S of n elements the number of partitions of the elements of S is the Bell number B_n (see Table 2.1 for $n \leq 10$). The most straightforward way to compute the Bell numbers is through the recursive relation

$$B_n = \sum_{k=0}^{n-1} \binom{n-1}{k} B_k, \quad B_0 \equiv 1, \tag{2.119}$$

which is easily proved observing that we can fix one element of the set S and consider the partitions in which this element appears with k other elements, $k = 0, \ldots, n-1$. The number of such partitions will be

$$\binom{n-1}{k} B_{n-1-k}\,; \tag{2.120}$$

then summing over k and using $\binom{n-1}{k} = \binom{n-1}{n-1-k}$ we obtain (2.119).

We similarly define the numbers F_n as

$$B_n = \sum_{k=0}^{n} \binom{n}{k} F_k, \quad F_0 \equiv 1. \tag{2.121}$$

F_n is the number of partitions of S whose blocks contain at least two elements. The proof is again elementary (see e.g. [63]). We divide all the B_n partitions of S into those containing exactly $k = 0, 1, \ldots, n$ isolated elements, and then we take partitions of the remaining $n-k$ elements in such way that no element is isolated. It is clear that we end up with (2.121).

Recalling the combinatorial identity $\binom{n+1}{k} = \binom{n}{k} + \binom{n}{k-1}$, expression (87) implies

$$B_{n+1} - B_n = \sum_{k=0}^{n} \binom{n}{k} F_{k+1}\,. \tag{2.122}$$

On the other hand, (2.119) gives $B_{n+1} = \sum_{k=0}^{n} \binom{n}{k} B_k$, and using (2.121) we derive

$$\sum_{k=0}^{n} \binom{n}{k} (F_{k+1} + F_k - B_k) = 0 \quad \forall n \geq 0\,. \tag{2.123}$$

By induction we finally obtain[42]

$$B_n = F_n + F_{n+1}\,. \tag{2.124}$$

The number of k-partitions (partitions into k non-empty subsets) of a set of n elements is the Stirling number $S(n,k)$. It satisfies $B_n = \sum_{k=1}^{n} S(n,k)$ from its definition, as well as the recursive equation

$$S(n,k) = k\,S(n-1,k) + S(n-1,k-1), \qquad n \geq k, \quad k \geq 1\,, \tag{2.125}$$

from the fact that we can obtain a k-partition of the set $\{x_1, \ldots, x_n\}$ adding x_n to one of the k blocks of a k-partition of the elements $\{x_1, \ldots, x_{n-1}\}$, or joining x_n as a single block to a $(k-1)$-partition of $\{x_1, \ldots, x_{n-1}\}$. The exponential generating function $\mathcal{S}_k(x) = \sum_{n \geq k} S(n,k) \frac{x^n}{n!}$ satisfies $\mathcal{S}_k'(x) = k\mathcal{S}_k(x) + \mathcal{S}_{k-1}(x)$, and is given by $\mathcal{S}_k(x) = \frac{1}{k!}(\mathrm{e}^x - 1)^k$. We also introduce the generalized Stirling number $\tilde{S}(n,k)$ as the number of k-partitions of a set of n elements whose blocks contain at least two elements (non-singleton k-partition); the relation

$$F_n = \sum_{k=1}^{n-1} \tilde{S}(n,k) \tag{2.126}$$

then expresses the decomposition of the total number of independent n-point spin correlation functions (which we take without isolated indices) into subsets with indices of k different colors. Non-singleton k-partitions of the set $\{x_1, \ldots, x_n\}$ are obtained adding x_n to one of the k blocks of a non-singleton k-partition of $\{x_1, \ldots, x_{n-1}\}$, or by joining the block $\{x_n, x_j\}$, for $j = 1, \ldots, n-1$, to a non-singleton $(k-1)$-partition of $\{x_1, \ldots, x_{j-1}, x_{j+1}, \ldots, x_{n-1}\}$. We have then

$$\tilde{S}(n,k) = k\tilde{S}(n-1,k) + (n-1)\tilde{S}(n-2,k-1), \quad n \geq k,\ k \geq 1. \tag{2.127}$$

The exponential generating function is $\tilde{\mathcal{S}}_k(x) = \frac{1}{k!}(\mathrm{e}^x - 1 - x)^k$ and solves $\tilde{\mathcal{S}}_k'(x) = k\tilde{\mathcal{S}}_k(x) + x\tilde{\mathcal{S}}_{k-1}(x)$. The first few $\tilde{S}(n,k)$ are collected in Table 2.2.

[42] Alternatively, one can recover (2.124) introducing the exponential generating functions $\mathcal{B}(x) = \sum_n \frac{B_n}{n!} x^n = \mathrm{e}^{\mathrm{e}^x - 1}$ and $\mathcal{F}(x) = \sum_n \frac{F_n}{n!} x^n = \mathrm{e}^{\mathrm{e}^x - 1 - x}$; the result then follows from $\mathcal{B}(x) = \mathcal{F}(x) + \mathcal{F}'(x)$.

n	1	2	3	4	5	6	7	8	9	10
F_n	0	1	1	4	11	41	162	715	3425	17722
$\tilde{S}(n,1)$	0	1	1	1	1	1	1	1	1	1
$\tilde{S}(n,2)$	0	0	0	3	10	25	56	119	246	501
$\tilde{S}(n,3)$	0	0	0	0	0	15	105	490	1918	6825
$\tilde{S}(n,4)$	0	0	0	0	0	0	0	105	1260	9450
$\tilde{S}(n,5)$	0	0	0	0	0	0	0	0	0	945

Table 2.2: The F_n independent n-point spin correlators without isolated indices decompose into subsets containing $\tilde{S}(n,k)$ correlators with indices of k different colors.

Appendix B

In this Appendix we determine the number $M_n(q)$ of S_q-nonequivalent, linearly independent n-point spin correlators (2.11) which determine magnetic correlations in the Potts model at $q = 2, 3, 4$. We exploit the fact, discussed in section 2.3, that at $q = 2, 3, 4$ the symmetric group factorizes as

$$S_q = K_q \rtimes S_{q-1}\,, \tag{2.128}$$

with $K_4 = D_2$, $K_3 = \mathbb{Z}_3$, $K_2 = \mathbb{Z}_2$, and that the Potts model is described by $q-1$ independent spin variables $t_1, \ldots, t_{q-1}$ charged under the abelian group K_q. Non vanishing correlation functions are neutral under K_q and invariant under permutations of the $q-1$ operators t_i.

At $q = 2$, the only independent variable is t_1 with charge $+1$ under $\mathbb{Z}_2$. The neutrality condition for the n-point correlation functions is

$$n \equiv 0 \mod 2, \tag{2.129}$$

giving $M_{2k}(2) = 1$, $M_{2k+1}(2) = 0$.

At $q = 3$, the independent spin variables are t_1 and t_2 with $\mathbb{Z}_3$ charge $+1$ and -1, respectively. Given a n-point correlation function containing n_1 variables t_1

and n_2 variables t_2 we require

$$n_1 + n_2 = n, \tag{2.130}$$

$$n_1 - n_2 \equiv 0 \mod 3, \tag{2.131}$$

or equivalently $n_1 + n \equiv 0 \mod 3$, with $n_1 = 0, \ldots, n$. Assigned the couple of integers $\{n_1, n_2\} = \{n_1, n-n_1\}$ satisfying the constraint (2.131), the total number of distinct correlation functions we can construct is the binomial coefficient $\binom{n}{n_1}$. The charge conjugation operation, however, exchanges n_1 with n_2, and correlation functions obtained by $n_1 \to n - n_1$ are equal; notice indeed that $\binom{n}{n_1} = \binom{n}{n-n_1}$. It follows[43]

$$M_n(3) = \frac{1}{2} \sum_{\substack{n=0 \\ n_1+n \equiv 0 \\ \mod 3}}^{n} \binom{n}{n_1}. \tag{2.132}$$

The elements of the sequence (2.132) (see the first few of them in Table 2.1) coincide with the Jacobsthal numbers [64] and satisfy the recursive relation

$$M_{n+1}(3) = M_n(3) + 2M_{n-1}(3)\,, \tag{2.133}$$

with $M_1(3) = 0$, $M_2(3) = 1$. We will not prove (2.133) directly but we will justify it through the following observation. Consider an hypertetrahedron with q vertices labeled by the numbers $1, \ldots, q$. The number $y^{(n)}$ of closed n-step paths starting from a given vertex, say 1, of the hyperterahedron satisfies the recursive relation (see Appendix C)

$$y^{(n)} = (q-2)y^{(n-1)} + (q-1)y^{(n-2)}\,, \tag{2.134}$$

with $y^{(1)} = 0$, $y^{(2)} = q-1$. The closed n-step paths $\gamma^{(n)}$ in (2.134) are considered distinct even when they differ by a permutation $\pi \in S_{q-1}$ of the $q-1$ vertices $2, \ldots, q$. At $q = 3$ there is only one possible permutation π, and it exchanges the vertices 2 and 3. The application of π to a path $\gamma^{(n)}$ generates the path reflected along the symmetry axis containing the vertex 1 of an equilateral triangle. The number of closed paths nonequivalent under permutations at $q = 3$ is then just

[43] If n is even and $n_1 = n/2$ the factor $1/2$ in (95) avoids the double counting of the correlation functions obtained exchanging in block the positions of the n_1 operators t_1 with the $n_2 = n_1$ operators t_2.

half of the total number of closed paths $y^{(n)}$, and in particular satisfies (2.134) with $q = 3$. Finally notice that closed n-step paths $\gamma^{(n)}$ nonequivalent under permutations are in one to one correspondence with independent n-point kink fields correlation functions[44] (2.26), whose number is $M_n(q)$. Consistency requires that $M_n(3)$ satisfies the recursive equation (2.134) with $q = 3$, which indeed coincides with (2.133).

For $q = 4$ we consider correlation functions of the three variables t_1, t_2 and t_3 with $D_2 = \mathbb{Z}_2 \times \mathbb{Z}_2$ charges $(1, 0)$, $(0, 1)$ and $(1, 1)$, respectively. A non-vanishing n-point correlation function with n_1 variables t_1, n_2 variables t_2 and n_3 variables t_3 satisfies

$$n_1 + n_2 + n_3 = n, \tag{2.135}$$

$$(n_1 + n_3, n_2 + n_3) \equiv (0, 0) \mod 2\,, \tag{2.136}$$

or, more symmetrically, $n_i \equiv n \mod 2$, $i = 1, 2, 3$. The number of distinct n-point correlation functions associated to the solution $\{n_1, n_2, n_3\}$ of (2.135) and (2.136) is $\frac{n!}{n_1!n_2!n_3!}$. Correlation functions obtained by permutations of the integers n_i are identified and we must therefore choose a definite order for them, for example $n_1 \le n_2 \le n_3$; $n_i = 0, \dots, n$. When two positive integers n_1 and n_2 coincide, the two correlation functions obtained by exchanging in block the positions of the n_1 operators t_1 with the n_2 operators t_2 are also equal and counted twice among the $\frac{n!}{n_1!n_2!n_3!}$ correlation functions. Similarly, if $n_1 = n_2 = n_3$ permutational symmetry does not distinguish among the 3! correlation functions obtained exchanging in block the positions of the n_i variables t_i for $i = 1, 2, 3$. The final result is then

$$M_n(4) = \sum_{\substack{n_1+n_2+n_3=n \\ n_i \equiv n \mod 2}} \frac{n!}{n_1!n_2!n_3!} \frac{1}{n_e(n_1, n_2, n_3)!}\,, \tag{2.137}$$

where the n_i are ordered, $n_i \le n_{i+1}$, and $n_e(n_1, n_2, n_3)$ is the number of non-zero equal integers in the tern $\{n_1, n_2, n_3\}$. The integer sequence (2.137) (see

[44] Any path $\gamma^{(n)}$ can be represented as the sequence of $n+1$ vertices $\{1, v_2, \dots, v_n, 1\}$ with $v_i \neq v_{i+1}$ and $v_i = 1 \dots q$. The associated kink fields correlation function is $\langle \mu_{1v_2}(x_1) \dots \mu_{v_n 1}(x_n) \rangle$. Alternatively $\gamma^{(n)}$ can be thought as a particular coloration of n points on a circle. See again Appendix C.

Table 2.1) is also known [65], and is solution of the recursive equation

$$M_{n+1}(4) = 2M_n(4) + 3M_{n-1}(4) - 1\,, \tag{2.138}$$

with $M_1(4) = 0$, $M_2(4) = 1$. Again we will not prove (2.138) directly, but will explain why a proper counting of closed paths $\gamma^{(n)}$ nonequivalent under permutations of the vertices on a tetrahedron is obtained subtracting 1 to the r.h.s. of (2.134) with $q = 4$. It is convenient to represent $\gamma^{(n)}$ as the sequence $\gamma^{(n)} = \{1, v_2, \ldots, v_n, 1\}$ with $v_i = 1, \ldots, 4$ and $v_i \neq v_{i+1}$, which is also a particular coloration of n points on a circle. The way an $(n+1)$-step closed path $\gamma^{(n+1)} = \{1, v_2, \ldots, v_n, v_{n+1}, 1\}$ is constructed by adding a new point v_{n+1} and taking care of permutational symmetry is the following[45]. First we identify the largest v_i, $i = 2, \ldots, n$, and then generate all the paths $\gamma^{(n+1)}$ for which $v_{n+1} \neq v_n, 1$, with $v_{n+1} = 2, \ldots, \min\{\max\{v_i\} + 1, 4\}$. The recursion (97) fails only if $\max\{v_i\} = 2$ and then $v_n = 1, 2$. In this case the closed paths $\gamma^{(n+1)}$ with $v_{n+1} = 3, 4$ are identified by permutational symmetry and the choice $v_{n+1} = 4$ must be discarded; this leads to (101).

We conclude noticing that n distinct vertices are sufficient (and necessary) to enumerate all closed n-step paths nonequivalent under permutations of the vertices on an hypertetrahedron. In particular the number $M_n(q)$ of closed n-step paths nonequivalent under permutations on an hypertetrahedron with q vertices is constant for any $q \geq n$, and we have already shown in section 2.2 that, when no restriction is assumed on the number of available vertices so that all closed nonequivalent paths are counted, this number coincides with F_n:

$$M_n(q) = F_n \quad \text{for} \quad q \geq n\,. \tag{2.139}$$

[45]Notice that there are two cases corresponding to $v_n = 1$ or $v_n \neq 1$. In the first case the new point v_{n+1} is added to some closed $(n-1)$-step path $\gamma^{(n-1)}$; in the second case the new point is added to an $(n-1)$-step open path. The number of $(n-1)$-step open paths is however equal to the number of closed n-step paths $\gamma^{(n)}$

Appendix C

Given the diagonal form (2.64) and the unitary matrix U, we have

$$C_\alpha^{\rho\sigma} = \sum_{\lambda,\nu} U^\dagger_{\rho\lambda}(q\delta_{\alpha\nu} - 1)\delta_{\lambda\nu}U_{\nu\sigma} \tag{2.140}$$

$$= qU^\dagger_{\rho\alpha}U_{\alpha\sigma} - \delta_{\rho\sigma}. \tag{2.141}$$

Requiring $C_\alpha^{\rho\rho} = 0$ for $\rho, \alpha = 1 \dots q$, gives

$$U_{\alpha\rho} = \frac{1}{\sqrt{q}} \mathrm{e}^{i\varphi_{\alpha\rho}}; \tag{2.142}$$

the equation (2.68) for the phases is then the self-consistent condition of unitarity of the matrix U. Substituting (2.142) back into (2.141) we obtain (2.67). The matrices C_α in (2.34) and (2.37) for $q = 2, 3$ are reproduced by the solution

$$\varphi_{\alpha\rho} = \pm\frac{2\pi}{q}\alpha\rho \tag{2.143}$$

of the phase equation (2.68). For $q = 4$, the matrix (2.42) corresponds instead[46] to the solution

$$\varphi_{\boldsymbol{\alpha\rho}} = \pm\pi(\alpha_1\rho_1 + \alpha_2\rho_2), \tag{2.144}$$

with $\boldsymbol{\alpha} = (\alpha_1, \alpha_2)$, $\boldsymbol{\rho} = (\rho_1, \rho_2)$, $\alpha_i, \rho_i = 1, 2$.

We conclude this appendix giving a simple geometrical interpretation of the relation (2.62). Without loss of generality we can choose the phases so that one of the matrices C_α, say C_q, is real, i.e.

$$C_q = \begin{pmatrix} 0 & 1 & \cdots & 1 \\ 1 & 0 & \cdots & 1 \\ \vdots & \vdots & \ddots & \vdots \\ 1 & 1 & \cdots & 0 \end{pmatrix}. \tag{2.145}$$

This is the adjacency matrix of a fully connected graph with q sites, i.e. the projection on the plane of a hypertetrahedron with q vertices. We can then use

[46] Of course (2.143) solves (2.68) also for $q = 4$. This solution, however, would lead to a matrix C_α associated to $K_4 = \mathbb{Z}_4$, inconsistent with our general discussion of section 2.3 (in particular, $\mathrm{Aut}(\mathbb{Z}_4) = \mathbb{Z}_2$).

the formula (2.62) to compute powers of C_q and obtain

$$C_q^n = y^{(n)} I + x^{(n)} C_q, \tag{2.146}$$

with the integers $x^{(n)}$ and $y^{(n)}$ satisfying the recursive equations

$$y^{(n+1)} = q_1 x^{(n)}, \tag{2.147}$$

$$x^{(n+1)} = q_2 x^{(n)} + y^{(n)}. \tag{2.148}$$

It is now simple to realize that $y^{(n)}$ and $x^{(n)}$ are, respectively, the number of closed paths of length n starting from a vertex v_1 of the hypertetrahedron and the number of open paths of length n from v_1 to v_k. Indeed, if we consider such an open path and we add the link (v_k, v_1) we obtain a closed path of length $n+1$; however, by permutational symmetry, all the locations of $v_k \neq v_1$ are equivalent, and we obtain (2.147). Suppose instead to remove from the original open path the last link (v_j, v_k); this gives a path of length $n-1$ from v_1 to v_j that can be open with multiplicity q_2 ($j \neq 1, k$), or closed with multiplicity one ($j = 1$), reproducing (2.148). The recursions (2.147) and (2.148) give for $y^{(n)}$ equation (2.134), whose solution is

$$y^{(n)} = \frac{1}{q}\big[(-1)^n q_1 + q_1^n\big], \tag{2.149}$$

which is q^{-1} times the chromatic polynomial $\pi_{C_n}(q)$ for the the cyclic graph C_n, i.e. the graph obtained putting n points on a circle. We conclude that the decompositions over kink fields of the correlator $\langle \mu_\alpha(x_1)\mu_\alpha(x_2)\dots\mu_\alpha(x_n)\rangle$ can be associated to closed n-step paths on a fully connected graph with q vertices, or to colorations of a ring of n points with q colors.

Chapter 3

Universality at criticality. The three-point connectivity

In this chapter we argue how the three-point connectivity P_{aaa} for critical random percolation can be related to Al. Zamolodchikov analytic continuation of the structure constants of the conformal minimal models. In particular we determine the value for the universal ratio $\frac{P_{aaa}(x_1,x_2,x_3)}{\sqrt{P_{aa}(x_1,x_2)P_{aa}(x_2,x_3)P_{aa}(x_1,x_3)}}$. At the end of the chapter we also discuss P_{aaa} away from criticality.

3.1 Critical three-point connectivity

As we have seen in the previous chapter the connectivity functions $P_{a\ldots a}(x_1,\ldots,x_n)$, i.e. the probabilities that n points belong to the same finite cluster a, play a fundamental role in percolation theory. In particular, their scaling limit determines the universal properties that clusters exhibit near the percolation threshold p_c. Although most quantitative studies focus on the two-point connectivity, which determines observables as the mean cluster size $S = \sum_x P_{aa}(x,0)$, also the connectivities with $n > 2$ carry essential information about the structure of the theory. In this chapter we consider the case $n = 3$ for clusters in random percolation and in the q-color Potts model ($q \leq 4$) in two dimensions, in the scaling limit on the infinite plane. In particular, we will determine exactly the universal

quantity

$$R(x_1, x_2, x_3) = \frac{P_{aaa}(x_1, x_2, x_3)}{\sqrt{P_{aa}(x_1, x_2) P_{aa}(x_1, x_3) P_{aa}(x_2, x_3)}} \tag{3.1}$$

at p_c, as well as some of its features below p_c. The connectivity combination (3.1) was studied in [66, 67] for the case in which two of the three points are located on the boundary of the half-plane, it was shown to be a constant at p_c and determined numerically and also analytically, exploiting the fact that points on the boundary yield linear differential equations for the connectivities at criticality [33]. It is not known how to write differential equations for random percolation connectivities if all the points are in the bulk.

Thanks to the FK mapping, see in particular the relation (2.14), the connectivity functions can be related to the correlation functions of the Potts order parameter $\sigma_\alpha(x) = q\delta_{s(x),\alpha} - 1$, $\alpha = 1, \ldots, q$; for $p \leq p_c$, namely when the probability of finding an infinite cluster is zero, the relation for the two- and three-point functions reads

$$P_{aa}(x_1, x_2) = \frac{1}{q-1} \langle \sigma_\alpha(x_1) \sigma_\alpha(x_2) \rangle \,, \tag{3.2}$$

$$P_{aaa}(x_1, x_2, x_3) = \frac{1}{(q-1)(q-2)} \langle \sigma_\alpha(x_1) \sigma_\alpha(x_2) \sigma_\alpha(x_3) \rangle \,, \tag{3.3}$$

where for random percolation the limit $q \to 1$ is understood in the r.h.s. The relations (3.2) and (3.3), evaluated for a generic q, give the connectivities in the random cluster model. The duality transformations (2.55) and (2.56) for the q-color Potts model allow also to rewrite

$$\langle \sigma_\alpha(x_1) \sigma_\alpha(x_2) \rangle_{J \leq J_c} = (q-1) \langle \mu_{\alpha\beta}(x_1) \mu_{\beta\alpha}(x_2) \rangle_{J^*} \,, \tag{3.4}$$

$$\langle \sigma_\alpha(x_1) \sigma_\alpha(x_2) \sigma_\alpha(x_3) \rangle_{J \leq J_c} = (q-1)(q-2) \langle \mu_{\alpha\beta}(x_1) \mu_{\beta\gamma}(x_2) \mu_{\gamma\alpha}(x_3) \rangle_{J^*} \,. \tag{3.5}$$

Comparison with (3.2), (3.3) shows that P_{aa} and P_{aaa} are related to the kink field correlators without any q-dependent prefactor[1].

In the scaling limit ($q \leq q_c$, $J \to J_c$, distances $|x_i - x_j| \equiv r_{ij}$ much larger than the lattice spacing) that we consider from now on, the lattice variables become fields of the Potts field theory. Up to overall constants depending on the

[1]For the case of points lying on the boundary of a simply connected domain of the plane we gave a geometrical explanation of (3.4) and (3.5) in the previous chapter.

arbitrary normalization of the field $\sigma_\alpha(x)$, the correlators in (3.2-3.3) are universal functions of the distances r_{ij} measured in units of the connectivity length. The normalization constants cancel in the combination (3.1), which is then completely universal.

At criticality, conformal invariance implies that the two- and three-point correlators of scalar fields $A_i(x)$ with scaling dimension X_i have the form [36]

$$\langle A_1(x_1)A_2(x_2)\rangle = \delta_{X_1,X_2} C_{12}\, r_{12}^{-2X_1}\,, \tag{3.6}$$

$$\langle A_1(x_1)A_2(x_2)A_3(x_3)\rangle = C_{123}\, r_{12}^{X_3-X_1-X_2} r_{13}^{X_2-X_1-X_3} r_{23}^{X_1-X_2-X_3}\,. \tag{3.7}$$

If the fields are chosen and normalized in such a way that $C_{ij} = \delta_{ij}$, the constants C_{ijk}, which are invariant under permutations of their indices, coincide with the coefficients C_{ij}^k of the operator product expansion (OPE)

$$A_i(x_1)A_j(x_2) = C_{ij}^k\, r_{12}^{X_k-X_i-X_j}\, A_k(x_2) + \dots\,. \tag{3.8}$$

Denoting X_s the scaling dimension of the Potts spin field $\sigma_\alpha(x)$, we see recalling (3.2-3.3) that $P_{aa} \propto r^{-2X_s}$, $P_{aaa} \propto (r_{12}r_{13}r_{23})^{-X_s}$, and

$$R(x_1,x_2,x_3) \equiv R_c = \frac{1}{(q-1)(q-2)}\, C_{\sigma_\alpha\sigma_\alpha\sigma_\alpha}\,, \qquad p = p_c\,, \tag{3.9}$$

where we have chosen according to the general discussion of section 2.4

$$C_{\sigma_\alpha\sigma_\alpha} = q-1. \tag{3.10}$$

As briefly discussed at the beginning of section 1.3, in the Potts model, the fields σ_α have in the Kac notation scaling dimension [37, 38]

$$X_s = X_{(t+1)/2,(t+1)/2} \tag{3.11}$$

and multiplicity[2] $q-1$ ($\sum_\alpha \sigma_\alpha = 0$). The field is degenerate only for $q=2$ (Ising model, $t=3$) and $q=3$ ($t=5$). Correlation functions of degenerate fields are solution of differential equations and in [68] this peculiarity was exploited to compute the OPE coefficients C_{ij}^k for the "diagonal" series of minimal models, in

[2]The non-integer multiplicity of the fields σ_α for q generic of course signals the unconventional nature of the field theoretical problem we deal with. The relevant point is that S_q invariance allows to treat q as a parameter which does not need to be integer, see below.

which all the primaries appear with multiplicity one. The Potts model belongs to this class for $q = 2$, but even for this case the results for the minimal OPE are not sufficient to determine R_c. Indeed, it is clear from (3.9) that a finite R_c requires $C_{\sigma_\alpha\sigma_\alpha\sigma_\alpha} = 0$ at $q = 2$, and this is trivially ensured by the spin reversal symmetry of the Ising model. Hence, even the determination of R_c at $q = 2$ requires the computation of the OPE coefficient for continuous values of q; even forgetting the problem with the multiplicity of the fields, the formulae of [68] can be evaluated only for the discrete values of t corresponding to minimal models.

Few years ago Al. Zamolodchikov [30] approached the problem of the derivation of the OPE coefficients of $c < 1$ minimal models within a conformal bootstrap method based on the use of correlators of four scalar fields, one of which being the degenerate primary with dimension $X_{1,2}$ or $X_{2,1}$. The other three fields are simply required to appear with multiplicity one; the mathematical treatment does not put any constraint on their scaling dimensions X_i, $i = 1, 2, 3$. The method leads to functional equations for the OPE coefficients which are related by analytic continuation to the functional equations arising in Liouville theory ($c \geq 25$) [69]. The solution for $c < 1$, however, is not an analytic continuation of the Liouville solution, and reads [30]

$$C^{X_3}_{X_1,X_2} = C_{X_1,X_2,X_3} = \tag{3.12}$$
$$\frac{A\,\Upsilon(a_1+a_2-a_3+\beta)\Upsilon(a_2+a_3-a_1+\beta)\Upsilon(a_3+a_1-a_2+\beta)}{[\Upsilon(2a_1+\beta)\Upsilon(2a_1+2\beta-\beta^{-1})\Upsilon(2a_2+\beta)\Upsilon(2a_2+2\beta-\beta^{-1})]^{1/2}}\times$$
$$\times\frac{\Upsilon(2\beta-\beta^{-1}+a_1+a_2+a_3)}{[\Upsilon(2a_3+\beta)\Upsilon(2a_3+2\beta-\beta^{-1})]^{1/2}},$$

with

$$\beta = \sqrt{t/(t+1)}\,, \tag{3.13}$$
$$X_i = 2a_i(a_i+\beta-\beta^{-1})\,, \tag{3.14}$$
$$A = \frac{\beta^{\beta^{-2}-\beta^2-1}[\gamma(\beta^2)\gamma(\beta^{-2}-1)]^{1/2}}{\Upsilon(\beta)}\,, \qquad \gamma(x) \equiv \frac{\Gamma(x)}{\Gamma(1-x)}\,, \tag{3.15}$$

$$\Upsilon(x) = \exp\left\{\int_0^\infty \frac{dt}{t}\left[\left(\frac{Q}{2}-x\right)^2 e^{-t} - \frac{\sinh^2\left[\left(\frac{Q}{2}-x\right)\frac{t}{2}\right]}{\sinh\frac{\beta t}{2}\sinh\frac{t}{2\beta}}\right]\right\}, \qquad Q = \beta+\beta^{-1}. \tag{3.16}$$

q	1	2	3	4
R_c	1.0220..	1.0524..	1.0923..	1.1892..
$\tilde{R}_c$	–	1.3767..	1.3107..	1.1892..
Γ^K_{KK}	1.0450..	1.1547..	1.3160..	1.8612..

Table 3.1: R_c and Γ^K_{KK} are the values of the quantities (3.9) and (3.27) for FK clusters; $q = 1$ corresponds to random percolation. $\tilde{R}_c$ is obtained from (3.24) with X_σ replaced by $X_{\tilde{\sigma}}$, the scaling dimension associated to spin clusters.

The integral in (3.16) is convergent for $0 < x < Q$; outside this range $\Upsilon(x)$ can be computed using the relations

$$\Upsilon(x+\beta) = \gamma(\beta x)\beta^{1-2\beta x}\Upsilon(x)\,, \tag{3.17}$$

$$\Upsilon(x+1/\beta) = \gamma(x/\beta)\beta^{2x/\beta-1}\Upsilon(x)\,. \tag{3.18}$$

The function (3.12) can be evaluated for continuous values of t and of the X_i's. Taken literally, it would give the OPE coefficients for a theory with arbitrary $c < 1$ and with a continuous spectrum of fields having multiplicity one. It is remarked in [30] that the consistency of such a theory, in particular from the point of view of modular invariance [40, 41], is an open question. Concerning the values of c corresponding to minimal models, (3.14) gives twice the scaling dimensions $h_{n,m}$ as in (1.32) for a_i equal to

$$a_{m,n} = \frac{(n-1)\beta}{2} - \frac{(m-1)\beta^{-1}}{2}\,. \tag{3.19}$$

Although a general proof is not available, checks case by case show that (3.12) reproduces the OPE coefficients of minimal models obtained in [68], at least when these differ from zero. In some cases for which the minimal OPE prescribes vanishing coefficients, (3.12) gives instead finite numbers whose interpretation is considered "mysterious" in [30]. As an example, (3.12) evaluated for $X_1 = X_2 = X_3 = X_{2,2}$ at $t = 3$ does not vanish, despite the fact that the spin three-point function is zero in the Ising model. Recall now from the previous chapter that the two-dimensional Potts model contains also kink fields, dual to the spin fields and with the same scaling dimension X_σ. They satisfy the OPE

$$\mu_{\alpha\beta}\,\mu_{\beta\gamma} = \delta_{\alpha\gamma}(I + C_\varepsilon\,\varepsilon + \ldots) + (1-\delta_{\alpha\gamma})(C_\mu\,\mu_{\alpha\gamma} + \ldots)\,, \tag{3.20}$$

where we omit the coordinate dependence for simplicity and the coefficient in front of the identity is fixed to 1 by (3.4) and (3.10). Use of (3.4-3.5) at the self-dual point then leads to the result $R_c = C_\mu$. S_q-invariance gives to (3.20) a two-channel structure ($\alpha = \gamma$ or $\alpha \neq \gamma$) equivalent to that produced by two fields μ and $\bar{\mu}$ satisfying[3]

$$\mu\,\bar{\mu} = I + C_\varepsilon\,\varepsilon + \dots\,, \tag{3.21}$$

$$\mu\,\mu + \bar{\mu}\,\bar{\mu} = C_\mu(\mu + \bar{\mu}) + \dots\,. \tag{3.22}$$

The field $\phi \equiv (\mu + \bar{\mu})/\sqrt{2}$ then satisfies

$$\phi\,\phi = I + C_\varepsilon\,\varepsilon + \frac{C_\mu}{\sqrt{2}}\,\phi + \dots\,, \tag{3.23}$$

namely a "neutral" OPE for fields with multiplicity one, as the one assumed in the derivation of (3.12). Notice also that, due to the neutrality of the fields in (3.23), C_μ has no reason to vanish for any value of q; in particular, this is not in conflict with the symmetries of the Ising model, because the absence for $q = 2$ of the vertex with three kink fields in (3.20) is enforced by the factor $1 - \delta_{\alpha\gamma}$. These observations may suggest the following interpretation for the function (3.12): it encodes the "dynamical" information about the OPE of conformal field theory for $c < 1$, and knows nothing about internal symmetries, which, on the other hand, are not uniquely determined by the value of c; symmetry considerations have to be developed separately and produce a dressing of (3.12) by factors which may vanish, suppressing the vertices not compatible with the given symmetry. Letting aside the general validity of this interpretation, the OPE's (3.20) and (3.23) make it plausible for the case we are discussing, and lead us to take

$$R_c = \sqrt{2}\,C_{X_s,X_s,X_s}\,, \tag{3.24}$$

[3]The two- and three-point kink correlators (the only ones we are concerned with in this chapter) are expressed in terms of the correlators of μ and $\bar{\mu}$ as

$$\langle \mu_{\alpha\beta}(x_1)\mu_{\beta\alpha}(x_2)\rangle = \langle \mu(x_1)\bar{\mu}(x_2)\rangle\,,$$

$$\langle \mu_{\alpha\beta}(x_1)\mu_{\beta\gamma}(x_2)\mu_{\gamma\alpha}(x_3)\rangle = (1/2)\,\langle (\mu+\bar{\mu})(x_1)(\mu+\bar{\mu})(x_2)(\mu+\bar{\mu})(x_3)\rangle\,.$$

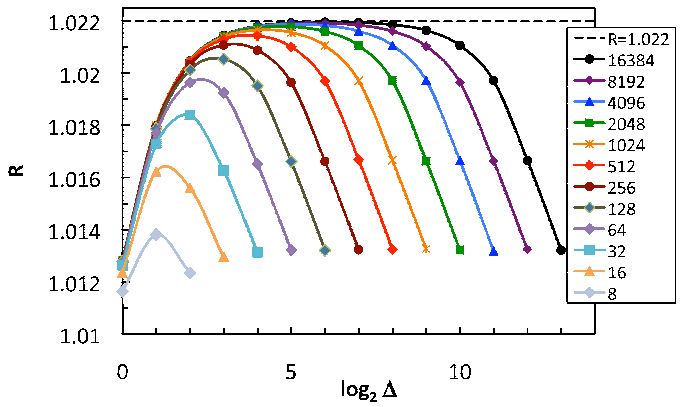

Figure 3.1: Montecarlo determination of the universal ratio R_c (called R in the figure, [31]). Simulations are performed on a $L \times L$ lattice with periodic boundary conditions, for the values of L listed on the right. The three points are taken at the vertices of an equilateral triangle of side Δ. Data clearly converge towards the theoretical result $1.022\ldots$ as L increases.

with X_s given in (3.11). The results for the integer values of q are given in Table 3.1. The value for $q = 4$ is obtained in the limit $t \to \infty$; C_μ is known to coincide with the r.h.s. of (3.24) for $q = 3$ (see e.g. [49] and [70]).

The result obtained for R_c at $q = 1$ has been checked numerically in [31]. The authors considered a a percolation problem defined on $L \times L$ lattice with periodic boundary conditions and put the points x_1, x_2 and x_3 at the vertices of an equilateral triangle of length-side Δ. Increasing L and for Δ in a range where lattice and finite size effects are negligible, R_c approaches the value predicted by (3.24), see Fig. 3.1.

The result (3.24) refers to FK clusters. Concerning the ordinary spin clusters, i.e. those obtained connecting nearest neighbors with the same value of the spin, they are also critical at J_c in two dimensions [71], with connectivities related to the correlation functions of the field with scaling dimension $X_{\tilde{s}} = X_{t/2,t/2}$ [72, 48]. For the Ising case, the best understood field theoretically [46, 21], the ratio (3.1) is expected to be given by (3.24) with X_s replaced by $X_{\tilde{s}}$. We give this value $\tilde{R}_c$ in Table 3.1; those obtained in the same way at $q = 3, 4$ are also quoted, but

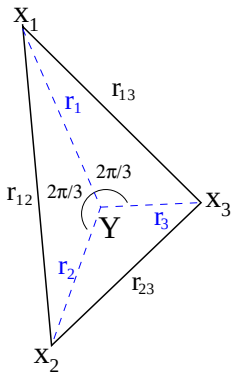

Figure 3.2: Triangle identified by the points x_1, x_2, x_3. The lines joining the vertices of the triangle to the Fermat (or Steiner) point Y form $2\pi/3$ angles.

these cases are less clear.

The OPE between σ_α and $\mu_{\beta\gamma}$ produces parafermionic fields. An analysis similar to that of [73] suggests that they have spin $X_{1,3}/2$; this is certainly the case for $q = 2, 3$ [49].

3.2 Three-point connectivity away from criticality

Away from criticality the Potts field theory is solved exactly in the framework of the factorized S-matrix, from which large distance expansions can be obtained for the correlation functions [62, 18]. The S_q symmetry is more transparently implemented working in the ordered phase ($J > J_c$), where the elementary excitations (kinks) are interpolated by the kink fields of section 2.7; the results for the disordered phase are obtained by duality. If x_1, x_2, x_3 are the vertices of a triangle whose internal angles are all smaller than $2\pi/3$, the asymptotic behavior of the correlator (3.5) when all the distances between the vertices become large reads [27] ([74] for a derivation)

$$\langle \mu_{\alpha\beta}(x_1)\mu_{\beta\gamma}(x_2)\mu_{\gamma\alpha}(x_3)\rangle_{J>J_c} = \frac{F_\mu^3}{\pi}\,\Gamma^K_{KK}\,K_0(r_Y/\xi) + O(\mathrm{e}^{-\rho/\xi})\,. \qquad (3.25)$$

Here F_μ is a shorthand notation for the one-kink form factor of the kink field, $K_0(x) = \int_0^\infty \mathrm{d}y\,\mathrm{e}^{-x\cosh y}$ is a Bessell function, and $r_Y \equiv r_1 + r_2 + r_3$ is the

sum of the distances of the vertices of the triangle from the Fermat (or Steiner) point Y, which has the property of minimizing such a sum (Fig. 3.2); $r_Y < \rho \equiv \min\{r_{12}+r_{13}, r_{12}+r_{23}, r_{13}+r_{23}\}$. ξ is the connectivity length (inverse of the kink mass), also determined by the large distance decay of the two-point function

$$\langle \mu_{\alpha\beta}(x_1)\mu_{\beta\alpha}(x_2)\rangle_{J>J_c} = \frac{F_\mu^2}{\pi} K_0(r_{12}/\xi) + O(\mathrm{e}^{-2r_{12}/\xi}) , \tag{3.26}$$

and Γ^K_{KK} is the three-kink vertex given by [27]

$$\Gamma^K_{KK} = \sqrt{\frac{1}{\lambda}\sin\frac{2\pi\lambda}{3}\, g(\lambda)} , \tag{3.27}$$

$$g(\lambda) = \exp\left[\int_0^\infty \mathrm{d}t \sinh\left(\frac{t}{3}\right) \frac{\sinh\left[\frac{t}{2}\left(1-\frac{1}{\lambda}\right)\right] - \sinh\left[\frac{t}{2}\left(\frac{1}{\lambda}-\frac{5}{3}\right)\right]}{t\sinh\frac{t}{2\lambda}\cosh\frac{t}{2}}\right] \tag{3.28}$$

with $q = 2\sin\frac{\pi\lambda}{3}$, $\lambda \in (0, 3/2)$. It follows from (3.4-3.5) that (3.25-3.26) are precisely the asymptotics for large separations of the connectivities (3.2-3.3) for KF clusters below p_c. It follows

$$R(x_1,x_2,x_3) \simeq \sqrt{\pi}\,\Gamma^K_{KK} \frac{K_0(r_Y/\xi)}{\sqrt{K_0(r_{12}/\xi)K_0(r_{13}/\xi)K_0(r_{23}/\xi)}}, \quad r_{ij} \gg \xi, \quad p \to p_c^- . \tag{3.29}$$

The dynamical information is entirely contained in the three-kink vertex, whose values for q integer are given[4] in Table 3.1. In the opposite limit, in which all the distances r_{ij} are much smaller than ξ (always remaining much larger than the lattice spacing), the function R tends to its constant critical value R_c.

Finally, consider the ordinary spin clusters for the Ising model. It was argued in [46] that in this case the scaling limit for $p \to p_c^-$ (in zero magnetic field) corresponds to a renormalization group trajectory with infinite connectivity length ending into a random percolation fixed point at large distances. Then one expects (3.1) to interpolate from $\tilde{R}_c|_{q=2}$, when all the distances between the points are small, to $R_c|_{q=1}$, when all of them are large. Although universal, this crossover could be easier to observe on the triangular lattice, which has $p_c = 1/2$ for site percolation and is expected to minimize the corrections to scaling [46]. If instead

[4]The value $\Gamma^K_{KK}|_{q=1}$ quoted in [27] is affected by a typo in the formula corresponding to our (3.28).

we work at the Ising critical temperature and add a magnetic field H, the connectivity length is finite and the large separation behavior of (3.1) for clusters of positive spins and $H \to 0^-$ has again the form (3.29), with $\Gamma^K_{KK} = 5.7675..$ given by (3.27) evaluated at $\lambda = 5/2$ [21]. Since the integral in (3.28) diverges for $\lambda \geq 3/2$, one uses the analytic continuation

$$g(\lambda) = \frac{\Gamma\left(1-\frac{2\lambda}{3}\right)\Gamma(1+\lambda)}{\Gamma\left(1+\frac{\lambda}{3}\right)} \times \\ \times \exp\left[\int_0^\infty \mathrm{d}t \sinh\left(\frac{t}{3}\right) \frac{\sinh\left[\frac{t}{2}\left(1-\frac{1}{\lambda}\right)\right] - \mathrm{e}^{-t}\sinh\left[\frac{t}{2}\left(\frac{1}{3}+\frac{1}{\lambda}\right)\right]}{t\sinh\frac{t}{2\lambda}\cosh\frac{t}{2}}\right] \tag{3.30}$$

for $3/2 \leq \lambda < 3$.

Chapter 4

Universality close to criticality. Amplitude ratios

In this chapter we describe the theoretical computation of universal amplitude ratios for random two-dimensional percolation. The two-kink form factors of the spin field at $q = 1$ are obtained exploiting integrability of the perturbed Potts field theory and then used to derive the results of Tab. 4.2. In particular we determine the ratio Γ^+/Γ^- of cluster size amplitudes below and above the critical threshold p_c. The numerical value of this quantity had been controversial for thirty years.

4.1 Introduction

Universal combinations of critical amplitudes represent the canonical way of encoding the universal information about the approach to criticality in statistical mechanics [75]. While critical exponents can be determined working *at* criticality, amplitude ratios characterize the scaling region *around* the critical point. They carry independent information about the universality class and their determination is in general theoretically more demanding. Field theory is the natural framework in which to address the problem, but the usual perturbative approach is not helpful if one has to work far below the upper critical dimension d_c.

For the best-known example of a geometric phase transition, namely isotropic

percolation ($d_c = 6$), it was shown in [62] how the field theoretical computation of universal amplitude ratios in two dimensions can be addressed non-perturbatively exploiting the fact that percolation can be seen as the $q \to 1$ limit of the q-color Potts model, see section 1.5, and that the latter is integrable even away from criticality, in the scaling limit for $q \leq 4$ as discussed in section 2.7. Starting from the exact S-matrix one can compute the Potts correlation functions, and from them the amplitude ratios, using the form factor approach. For example consider the ratio of the cluster size amplitudes Γ^+ and Γ^- we introduced in section 1.5. This is expressed as the ratio of Potts susceptibilities in the limit $q \to 1$

$$\frac{\Gamma^+}{\Gamma^-} = \lim_{q\to 1} \frac{\int \mathrm{d}^2x \langle \Omega|\sigma_\alpha(x)\sigma_\alpha(0)|\Omega\rangle}{\int \mathrm{d}^2x \langle \Omega_\alpha|\sigma_\alpha(x)\sigma_\alpha(0)|\Omega_\alpha\rangle_c}, \tag{4.1}$$

where $|\Omega_\alpha\rangle$ is the Potts vacuum in the spontaneously broken phase of color α and $|\Omega\rangle$ is the Potts S_q invariant vacuum. The correlation function in the broken phase is the connected one. The scattering theory of the q-color Potts model is formulated in the ordered phase where lightest mass excitations are kinks. The computation of the numerator in (4.1) is then possible exploiting the duality transformation discussed in chapter 2

$$\langle \Omega|\sigma_\alpha(x)\sigma_\alpha(0)|\Omega\rangle = (q-1)\langle \Omega_\alpha|\mu_{\alpha\beta}(x)\mu_{\beta\alpha}(0)|\Omega_\alpha\rangle, \tag{4.2}$$

and within the two-kink form factor approximation the correlation functions are[1]

$$\langle \Omega_\alpha|\sigma_\alpha(x)\sigma_\alpha(0)|\Omega_\alpha\rangle_c = \frac{q-1}{2\pi^2}\int_0^\infty d\theta\ K_0\big(2m|x|\cosh\theta/2\big)|F^{\sigma_\alpha}_{\alpha\beta\alpha}(\theta)|^2 + o\big(\mathrm{e}^{-2m|x|}\big) \tag{4.3}$$

$$\langle \Omega_\alpha|\mu_{\alpha\beta}(x)\mu_{\beta\alpha}(0)|\Omega_\alpha\rangle = \frac{K_0(m|x|)}{\pi}|F^{\mu_{\alpha\beta}}_{\beta\alpha}|^2 \tag{4.4}$$

$$+ \frac{q-2}{2\pi^2}\int_0^\infty d\theta\ K_0\big(2m|x|\cosh\theta/2\big)|F^{\mu_{\alpha\beta}}_{\beta\gamma\alpha}(\theta)|^2 + o\big(\mathrm{e}^{-2m|x|}\big), \tag{4.5}$$

[1] By rotational invariance the Euclidean point x has been taken $(|x|, 0)$.

with $K_0(x) = \int_0^\infty \mathrm{d}\xi\ \mathrm{e}^{-x\cosh\xi}$ a modified Bessel function. The notation for the two-kink form factor is that of section 2.7, i.e.

$$F^{\Phi}_{\alpha_1\alpha_2\alpha_3}(\theta) = \langle \Omega_{\alpha_1}|\Phi(0,0)|K_{\alpha_1\alpha_2}(\theta)K_{\alpha_2\alpha_3}(0)\rangle \tag{4.6}$$

and the functional equations solved by the matrix element (4.6) are briefly quoted in (2.116), (2.117) and (2.118) for the case of a neutral field. For more details we refer to [62]. In the next section we will discuss the computation of the two-kink spin field and kink field form factors in the Potts model and in particular in the limit $q \to 1$.

4.2 Two-kink form factors for the spin and kink field

Parameterizing $\sqrt{q} = 2\sin(\pi\lambda/3)$, the two-kink form factor of the spin field has the following analytic form, [62]

$$F^{\sigma_\alpha}_{\alpha\beta\alpha}(\theta) = F_\Lambda(\theta)\Omega_q(\theta), \tag{4.7}$$

with the integral representation for function $F_\Lambda(\theta)$

$$F_\Lambda(\theta) = -i\sinh\theta/2\,\exp\left[\int_0^\infty \frac{dx}{x}\frac{g_1(x)+g_\varepsilon(x)}{\sinh x}\sin^2\frac{(i\pi-\theta)x}{2\pi}\right] \tag{4.8}$$

and

$$g_a(x) = 2\frac{\sinh\left(\frac{1}{2\lambda}-a\right)x}{\sinh\frac{x}{2\lambda}}, \tag{4.9}$$

$$g_\varepsilon = 2\frac{\sinh\frac{x}{3}\cosh\left(\frac{1}{3}-\frac{1}{\lambda}\right)\frac{x}{2}}{\sinh\frac{x}{2\lambda}\cosh\frac{x}{2}}. \tag{4.10}$$

The function $\Omega_q(\theta)$ is characterized by the following properties:

i) is a meromorphic function of θ whose only singularity in the strip $\mathrm{Im}\,\theta \in (0, 2\pi)$ is a simple pole at $\theta = i\pi$ with residue

$$\mathrm{Res}_{\theta=i\pi}\Omega_q(\theta) = i\frac{1}{q-1}\langle\sigma_\alpha\rangle_\alpha, \tag{4.11}$$

where $\langle\sigma_\alpha\rangle_\alpha$ denotes the Potts spontaneous magnetization;

ii) is solution of the functional equations

$$\Omega_q(\theta) = \Omega_q(-\theta), \tag{4.12}$$

$$2\cos\frac{\pi\lambda}{3}\sinh\lambda\theta\,\Omega_q(\theta) = \sinh\lambda(i\pi+\theta)\,\Omega_q(2i\pi-\theta) - \sinh\lambda(i\pi-\theta)\,\Omega_q(2i\pi+\theta)\,, \tag{4.13}$$

with the asymptotic behavior

$$\Omega_q(\theta) \sim \exp\left[\left(\frac{2}{3}\lambda - 1\right)\theta\right], \qquad \theta \to +\infty. \tag{4.14}$$

For $q \leq 3$, where the Potts scattering theory possesses no bound states, the properties i) and ii) uniquely identify $\Omega_q(\theta)$, and then the spin field of the scaling Potts model[2].

In [62] $\Omega_q(\theta)$ was determined only for $q = 2, 3, 4$, where it takes a simple form. We now show that $\Omega_1(\theta)$ can be obtained taking a mathematical detour in the sine-Gordon model. For the latter, which is defined by the action

$$\mathcal{A}_{SG} = \int \mathrm{d}^2x\ \frac{1}{2}\left(\partial_\nu\varphi\right)^2 + \mu\cos\beta\varphi, \tag{4.15}$$

Lukyanov computed in [77] the soliton-antisoliton form factors

$$F^a_{\varepsilon_1\varepsilon_2}(\theta) = \langle 0|e^{ia\beta\varphi(0)}|A_{\varepsilon_1}(\theta_1)A_{\varepsilon_2}(\theta_2)\rangle, \qquad \varepsilon_i = \pm 1, \quad \varepsilon_1\varepsilon_2 = -1, \tag{4.16}$$

obtaining a result that in our notations[3] reads

$$F^a_{\pm\mp}(\theta) = -\langle e^{ia\beta\varphi}\rangle\,\frac{F_0(\theta)}{F_0(i\pi)}A^a_\pm(\theta), \tag{4.17}$$

$$A^a_\pm(\theta) = e^{\mp\frac{\pi}{2\xi}(i\pi-\theta)}[e^{\mp 2i\pi a}I_a(-\theta) + I_a(\theta - 2i\pi)], \tag{4.18}$$

where $\xi = \pi\beta^2/(8\pi - \beta^2)$, $F_0(\theta)$ is a function on which we comment below, and $I_a(\theta)$ is specified *for real values of* θ and $a \in (-\frac{1}{2} - \frac{\pi}{\xi}, \frac{1}{2})$ as

$$I_a(\theta) = \mathcal{C}\int_{-\infty}^{+\infty}\frac{\mathrm{d}x}{2\pi}\,W\left(-x - \frac{\theta}{2} + i\pi\right)W\left(-x + \frac{\theta}{2} + i\pi\right)e^{-\left(\frac{\pi}{\xi}+2a\right)x}, \tag{4.19}$$

[2]See [76, 73] for the correspondence between fields and solutions of the form factor equations in integrable field theory.

[3]In particular, switching from Lukyanov's notations to ours involves the replacements $\theta \to -\theta$, $\xi \to \xi/\pi$, $a \to \beta a$.

with

$$W(\theta) = -\frac{2}{\cosh\theta}\,\exp\left[-2\int_0^\infty \frac{\mathrm{d}t}{t}\,\frac{\sinh\frac{t}{2}\left(1-\frac{\xi}{\pi}\right)}{\sinh t\,\sinh\frac{\xi t}{2\pi}}\sin^2\frac{t}{2\pi}(i\pi-\theta)\right], \tag{4.20}$$

and

$$\mathcal{C} = \frac{1}{4}\exp\left[-4\int_0^\infty \frac{\mathrm{d}t}{t}\,\frac{\sinh^2\frac{t}{4}\,\sinh\frac{t}{2}\left(1-\frac{\xi}{\pi}\right)}{\sinh t\,\sinh\frac{\xi t}{2\pi}}\right]. \tag{4.21}$$

These results were presented in [77] within a framework known as free field representation, which differs from the usual approach to form factors based on functional relations. Of course, this latter approach can be adopted also for the matrix elements (4.17), using as input the sine-Gordon S-matrix and the fact that the soliton is semi-local with respect to $e^{ia\beta\varphi}$, with a semi-locality phase $e^{2i\pi a}$. The corresponding functional equations then read [78]

$$F^a_{\varepsilon_1\varepsilon_2}(\theta) = S_T(\theta)F^a_{\varepsilon_2\varepsilon_1}(-\theta) + S_R(\theta)F^a_{\varepsilon_1\varepsilon_2}(-\theta), \tag{4.22}$$

$$F^a_{\varepsilon_1\varepsilon_2}(\theta+2i\pi) = e^{2i\pi a\varepsilon_2}\,F^a_{\varepsilon_2\varepsilon_1}(-\theta), \tag{4.23}$$

where

$$S_T(\theta) = -\frac{\sinh\frac{\pi\theta}{\xi}}{\sinh\frac{\pi}{\xi}(\theta-i\pi)}\,S(\theta), \tag{4.24}$$

$$S_R(\theta) = -\frac{\sinh\frac{i\pi^2}{\xi}}{\sinh\frac{\pi}{\xi}(\theta-i\pi)}\,S(\theta), \tag{4.25}$$

are the transmission and reflection amplitudes; the explicit form in the present notations of $S(\theta)$ and $F_0(\theta)$ can be found for example in [50], but here we only need to know that

$$F_0(\theta) = S(\theta)F_0(-\theta), \qquad F_0(\theta+2i\pi) = F_0(-\theta). \tag{4.26}$$

This implies in particular that (4.23) is automatically satisfied by (4.17). Since $A^a_\pm$ are meromorphic functions of θ, also I_a, as a linear combination of A^a_+ and A^a_- with entire coefficients, is meromorphic. It particular, analyticity implies that the property

$$I_a(\theta) = I_a(-\theta), \tag{4.27}$$

which for real θ is apparent in (4.19), extends to the whole complex plane. Requiring (4.22) leads now to the equation

$$2\cos\left(\frac{\pi^2}{\xi}+2\pi a\right)\sinh\frac{\pi\theta}{\xi}\,I_a(\theta)=\sinh\frac{\pi}{\xi}(i\pi-\eta\theta)\,I_a(2i\pi-\theta)+ \\ -\sinh\frac{\pi}{\xi}(i\pi+\eta\theta)\,I_a(2i\pi+\theta)\,, \tag{4.28}$$

with $\eta=1$. Making the identifications

$$\xi=\frac{\pi}{\lambda}, \qquad\qquad a=-\frac{\lambda}{2}\left(1\pm\frac{1}{3}\right)+k, \qquad k\in\mathbb{Z} \tag{4.29}$$

we rewrite (4.28) as

$$2\cos\frac{\pi\lambda}{3}\sinh\lambda\theta\,I_a(\theta)=\sinh\lambda(i\pi-\eta\theta)\,I_a(2i\pi-\theta)-\sinh\lambda(i\pi+\eta\theta)\,I_a(2i\pi+\theta)\,, \tag{4.30}$$

always with $\eta=1$. On the other hand, this equation coincides with (4.13) when $\eta=-1$. At $q=1$ (i.e. $\lambda=1/2$), however, the sign of η becomes immaterial and (4.30) exactly coincides with the equation satisfied by Ω_1. The functional equation (4.30) has infinitely many solutions (a solution multiplied by a $2i\pi$-periodic function of θ is a new solution) and it remains to be seen whether (4.19) with the identifications (4.29) and $\lambda=1/2$ can yield the function Ω_1 relevant for the percolation problem. From the known asymptotic behavior (see e.g. [78]) of the form factors (4.17) one deduces that $I_a(\theta)$ behaves as $\exp\left[\left(a-\frac{1}{2}\right)\theta\right]$ as $\theta\to+\infty$, a result which is not obvious from (4.19) but can be checked numerically. Comparing with (4.14) we see that I_a behaves asymptotically as Ω_1 provided we take $a=-1/6$, corresponding to the lower sign and $k=0$ in (4.29) with $\lambda=1/2$. The value $\xi=2\pi$ (i.e. $\lambda=1/2$) falls in the repulsive regime of the sine-Gordon model in which the only singularity of the form factors (4.17) within the strip $\mathrm{Im}\,\theta\in(0,2\pi)$ is the annihilation pole at $\theta=i\pi$. Since $F_0(\theta)$ is free of poles in the strip, the annihilation pole must be carried by $A^a_\pm$, and then by I_a. Any other pole of I_a in the strip could not cancel simultaneously in A^a_+ and A^a_-, and then $I_a(\theta)\big|_{\xi=2\pi}$ possesses a single pole at $\theta=i\pi$ in the strip $\mathrm{Im}\,\theta\in(0,2\pi)$, exactly as it is the case for $\Omega_q(\theta)$ in the Potts model. Summarizing, the functions $I_{-1/6}(\theta)\big|_{\xi=2\pi}$ and $\Omega_1(\theta)$ satisfy the same functional relations, have the same

asymptotic behavior and the same singularity structure; then we conclude that they coincide up to a normalization. Since we know that [78]

$$\mathrm{Res}_{\theta=i\pi} F^{a}_{+-}(\theta) = i(1-e^{-2i\pi a})\langle e^{ia\beta\varphi}\rangle, \tag{4.31}$$

we read from (4.17), (4.18) and (4.27) that $I_a(\theta)$ has residue i on the pole. Knowing also that the percolative order parameter P (probability that a site belongs to an infinite cluster) is related to the Potts magnetization as in (1.50)

$$P = \lim_{q\to 1} \frac{\langle\sigma_\alpha\rangle_\alpha}{q-1}, \tag{4.32}$$

and recalling (4.11), we conclude that $\Omega_1(\theta)$ has residue iP on the pole, and therefore

$$\Omega_1(\theta) = P\; I_{-1/6}(\theta)\big|_{\xi=2\pi}\,. \tag{4.33}$$

The values $\xi = 2\pi$, $a = -1/6$ fall in the range where (4.19) can be used to compute $\Omega_1(\theta)$ for real values of θ, which is sufficient for our purposes.

The two-kink form factor of the kink field $\mu_{\alpha\beta}$ was derived in [62] and it has the form

$$F^{\mu_{\alpha\beta}}_{\alpha\beta\gamma} = -\frac{\sqrt{3}\Gamma^K_{KK}}{4F_\Sigma(2\pi i/3)} F^{\mu_{\alpha\beta}}_{\beta\alpha} \frac{F_\Sigma(\theta)}{\sinh\frac{1}{2}\big(\theta+\frac{2\pi i}{3}\big)\sinh\frac{1}{2}\big(\theta-\frac{2\pi i}{3}\big)}, \tag{4.34}$$

with F_Σ and Γ^K_{KK} defined by

$$F_\Sigma(\theta) = -i\sinh\theta/2\,\exp\left[\int_0^\infty \frac{dx}{x}\frac{g_{\frac{2}{3}}(x)+g_\varepsilon(x)}{\sinh x}\sin^2\frac{(i\pi-\theta)x}{2\pi}\right], \tag{4.35}$$

$$\Gamma^K_{KK} = \Big[\frac{1}{\lambda}\sin\frac{2\pi\lambda}{3}\mathrm{e}^{\mathcal{A}(i\pi/3)}\Big]^{1/2}, \tag{4.36}$$

$\mathcal{A}(\theta)$ was considered in (2.107).

Form factors of the spin field σ_α and of the kink field $\mu_{\alpha\beta}$ are computed independently even tough they must be consistent with (4.2). The relative normalization is fixed by the asymptotic factorization property [79]

$$\lim_{\theta\to\infty} F^{\sigma_\alpha}_{\alpha\beta\alpha}(\theta) = \frac{q-1}{\langle\sigma_\alpha\rangle_\alpha}|F^{\mu_{\alpha\beta}}_{\beta\alpha}|^2, \tag{4.37}$$

	Triangular	**Square**
A^+	-4.37^a	-
Γ^+	0.0720^b	0.102^b
B	0.780^b	0.910^b
$2f^+_{2nd}$	0.520^b	0.520^b

Table 4.1: Lattice estimates of critical amplitudes for site percolation on triangular and square lattice. The superscripts *a, b* indicate Refs. [81, 82], respectively.

which in the limit $q \to 1$ reads

$$\lim_{\theta\to\infty} F^{\sigma_\alpha}_{\alpha\beta\alpha}(\theta)|_{q=1} = \frac{1}{P}|F^{\mu_{\alpha\beta}}_{\beta\alpha}|^2_{q=1}. \tag{4.38}$$

We observe that the factors $(q-1)$ can be explicitly isolated and cancel in the computation of the ratio (4.1). The same can be shown for the other amplitudes.

4.3 The universal amplitude ratios of random percolation

Near the percolation threshold the relations

$$S \simeq \Gamma^{\pm}|p-p_c|^{-\gamma}, \tag{4.39}$$

$$\xi \simeq f^{\pm}|p-p_c|^{-\nu}, \tag{4.40}$$

$$P \simeq B(p-p_c)^{\beta}, \tag{4.41}$$

$$\frac{\langle N_c\rangle}{N} \simeq A^{\pm}|p-p_c|^{2-\alpha}. \tag{4.42}$$

define the critical amplitudes for the mean cluster size, the correlation length, the order parameter and the mean cluster number per site, respectively; the superscripts $\pm$ refer to p_c being approached from below or from above. Below we consider both the second moment correlation length

$$\xi^2_{2nd} = \frac{1}{4}\frac{\int \mathrm{d}^2x\ |x|^2 P_{aa}(x)}{\int \mathrm{d}^2x\ P_{aa}(x)}, \tag{4.43}$$

and the true correlation length ξ_t defined by

$$P_{aa}(x) \sim e^{-|x|/\xi_t}, \qquad |x| \to \infty, \tag{4.44}$$

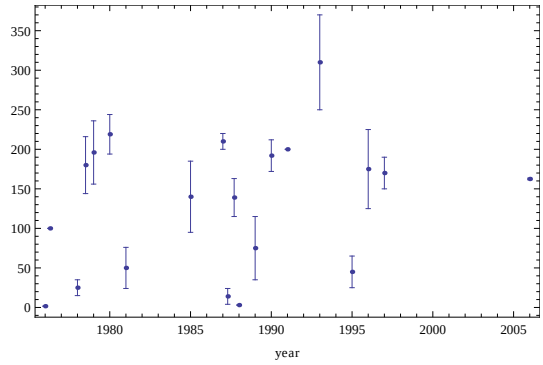

Figure 4.1: Numerical estimations for the amplitude size ratio Γ^+/Γ^-, obtained since 1976. See [86] for references.

where $P_{aa}(x)$ is the probability that x and the origin belong to the same finite cluster. It was shown in [62] that, in terms of the Potts kink mass m, ξ_t is $1/m$ at $p < p_c$ and $1/2m$ at $p > p_c$, and that

$$A^{\pm} = -\frac{1}{2\sqrt{3}\,(f_t^+)^2}. \tag{4.45}$$

Defining the amplitude combinations

$$R_\xi^+ = \left[\alpha(1-\alpha)(2-\alpha)A^+\right]^{1/2} f^+, \qquad U = 4\frac{B^2(f_{2nd}^+)^2}{\Gamma^+}, \tag{4.46}$$

which are universal due to the scaling relations $2-\alpha = 2\nu$ and $2\nu = 2\beta+\gamma$, (4.45) together with $\alpha = -2/3$ imply in particular

$$R_{\xi_t}^+ = \left[\frac{40}{27\sqrt{3}}\right]^{1/2} = 0.9248.., \tag{4.47}$$

a result recovered from a lattice computation in [80]. The result for $R_{\xi_{2nd}}^+$ in the two-kink approximation was computed in [62] and compares quite well with the lattice estimate obtained from the combination of the data collected in Table 1. The result (4.33) allows us to complete the two-kink computation of the universal ratios involving the amplitudes f_{2nd}^-, Γ^-, B. The field theoretical results for the complete list of *independent*[4] ratios involving the amplitudes (4.39–4.42) are

[4] In [62] the ratio $R_c = 4(R_{\xi_{2nd}}^+)^2/U$ was considered instead of U. The result R_c= 1.56 we obtain should be compared with ≈ 1.53 following from Table 4.1.

	Field Theory	**Lattice**
A^+/A^-	1	1^a
f_t^+/f_t^-	2	-
f_{2nd}^+/f_t^+	1.001	-
f_{2nd}^+/f_{2nd}^-	3.73	4.0 ± 0.5^c
Γ^+/Γ^-	160.2	162.5 ± 2^d
U	2.22	2.23 ± 0.10^e
$R_{\xi_{2nd}}^+$	0.926	$\approx 0.93^{a+b}$

Table 4.2: Universal amplitude ratios in two-dimensional percolation. The field theory results in the first two lines are exact, the others are obtained in the two-kink approximation. The superscripts *a, b, c, d, e* indicate Refs. [81, 82, 83, 84, 85], respectively.

summarized in Table 4.2 together with the most accurate lattice estimates. As remarked above, the comparison confirms in particular the effectiveness of the two-particle approximated form factor results in integrable field theory. The value 160.2 for the finite cluster size amplitude ratio is particularly interesting since the status of numerical results obtained in the past decades for this quantity was particularly controversial, see Fig. 4.1. Our theoretical result agrees with the last very accurate lattice determination by Jensen and Ziff [84].

Chapter 5

Crossing probability and number of crossing clusters away from criticality

In this chapter we discuss another classical observable of two-dimensional percolation, the vertical crossing probability P_v, i.e. the probability that on a rectangular geometry there exits at least a cluster connecting the horizontal sides. We reproduce in section 5.1 the result by Cardy at criticality. In the rest of the chapter we provide asymptotic formulae for P_v in the scaling limit above and below p_c, for the case in which both sides of the rectangle are much larger than the correlation length ξ. Our result agrees with available numerical data.

5.1 Cardy formula for the critical case

Consider a bond percolation problem defined on a regular two-dimensional lattice where bonds are occupied with probability p and focus on a rectangular window $\mathcal{L}$ of width L and height R. Configurations will contain or not at least one cluster of occupied bonds spanning between the two horizontal sides of the rectangle, see Fig. 5.1. The probability to generate a configuration with a vertical crossing (vertical crossing probability) is $P_v(L, R, p)|_{\mathcal{L}}$. Clearly if P_h is the horizontal

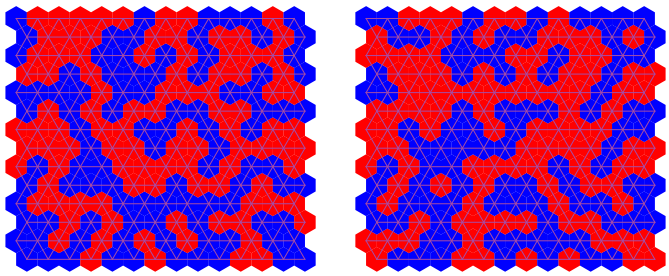

Figure 5.1: Critical site percolation problem on a square. The underlying lattice is triangular. Percolative clusters are red hexagons on the dual hexagonal lattice and the configuration on the right contains a vertically spanning cluster.

crossing probability,

$$P_v(L,R,p)|_{\mathcal{L}} = 1 - P_h(L,R,p^*)|_{\mathcal{L}^*} \tag{5.1}$$

and $P_v(L,R,p) = P_h(R,L,p)$, see Fig. 5.2. In (5.1) the duality transformation for percolation[1] corresponds to the replacement $p \to p^* = 1-p$ in the partition function

$$\sum_{\mathcal{G}\subseteq\mathcal{L}} p^{|E(\mathcal{G})|}(1-p)^{|E(\mathcal{L})|-|E(\mathcal{G})|}, \tag{5.2}$$

where we recall that $|E(\mathcal{L})| = |E(\mathcal{L}^*)|$ and $|E(\mathcal{G}')| + |E(\mathcal{G})| = |E(\mathcal{L})|$, $\mathcal{G}'$ being the complementary graph of $\mathcal{G}$ defined in section 1.1.

It is well known, since the numerical work of Langlands et al. [32], that in the scaling limit P_v is universal, i.e. its value does not dependent on the lattice and on the type of random percolation problem (site or bond) considered. In 1992 Cardy [33] determined the function $P_v(L,R,p_c)$ at the critical point with techniques of conformal field theory[2]. The derivation is a classic and simple example of the power of conformal invariance in two dimensions and we will present it now.

As we have seen many times in this thesis, an efficient theoretical approach to random percolation is to see it as a limiting case of the q-color Potts model. Consider the Potts partition function Z_{ud}^{lr} on the rectangle with boundary conditions

[1] We do not consider subtleties with the boundary of $\mathcal{L}$.

[2] See [87] for the probability of simultaneous horizontal and vertical crossing.

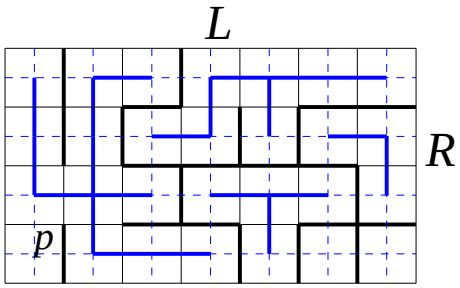

Figure 5.2: A particular configuration in a bond percolation problem on a square lattice. The graph $\mathcal{G}$ is shown in the figure (in black) together with its complementary graph $\mathcal{G}'$ (in blue). The edges of $\mathcal{G}'$ are all the edges of $\mathcal{L}^*$ which do not intersect the edges of $\mathcal{G}$. Clearly a vertical crossing in $\mathcal{G}$ forbids an horizontal crossing in $\mathcal{G}'$.

u, d, l and r on the upper, lower, left and right side, respectively. The boundary lattice spins can be fixed to have color α (α) or free (f). In the FK expansion of the Potts partition function, FK clusters touching a boundary with fixed boundary conditions carry one color, while FK clusters connected to a free boundary carry q colors. In particular if the spins on the upper side of the rectangle are fixed to have color β with $\beta \neq \alpha$, $Z^{ff}_{\alpha\beta}$ cannot contain vertically spanning clusters and we conclude

$$P_v = 1 - Z^{ff}_{\alpha\beta}|_{q=1}. \tag{5.3}$$

We observe for later purposes that the mean number of vertically spanning clusters $\bar{N}_v$ can be also computed starting from the FK representations

$$Z^{ff}_{\alpha\alpha} = \sum_{\mathcal{G}} p^{|E(\mathcal{G})|}(1-p)^{|E(\mathcal{L})|-|E(\mathcal{G})|} q^{N_b}, \tag{5.4}$$

$$Z^{ff}_{ff} = \sum_{\mathcal{G}} p^{|E(\mathcal{G})|}(1-p)^{|E(\mathcal{L})|-|E(\mathcal{G})|} q^{N_b+N_v+N_u+N_d}, \tag{5.5}$$

$$Z^{ff}_{\alpha f} = \sum_{\mathcal{G}} p^{|E(\mathcal{G})|}(1-p)^{|E(\mathcal{L})|-|E(\mathcal{G})|} q^{N_b+N_d}, \tag{5.6}$$

$$Z^{ff}_{f\alpha} = \sum_{\mathcal{G}} p^{|E(\mathcal{G})|}(1-p)^{|E(\mathcal{L})|-|E(\mathcal{G})|} q^{N_b+N_u}, \tag{5.7}$$

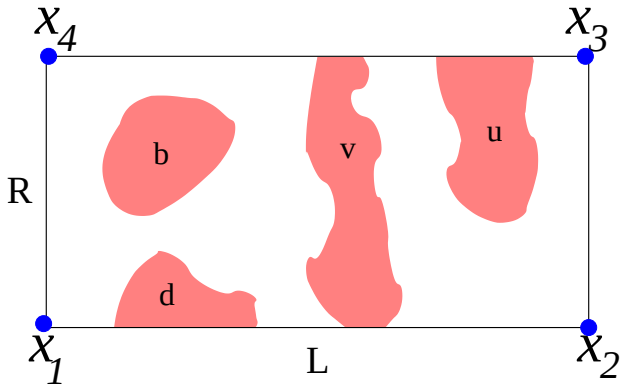

Figure 5.3: The different types of clusters which, depending on boundary conditions, determine the q-dependence of the Potts partition functions (5.4-5.7).

where N_b is the number of clusters which do not touch the horizontal boundaries, N_u (N_d) the number of clusters which touch the upper (lower) but not the lower (upper) boundary, and N_v the number of those touching both horizontal boundaries (see Fig. 5.3). It follows

$$\bar{N}_v = \lim_{q\to 1} \partial_q \log \frac{Z^{ff}_{ff} Z^{ff}_{\alpha\alpha}}{Z^{ff}_{\alpha f} Z^{ff}_{f\alpha}} \,. \tag{5.8}$$

We are now ready to derive the vertical crossing probability at criticality, where by scale invariance it is a function of the aspect ratio $r = R/L$ of the rectangle only.

In a conformal field theory the change of boundary conditions from a to b in the point x of the boundary is implemented by a local operator $\phi_{ab}(x)$, the so-called boundary condition changing operator, according to the general theory developed in [88]. The partition function $Z^{ff}_{\alpha\beta}$ is then a correlation function of four boundary conditions changing operators $\phi_{\alpha f}$ inserted at the vertices of the rectangle x_1, x_2, x_3 and x_4, Fig. 5.3

$$\langle \phi_{f\alpha}(x_1)\phi_{\alpha f}(x_2)\phi_{f\beta}(x_3)\phi_{\beta f}(x_4)\rangle. \tag{5.9}$$

The crucial point is the identification of the boundary condition changing operator $\phi_{\alpha f}$. The argument is the following. Consider the boundary condition changing

operator $\phi_{\alpha\beta}$, i.e. the kink field in the broken phase of the q-color Potts model. At the self dual point, its insertion at the boundary is equivalent to the insertion of the Potts order parameter σ_α with free boundary conditions. Such operator corresponds to the degenerate field $\phi_{1,3}$ for $q = 2$ and $q = 3$. Assuming that such identification also holds at $q = 1$ the field $\phi_{\alpha f}$ must satisfy the OPE

$$\phi_{\alpha f} \cdot \phi_{f\beta} \sim \delta_{\alpha\beta} + \phi_{\alpha\beta} + \dots \tag{5.10}$$

In particular $\phi_{1,2}$ obeys $\phi_{1,2} \cdot \phi_{1,2} \sim I + \phi_{1,3}$ and we conjecture that $\phi_{\alpha f}$ coincides with $\phi_{1,2}$ also at $q = 1$. The Verma module of $\phi_{1,2}$ contains a null vector at level two expressed as the linear combination of Laurent modes

$$\Big[\frac{3}{2(1+2h_{1,2})}L_{-1}^2 - L_{-2}\Big]|h_{1,2}\rangle, \tag{5.11}$$

leading to the differential equation in the complex plane

$$\left[\frac{3}{2(1+2h_{1,2})}\partial_{z_1}^2 + \sum_{p=2}^{4}\frac{1}{z_1 - z_p}\partial_{z_p}\right]\langle\phi_{1,2}(z_1)\phi_{1,2}(z_2)\phi_{1,2}(z_3)\phi_{1,2}(z_4)\rangle = 0 \tag{5.12}$$

for the four-point correlation function. From the Riemann mapping theorem we can suppose the z_i's with $z_i < z_{i+1}$ images on the real axis of the vertices of the rectangle. The conformal weight[3] $h_{1,2}$ vanishes at $q = 1$ and as a consequence the correlation function of the field $\phi_{1,2}$ is a function $F(\eta)$ of the harmonic ratio $\eta = \frac{z_{12}z_{34}}{z_{13}z_{24}}$ only. The points z_i, $i = 1, \dots, 4$ can be fixed on the real axis to be $z_1 = \eta$, $z_2 = 0$, $z_3 = \infty$ and $z_4 = 1$ by a Moebius transformation and the differential equation (5.12) simplifies to the hypergeometric equation

$$\Big[\eta(1-\eta)\frac{d^2}{d\eta^2} + \big(\frac{2}{3} - \frac{4}{3}\eta\big)\frac{d}{d\eta}\Big]F(\eta) = 0. \tag{5.13}$$

There are two independent solutions of this equation

$$F_1(\eta) = 1, \tag{5.14}$$

$$F_2(\eta) = 3\frac{\Gamma\big(\frac{2}{3}\big)}{\Gamma\big(\frac{1}{3}\big)^2}(1-\eta)^{1/3}{}_2F_1(\frac{1}{3}, \frac{2}{3}, \frac{4}{3}, 1-\eta) \tag{5.15}$$

[3]This can be checked from the formulae (1.32) substituting $t = 2$ which yields $c = 0$.

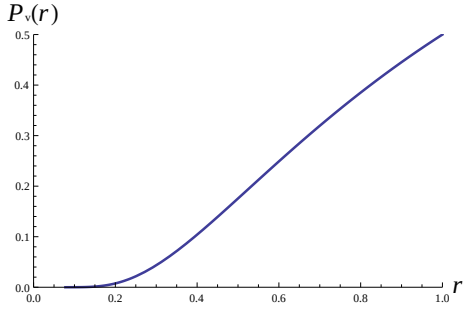

Figure 5.4: The vertical critical crossing probability $P_v(r)$ as a function of the aspect ratio r of the rectangle. Notice that $P_v(1) = 1/2$ as a consequence of the duality $P_v(r) + P_h(r) = 1$.

and we must establish to which linear combination of them $Z^{ff}_{\alpha\beta}$ corresponds. This is easily seen taking the limit $z_2 \to z_3$ corresponding to $\eta \to 1$. In this limit the OPE $\phi_{\alpha f}(z_2) \cdot \phi_{f\beta}(z_3)$ produces the field $\phi_{\alpha\beta}$ and must therefore be singular. We conclude $Z^{ff}_{\alpha\beta} = F_2(\eta)$, the other solution is the partition function $Z^{ff}_{\alpha\alpha}$ correctly normalized to one. The numerical prefactor in (5.15) ensures $Z^{ff}_{\alpha\beta}(0) = 1$ and the final result for the vertical crossing probability is then

$$P_v(\eta) = 1 - 3\frac{\Gamma\left(\frac{2}{3}\right)}{\Gamma\left(\frac{1}{3}\right)^2}(1-\eta)^{1/3}{}_2F_1(\frac{1}{3},\frac{2}{3},\frac{4}{3},1-\eta) \tag{5.16}$$

$$= 3\frac{\Gamma\left(\frac{2}{3}\right)}{\Gamma\left(\frac{1}{3}\right)^2}\eta^{1/3}{}_2F_1(\frac{1}{3},\frac{2}{3},\frac{4}{3},\eta). \tag{5.17}$$

The points on the real axis $z_1 = -k^{-1}$, $z_2 = -1$, $z_3 = 1$ and $z_4 = k^{-1}$ are the images under the Schwarz-Christoffel transformation of the vertices of rectangle with aspect ratio $r = \frac{K(1-k^2)}{2K(k^2)}$ where $K(u)$ is the complete elliptic integral of the first kind

$$K(u) = \int_0^1 \frac{dt}{\sqrt{(1-t^2)(1-ut^2)}}. \tag{5.18}$$

The prediction is then that the crossing probability is given by (5.16) with $\eta = \left((1-k)/(1+k)\right)^2$. A plot of $P_v(r)$ is given in Fig. 5.4.

We conclude noticing that the result for the crossing probability (5.16) has

been proved rigorously by SLE methods in [42]. Cardy also determined the mean number $\bar{N}_v$ of crossing clusters [89, 90] at p_c.

5.2 Off-critical percolation on the rectangle

5.2.1 Introduction

In the rest of this chapter we consider crossing probability and mean number of crossing clusters in the scaling limit close to p_c, where, due to the presence of a finite correlation length ξ (much larger than the lattice spacing), they separately depend on L/ξ and R/ξ. We consider the limit $L \gg \xi$ and use boundary integrable field theory to determine the mean number of vertically crossing clusters, i.e. the clusters which span between the sides of the rectangle separated by the distance R, in the limit $R \gg \xi$. The result we obtain below p_c is given in (5.63), (5.62). On the other hand, we can observe that for $R \to \infty$ below p_c vertical crossing becomes extremely rare, so that $P_v \equiv \mathrm{Prob}(N_v > 0) \sim \mathrm{Prob}(N_v = 1) \sim \bar{N}_v$; from the leading term in (5.62) we then obtain for the vertical crossing probability in the scaling limit below p_c the universal result

$$P_v(L,R) \sim A\,\frac{L}{\xi}\,\mathrm{e}^{-R/\xi}\,, \qquad L \gg \xi\,, \quad R \gtrsim L\,, \tag{5.19}$$

where

$$A = \frac{1}{2}\,(3-\sqrt{3})\,. \tag{5.20}$$

The correlation length ξ we refer to is defined by the decay of the probability $P_{aa}(r)$ that two points separated by a distance r are in the same finite cluster:

$$P_{aa}(r) \propto r^{-a}\,e^{-r/\xi}\,, \qquad r \to \infty\,, \tag{5.21}$$

with $a = 1/2$ below p_c and $a = 2$ above p_c [18]; ξ is related to the mass m appearing in (5.62) and throughout the chapter as

$$\xi = \begin{cases} 1/m\,, & p < p_c\,, \\ 1/2m\,, & p > p_c\,. \end{cases} \tag{5.22}$$

We will also give a direct derivation of (5.19) which also yields the next term, given by (5.65), in the large R expansion. The corresponding results in the scaling limit above p_c are given in (5.61) and (5.66).

It has been previously known [91, 92] that for $R = L \gg \xi$ the crossing probability is a function of $L|p - p_c|^\nu$ which decays exponentially to zero below p_c and to one above, a feature investigated numerically in [92, 93, 94, 95].

5.2.2 Field theory and massive boundary states

Let us begin our field theoretical considerations for the scaling limit considering an infinitely long horizontal strip of height R. With imaginary time running upwards, the partition functions on the strip can be written as

$$Z_{ud}^{lr} = \langle B_u | \mathrm{e}^{-RH} | B_d \rangle_{l,r} \,, \tag{5.23}$$

where H is the Hamiltonian of the quantum system living in the infinite horizontal dimension, $|B_{d,u}\rangle$ are boundary states specifying initial and final conditions, and the vertical boundary conditions at infinity have the role of selecting the states which can propagate between the horizontal boundaries. Integrability of the scaling Potts model [27] allows us to work in the framework of integrable field theories for which the bulk dynamics is entirely specified by the Faddeev-Zamolodchikov commutation rules (see e.g. [60])

$$A_i^\dagger(\theta_1) A_j^\dagger(\theta_2) = S_{ij}^{i'j'}(\theta_1 - \theta_2) A_{j'}^\dagger(\theta_2) A_{i'}^\dagger(\theta_1) \,, \tag{5.24}$$

$$A^i(\theta_1) A_j^\dagger(\theta_2) = S_{ji'}^{j'i}(\theta_2 - \theta_1) A_{j'}^\dagger(\theta_2) A^{i'}(\theta_1) + 2\pi \delta_j^i \delta(\theta_1 - \theta_2) \,, \tag{5.25}$$

where $A_i^\dagger(\theta)$ and $A^i(\theta)$ are creation and annihilation operators for a particle of species i with rapidity[4] θ, and $S_{ij}^{i'j'}(\theta)$ are two-body scattering amplitudes satisfying, in particular, unitarity

$$S_{ij}^{i'j'}(\theta) S_{i'j'}^{i''j''}(-\theta) = \delta_i^{i''} \delta_j^{j''} \tag{5.26}$$

and crossing symmetry

$$S_{ij}^{i'j'}(\theta) = S_{j\bar{i}'}^{j'\bar{i}}(i\pi - \theta). \tag{5.27}$$

Generic boundary states $|B_a\rangle$ can be written as superpositions of asymptotic states of the particles created by $A_i^\dagger$, with vanishing total momentum in order to preserve horizontal translation invariance. The additional constraints coming

[4]Energy and momentum of a particle with mass m are given by $(e, p) = (m \cosh\theta, m \sinh\theta)$.

from the requirement that a boundary condition preserves integrability were discovered in [96]. In particular, particles carrying momentum can only appear in pairs with vanishing total momentum. On the other hand, for the case of our interest of a theory satisfying

$$S_{ij}^{i'j'}(0) = (-1)\,\delta_i^{j'}\,\delta_j^{i'}\,, \tag{5.28}$$

states containing $k \geq 2$ particles of zero momentum are forbidden by (5.24). Finally $|B_a\rangle$ takes the form

$$|B_a\rangle = \mathcal{S}_a \exp\Big[\frac{1}{2}\int_{-\infty}^{\infty}\frac{d\theta}{2\pi}\;\mathcal{P}_a(\theta)\Big]|\Omega\rangle\,, \tag{5.29}$$

where $|\Omega\rangle$ is the vacuum state and

$$\mathcal{S}_a = 1 + \tilde{g}_a^i A_i^\dagger(0)\,, \tag{5.30}$$

$$\mathcal{P}_a(\theta) = K_a^{ij}(\theta)A_i^\dagger(-\theta)A_j^\dagger(\theta)\,. \tag{5.31}$$

The boundary pair emission amplitudes $K_a^{ij}(\theta)$ satisfy equations involving the bulk amplitudes $S_{ij}^{i'j'}(\theta)$, and the constants $\tilde{g}_a^i$ follow from the relations[5]

$$2i\,\mathrm{Res}_{\theta=0}K_a^{ij}(\theta) = g_a^i g_a^j\,, \tag{5.32}$$

$$\tilde{g}_a^i = \frac{g_a^i}{2}\,. \tag{5.33}$$

The exponential form of the boundary state is a consequence of the boundary Yang-Baxter equations, which give in particular $[\mathcal{P}_a(\theta), \mathcal{P}_a(\theta')] = [\mathcal{P}_a(\theta), \mathcal{S}_a] = 0$ [96].

We are now ready to use this formalism to evaluate the Potts partition functions entering (5.8). The Potts field theory, i.e. the integrable field theory which describes the scaling limit of the Potts model in two dimensions, was solved exactly in [27] in the language of the spontaneously broken phase above J_c, in which the elementary excitations are kinks $A_{\beta\alpha}^\dagger(\theta)|\Omega_\alpha\rangle$ interpolating between degenerate ferromagnetic vacua $|\Omega_\alpha\rangle$ and $|\Omega_\beta\rangle$ with different color. The vacua satisfy $\langle\Omega_\alpha|\Omega_\beta\rangle = \delta_{\alpha\beta}$ and the admissible multi-kink states have the form

$$A_{\alpha_{n+1}\alpha_n}^\dagger(\theta_n)\ldots A_{\alpha_3\alpha_2}^\dagger(\theta_2)A_{\alpha_2\alpha_1}^\dagger(\theta_1)|\Omega_{\alpha_1}\rangle\,. \tag{5.34}$$

[5] See [97, 98] for the factor 1/2 in (5.33).

For these topological excitations the Faddeev-Zamolodchikov commutation relations take the form,

$$A^\dagger_{\alpha\beta}(\theta_1)A^\dagger_{\beta\gamma}(\theta_2) = \sum_\delta S^{\beta\delta}_{\alpha\gamma}(\theta_1-\theta_2)A^\dagger_{\alpha\delta}(\theta_2)A^\dagger_{\delta\gamma}(\theta_1)\,, \tag{5.35}$$

$$A_{\alpha\beta}(\theta_1)A^\dagger_{\beta\gamma}(\theta_2) = \sum_\delta S^{\gamma\alpha}_{\beta\delta}(\theta_2-\theta_1)A^\dagger_{\alpha\delta}(\theta_2)A_{\delta\gamma}(\theta_1) + 2\pi\delta_{\alpha\gamma}\delta(\theta_1-\theta_2)\,, \tag{5.36}$$

where invariance of the theory under permutations of the colors allows for the four nonequivalent scattering amplitudes; they are given explicitly in section 2.7 and obey (5.28) in the form

$$S^{\beta\delta}_{\alpha\gamma}(0) = (-1)\,\delta_{\beta\delta}\,. \tag{5.37}$$

Both fixed (to a color α) and free (f) boundary conditions are integrable and the corresponding pair emission amplitudes were determined in [99]. They determine the boundary states $|B_\alpha\rangle$ and $|B_f\rangle$ in the form that we now specify; in the following q will be parameterized as $q = 4\sin^2\!\big(\frac{\pi\lambda}{3}\big)$, so that $\lambda \to 1/2$ corresponds to the percolation limit. For fixed boundary conditions we have

$$|B_\alpha\rangle = \exp\Big[\frac{1}{2}\int_{-\infty}^{\infty}\frac{d\theta}{2\pi}\;\mathcal{P}_\alpha(\theta)\Big]|\Omega_\alpha\rangle\,, \tag{5.38}$$

with

$$\mathcal{P}_\alpha(\theta) = K_0(\theta)\sum_{\beta\neq\alpha}A^\dagger_{\alpha\beta}(-\theta)A^\dagger_{\beta\alpha}(\theta)\,, \tag{5.39}$$

$$K_0(\theta) = i\tanh\Big(\frac{\theta}{2}\Big)\exp\bigg[-\int_0^\infty\frac{dt}{t}\,\frac{n_\lambda(t)}{2\cosh t}\sinh\Big(t-\frac{2\theta t}{i\pi}\Big)\bigg], \tag{5.40}$$

$$n_\lambda(t) = \frac{\sinh\big(\frac{t}{6}+\frac{t}{2\lambda}\big)-\sinh\big(\frac{3t}{2}-\frac{t}{2\lambda}\big)}{\sinh\big(\frac{t}{2\lambda}\big)\cosh\big(\frac{t}{2}\big)}\,; \tag{5.41}$$

the integral in (5.40) is convergent for $1/2 \le \lambda < 1$. $K_0(\theta)$ satisfies the boundary "cross-unitarity" relation

$$K_0(\theta) = \big[S^{\beta\beta}_{\alpha\alpha}(2\theta) + (q-2)S^{\beta\gamma}_{\alpha\alpha}(2\theta)\big]K_0(-\theta)\,, \tag{5.42}$$

which together with (5.37) implies $K_0(0) = 0$, as already apparent from (5.40); the absence of a pole at $\theta = 0$ explains $\mathcal{S}_\alpha = 1$.

For free boundary conditions we have instead

$$|B_f\rangle = \sum_\alpha \mathcal{S}_f^\alpha \, \exp\Big[\frac{1}{2}\int_{-\infty}^{\infty} \frac{d\theta}{2\pi}\, \mathcal{P}_f^\alpha(\theta)\Big]|\Omega_\alpha\rangle\,, \tag{5.43}$$

with

$$\mathcal{P}_f^\alpha(\theta) = \sum_{\beta\neq\alpha}\left[K_1(\theta)\, A^\dagger_{\alpha\beta}(-\theta)A^\dagger_{\beta\alpha}(\theta) + K_2(\theta)\sum_{\gamma\neq\alpha,\beta} A^\dagger_{\gamma\beta}(-\theta)A^\dagger_{\beta\alpha}(\theta)\right], \tag{5.44}$$

$$K_1(\theta) = (q-3)\frac{\sinh\big[\lambda(4i\pi/3-2\theta)\big]}{\sinh\big(2\lambda\theta\big)}\frac{\Gamma\big(-4\lambda/3+2\hat\theta+1\big)\Gamma\big(7\lambda/3-2\hat\theta\big)}{\Gamma\big(2\lambda/3-2\hat\theta+1\big)\Gamma\big(\lambda/3+2\hat\theta\big)}\,Q(\theta)\,, \tag{5.45}$$

$$K_2(\theta) = \frac{\sin\frac{2\pi\lambda}{3}}{\sin\frac{\pi\lambda}{3}}\frac{\sinh\big[\lambda(i\pi-2\theta)\big]}{\sinh\big(2\lambda\theta\big)}\frac{\sinh\big[\lambda(4i\pi/3-2\theta)\big]}{\sinh\big[\lambda(-2i\pi/3+2\theta)\big]}\times \\ \times\frac{\Gamma\big(-4\lambda/3+2\hat\theta+1\big)\Gamma\big(7\lambda/3-2\hat\theta\big)}{\Gamma\big(2\lambda/3-2\hat\theta+1\big)\Gamma\big(\lambda/3+2\hat\theta\big)}\,Q(\theta)\,, \tag{5.46}$$

$$Q(\theta) = \exp\left[-\int_0^\infty \frac{dt}{t}\,\frac{\mathrm{e}^{-2t}\sinh\big(\frac{5t}{6}-\frac{t}{2\lambda}\big)-\sinh\big(\frac{3t}{2}-\frac{t}{2\lambda}\big)}{2\cosh t\sinh\big(\frac{t}{2\lambda}\big)\cosh\big(\frac{t}{2}\big)}\sinh\Big(t-\frac{2\theta t}{i\pi}\Big)\right], \tag{5.47}$$

where $\hat\theta \equiv \frac{\lambda\theta}{i\pi}$; the integral in (5.47) is again convergent for $1/2 \le \lambda < 1$. In this case the residue at $\theta = 0$ is non-zero and gives[6]

$$\tilde g_f^2 = \frac{i}{2}\mathrm{Res}_{\theta=0}K_1(\theta) = \frac{i}{2}\mathrm{Res}_{\theta=0}K_2(\theta) = \frac{(3-q)}{4}\frac{\sin\frac{4\pi\lambda}{3}}{\lambda}\frac{\Gamma\big(1-\frac{4\lambda}{3}\big)\Gamma\big(\frac{7\lambda}{3}\big)}{\Gamma\big(1+\frac{2\lambda}{3}\big)\Gamma\big(\frac{\lambda}{3}\big)}Q(0)\,, \tag{5.48}$$

$$\mathcal{S}_f^\alpha = 1 + \tilde g_f \sum_{\beta\neq\alpha} A^\dagger_{\beta\alpha}(0)\,. \tag{5.49}$$

We also quote the boundary cross-unitarity conditions

$$K_1(\theta) = \big[S^{\beta\beta}_{\alpha\alpha}(2\theta) + (q-2)S^{\beta\gamma}_{\alpha\alpha}(2\theta)\big]K_1(-\theta), \tag{5.50}$$

$$K_2(\theta) = \big[S^{\beta\beta}_{\alpha\gamma}(2\theta) + (q-3)S^{\beta\delta}_{\alpha\gamma}(2\theta)\big]K_2(-\theta). \tag{5.51}$$

[6]There appears to be a typo in eq. (48) of [99]. In particular it does not reproduce $\tilde g_f^2\big(\frac{3}{4}\big) = 1$ for the Ising model (q=2).

5.2.3 Partition functions and final results

In principle, the knowledge of the bulk and boundary amplitudes should allow the study of partition functions on the strip for any R through the boundary version [100] of the thermodynamic Bethe ansatz (TBA) [101]. In practice, however, the very non-trivial structure of Potts field theory seriously complicates the task[7]. More pragmatically, here we plug the explicit expressions for $|B_\alpha\rangle$ and $|B_f\rangle$ into (5.23) and exploit the fact that the states (5.34) are eigenstates of the Hamiltonian H with eigenvalues $m\sum_{i=1}^n \cosh\theta_i$, m being the mass of the kinks. This leads to a large R expansion for the partition functions for which we compute below the terms coming from one- and two-kink states.

Since we work in the kink basis, the partition functions we obtain in this way are those above J_c, that we denote $\tilde{Z}^{lr}_{ud}$, keeping the notation Z^{lr}_{ud} for those below J_c. As an illustration, for $\tilde{Z}^{ff}_{\alpha\alpha}$ expansion of the boundary state leads to

$$\tilde{Z}^{ff}_{\alpha\alpha}(R) = 1+\frac{1}{4}\int_{-\infty}^{\infty}\frac{\mathrm{d}\theta\mathrm{d}\theta'}{(2\pi)^2}K_0^*(\theta')K_0(\theta)\mathrm{e}^{-2mR\cosh\theta}\sum_{\beta,\gamma\neq\alpha}M_{\alpha\beta\gamma\alpha}(\theta,\theta')+O(\mathrm{e}^{-4mR})\,, \tag{5.52}$$

$$\begin{aligned} M_{\alpha\beta\gamma\alpha}(\theta,\theta') &\equiv \langle\Omega_\alpha|A_{\alpha\beta}(\theta')A_{\beta\alpha}(-\theta')A^\dagger_{\alpha\gamma}(-\theta)A^\dagger_{\gamma\alpha}(\theta)|\Omega_\alpha\rangle \\ &= (2\pi)^2\big[\delta(\theta'-\theta)\big]^2\delta_{\beta\gamma}+(2\pi)^2\big[\delta(\theta'+\theta)\big]^2S^{\gamma\beta}_{\alpha\alpha}(2\theta')\,; \end{aligned} \tag{5.53}$$

the last equality follows from formal use of (5.36) and can be associated to the diagrams shown in Fig. 5.5. If $L\to\infty$ denotes the horizontal size of the system, the squared delta functions in (5.53) admit the usual regularization[8]

$$\big[\delta(\theta'\pm\theta)\big]^2 \to \delta(\theta'\pm\theta)\,\frac{mL}{2\pi}\,\cosh\theta\,; \tag{5.54}$$

free vertical boundary conditions have been imposed making no selection on the kink states which propagate between the horizontal boundaries. Exploiting boundary cross-unitarity (5.42) and real analiticity $K_0(-\theta)=K_0^*(\theta)$, $\theta\in\mathbb{R}$, we then obtain

[7] See [102] for the state of the art of TBA in the Potts model.

[8] It is important to stress that, as observed for other models in [100] (see also [103]), contributions to (5.23) coming from states with more than two particles produce singularities whose regularization depends in general on the interaction. This is what makes difficult the determination of additional terms in the large R expansion within the approach we are following.

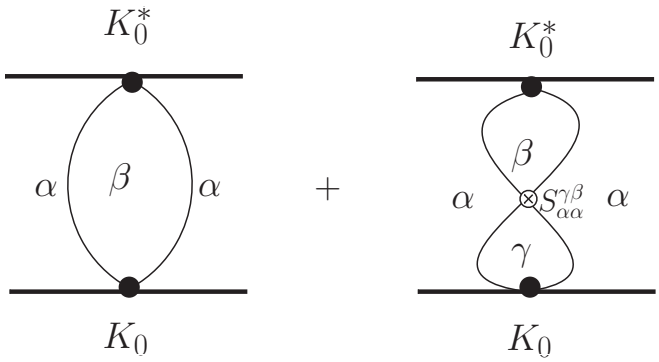

Figure 5.5: Diagrammatic interpretation of the two contributions entering the matrix element (5.53).

$$\tilde{Z}^{ff}_{\alpha\alpha}(L,R) = 1 + (q-1)\, mL\, F_{\alpha\alpha}(R) + O(\mathrm{e}^{-4mR})\,, \qquad mL \gg 1\,, \tag{5.55}$$

$$F_{\alpha\alpha}(R) = \int_0^\infty \frac{\mathrm{d}\theta}{2\pi}\ \cosh\theta\ |K_0(\theta)|^2\ \mathrm{e}^{-2mR\cosh\theta}\,. \tag{5.56}$$

Similarly one finds for $mL \gg 1$

$$\tilde{Z}^{ff}_{ff}(L,R) = q\left[1 + (q-1)\, mL\left(\tilde{g}_f^2\ \mathrm{e}^{-mR} + F_{ff}(R)\right)\right] + O(\mathrm{e}^{-3mR}), \tag{5.57}$$

$$F_{ff}(R) = \int_0^\infty \frac{\mathrm{d}\theta}{2\pi}\ \cosh\theta\ \left(|K_1(\theta)|^2 + (q-2)|K_2(\theta)|^2\right)\ \mathrm{e}^{-2mR\cosh\theta}\,, \tag{5.58}$$

$$\tilde{Z}^{ff}_{\alpha f}(L,R) = 1 + (q-1)\, mL\, F_{\alpha f}(R) + O(\mathrm{e}^{-4mR}), \tag{5.59}$$

$$F_{\alpha f}(R) = \int_0^\infty \frac{\mathrm{d}\theta}{2\pi}\ \cosh\theta\, \mathrm{Re}\big[K_0^*(\theta) K_1(\theta)\big]\ \mathrm{e}^{-2mR\cosh\theta}\,, \tag{5.60}$$

and $\tilde{Z}^{ff}_{f\alpha} = \tilde{Z}^{ff}_{\alpha f}$. The partition functions $\tilde{Z}^{\beta\alpha}_{ud}$ with fixed vertical boundary conditions are obtained taking off from $\tilde{Z}^{ff}_{ud}$ the contribution of the states which are not of the form (5.34) with $\alpha_1 = \alpha$ and $\alpha_{n+1} = \beta$.

From these results we obtain for the mean number of crossing clusters in the scaling limit above p_c the universal result

$$\tilde{\bar{N}}_v(L,R) = \lim_{q\to 1} \partial_q \log \frac{\tilde{Z}^{ff}_{\alpha\alpha}\,\tilde{Z}^{ff}_{ff}}{\tilde{Z}^{ff}_{f\alpha}\,\tilde{Z}^{ff}_{\alpha f}} \sim 1 + mL\left[\Phi(R) + O(\mathrm{e}^{-3mR})\right] , \qquad mL \gg 1 , \tag{5.61}$$

$$\Phi(R) = A\,\mathrm{e}^{-mR} + \left[F_{ff}(R) + F_{\alpha\alpha}(R) - 2F_{\alpha f}(R)\right]_{q=1} , \tag{5.62}$$

where $A = \tilde{g}_f^2|_{q=1}$ reduces to (5.20). The additive term 1 in (5.61) is produced by the overall factor q in (5.57) and accounts for the contribution of the infinite cluster in the limit $R \to \infty$. Notice that any normalization of the boundary states other than the one we used would anyway cancel in the combination of partition functions in (5.61).

In order to determine the mean number of crossing clusters below p_c we have to use the duality [22] of the Potts model to connect the partition functions (5.4-5.7) below J_c to the partition functions $\tilde{Z}^{lr}_{ud}$ above J_c we have computed. Duality maps free boundary conditions into fixed boundary conditions and viceversa (see e.g. [53]). For our present purpose of counting the vertically crossing clusters, it is useful to observe that fixing the spins to the color α on both vertical sides, rather than leaving them free, has the only effect that the clusters touching at least one vertical side are not counted. Below p_c, where all clusters are finite with a mean linear extension of order ξ, such a boundary term does not affect $\bar{N}_v$, which is extensive in L in the limit $L/\xi \to \infty$ we are considering. So we can use (5.8) with the replacement $ff \to \alpha\alpha$ in the vertical boundary conditions, and use duality[9] to obtain in the scaling limit below p_c

$$\bar{N}_v(L,R) \sim \left[\lim_{q\to 1} \partial_q \log \frac{\tilde{Z}^{ff}_{\alpha\alpha}\,\tilde{Z}^{ff}_{ff}}{\tilde{Z}^{ff}_{f\alpha}\,\tilde{Z}^{ff}_{\alpha f}}\right]_{\text{extensive part}} = mL\left[\Phi(R) + O(\mathrm{e}^{-3mR})\right] , \qquad mL \gg 1 . \tag{5.63}$$

A different derivation of this result is given in the Appendix.

The functions $F_{ff}(R)|_{q=1}$ and $F_{\alpha f}(R)|_{q=1}$ in (5.62) are well defined in spite of the poles at $\theta = 0$ in the amplitudes $K_1(\theta)$ and $K_2(\theta)$ contained in the integrands

[9] In principle $Z^{\alpha\alpha}_{ff}$ could be mapped into a linear combination of $\tilde{Z}^{ff}_{\alpha\alpha}$ and $\tilde{Z}^{ff}_{\alpha\beta}$, $\alpha \neq \beta$. However, it follows from (5.38) that the latter partition function vanishes identically on the infinitely long strip; at large L it is suppressed as e^{-mL}.

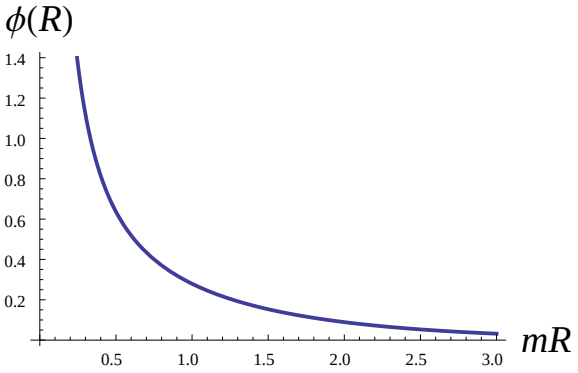

mR	$\Phi(R)$
0.5	0.63684
1	0.27929
1.5	0.15304
2	0.08910
2.5	0.05304
3	0.03188

Figure 5.6: Plot of the function (5.62); few values are given in the table.

in (5.58) and (5.60). If the convergence of (5.60) simply follows from $K_0(0) = 0$, the case of F_{ff} is more subtle. Consider indeed the Laurent expansions $K_i(\theta) = a_{-1}/\theta + a_0^{(i)} + a_1^{(i)}\,\theta + \ldots$, $i = 1, 2$. If $\theta \in \mathbb{R}$, due to the relation $K_i^*(\theta) = K_i(-\theta)$ the coefficients $a_{2k-1}^{(i)}$ are purely imaginary and the coefficients $a_{2k}^{(i)}$ are instead real for all non-negative integers k; this in turn implies that the combination $|K_1(\theta)|^2 - |K_2(\theta)|^2$ entering $F_{ff}(R)|_{q=1}$ does not contain any double or single pole at $\theta = 0$.

The function (5.62) is plotted in Fig. 5.6, where some numerical values are also listed. Since (5.63) is extensive in L for any R, it is tempting to check what our large R result gives in the conformal limit $mR \to 0$, for which the result $\bar{N}_v \sim (\sqrt{3}/4)L/R = (0.433..)L/R$, $L \gg R$, is known from [89]. Using the large θ limits $K_0 \to \mathrm{e}^{i\pi/3}$, $K_1 \to -2\mathrm{e}^{i\pi/3}$ and $K_2 \to -\sqrt{3}\mathrm{e}^{i\pi/6}$ at $q = 1$, (5.63) gives[10] $3/(2\pi)(L/R) = (0.477..)L/R$, with a 10% deviation from the exact result suggesting that (5.62) may still provide a good approximation for mR of order 1.

We already explained how (5.19) follows from (5.63). The same result also follows from (5.2) which in the scaling limit leads to

$$P_v = 1 - \tilde{P}_h = \lim_{q\to 1} \tilde{Z}_{ff}^{\alpha\beta}\,. \tag{5.64}$$

The partition function $\tilde{Z}_{ff}^{\alpha\beta}$ is obtained picking up in (5.57) only the contributions of the states compatible with the vertical boundary conditions $\alpha\beta$. In particular,

[10] Given $F(y) = \int_0^\infty \mathrm{d}x\ \cosh x\ \mathrm{e}^{-y\cosh x} f(x)$, with $\lim_{x\to\infty} f(x) = \alpha$, we have $F(y) \to \alpha/y$ for $y \to 0$.

since we are no longer summing over α and β, the one-kink contribution in e^{-mR} now appears with multiplicity one rather than $q(q-1)$, and this gives (5.19) back[11]. Concerning the two-kink contribution, only the term containing $|K_2|^2$ survives now, again without the prefactor $q(q-1)$; $|K_2|^2$ contains a singularity of the form $4\tilde{g}_f^4/\theta^2$ at $\theta = 0$ which has to be subtracted[12] because produced by the propagation of states created by $A^\dagger_{\alpha\gamma}(0)A^\dagger_{\gamma\beta}(0)$ which, as already observed, are not compatible with (5.35) and (5.37). Hence, the contribution of order $e^{-2R/\xi}$ to be added to (4.32) is

$$U(L,R) = -mL \int_0^\infty \frac{\mathrm{d}\theta}{2\pi}\ \cosh\theta\ \left(|K_2(\theta)|^2_{q=1}\, \mathrm{e}^{-2mR\cosh\theta} - \frac{4A^2}{\sinh^2\theta}\, \mathrm{e}^{-2mR} \right). \quad (5.65)$$

The replacement $1/\theta^2 \to 1/\sinh^2\theta$, relevant for the convergence of the integral, comes from the fact that $m\int d\theta \cosh\theta = \int dp$, and in the momentum variable p the function $|K_2|^2$ diverges as $1/p^2$.

The vertical crossing probability above p_c is $\tilde{P}_v = 1 - \lim_{q\to 1} \tilde{Z}^{ff}_{\alpha\beta}$. We already observed that $\tilde{Z}^{ff}_{\alpha\beta}$ vanishes exponentially at large L, in agreement with the expectation that, due to the presence of an infinite cluster, above p_c the crossing probability tends to 1 as we enlarge the window. More precisely, duality gives

$$\begin{aligned} \tilde{P}_v(L,R) &= 1 - P_h(L,R) \\ &\sim 1 - A\,\frac{R}{2\xi}\,\mathrm{e}^{-L/2\xi} - U(R,L)\,, \qquad R \gg \xi\,,\quad L \gtrsim R\,, \end{aligned} \quad (5.66)$$

where the last line takes (5.22) into account and holds at order $e^{-L/\xi}$.

A scaling analysis of Monte Carlo data for $P_v(L,R)$ in terms of a single scaling variable was performed in [34] and further discussed in [104, 105]. It is relevant that the data of [34] allow a comparison with our results. The inset of Fig. 5.7 shows the data of [34] for the crossing probability in bond percolation on the square lattice of size $L = R = 256$ lattice units; they satisfy the duality relation (5.64) for the crossing probability above and below p_c (which for $R = L$ specializes

[11] Notice that our normalization of the boundary states ensures the conditions $\lim_{q\to 1} \tilde{Z}^{ff}_{ff} = \lim_{q\to 1} \tilde{Z}^{\alpha\alpha}_{\alpha\alpha} = 1$ required for percolation.

[12] The result obtained in [103] for simpler models (with purely transmissive scattering) by a TBA analysis amounts to such a subtraction.

to $P_v = 1 - \tilde{P}_v$) up to discrepancies to be ascribed to a mixing of finite size effects, corrections to scaling and statistical errors. In principle comparison of the data to (4.32), (5.20) and (5.66) allows to fit the value of the only unknown parameter, i.e. the non-universal amplitude m_0 entering the relation $m = m_0|p - p_c|^\nu$, $\nu = 4/3$. We fit $m_0 \approx 5.7$ from the tail of the crossing probability below p_c, and $m_0 \approx 5.9$ from the tail above p_c; consider that for $R = 256$ and mR around 10, ξ is around 25 below p_c and around 12 above, so that the analysis is almost certainly affected by non-negligible corrections to scaling. On the other hand, the value $2\xi^0_{2nd} \approx 0.37$ was measured in [85] for the amplitude of the second moment correlation length in bond percolation on the square lattice below p_c, and it is known from [18] that $m_0 = a/\xi^0_{2nd} \approx 5.4\, a$, with a equal 1 up to corrections that are not expected to exceed few percents. A comparison between the data for the tails and (4.32), (5.20) is given in Fig. 5.7; the subleading term (5.65) is always very small and totally negligible in the range of mR shown in the figure. Putting all together, our conclusion is that the data[13] of [34] are consistent with the results of this chapter within the numerical uncertainties; an unambiguous verification will require simulations expressly targeting the tails on larger lattices.

Appendix

Let us denote by $\phi_{ab}(x)$ the field [88] whose insertion at point x on the boundary changes the boundary condition from a to b; of course ϕ_{aa} coincides with the identity I. If $x_1, \ldots, x_4$ are the coordinates of the corners of the rectangle starting from the left upper corner and moving clockwise, we have[14]

$$G_{lurd} \equiv \langle \phi_{lu}(x_1)\phi_{ur}(x_2)\phi_{rd}(x_3)\phi_{dl}(x_4)\rangle_{J \le J_c} = Z^{lr}_{ud}/Z^{ll}_{ll}\,, \tag{5.67}$$

$$\tilde{G}_{lurd} \equiv \langle \phi_{lu}(x_1)\phi_{ur}(x_2)\phi_{rd}(x_3)\phi_{dl}(x_4)\rangle_{J^* \ge J_c} = \tilde{Z}^{lr}_{ud}/\tilde{Z}^{ll}_{ll}\,. \tag{5.68}$$

The fields ϕ_{ab} obey the natural operator product expansion [33]

$$\phi_{\alpha f} \cdot \phi_{f\beta} = \delta_{\alpha\beta}\, I + c\,(1 - \delta_{\alpha\beta})\mu_{\alpha\beta} + \cdots\,, \tag{5.69}$$

[13] Aspect ratios $L/R > 1$ were also analyzed in [34], but for these cases the range of mL covered by the data is not large enough to allow comparison with (5.66).

[14] At J_c analogous relations were used in [33, 89].

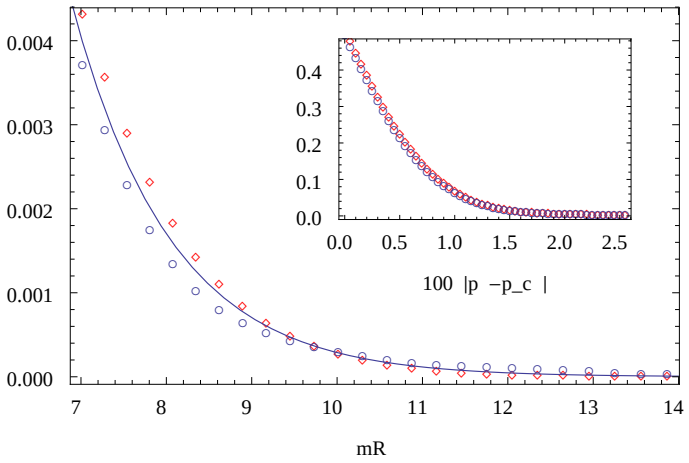

Figure 5.7: The inset shows Monte Carlo data from [34] for the crossing probability below p_c (diamonds) and for the complement to 1 of the crossing probability above p_c (circles); the data refer to bond percolation on the square lattice with $L = R = 256$. The tails are plotted against mR using $m = m_0|p - p_c|^{4/3}$, with $m_0 = 5.8$. The continuous curve is the result (4.32), (5.20), (5.66), i.e. $A\, mR\, e^{-mR}$.

that we write symbolically omitting the coordinate dependence, and using the notation $\mu_{\alpha\beta} = \phi_{\alpha\beta}$ for the kink field which switches between fixed boundary conditions with different colors. The field $\mu_{\alpha\beta}(x)$ is dual to the Potts spin field $\sigma_\alpha(x) = q\delta_{s(x),\alpha} - 1$, and the relation

$$\langle \sigma_\alpha(x)\sigma_\beta(y)\rangle_{J\le J_c} = (q\delta_{\alpha\beta} - 1)\,\langle \mu_{\gamma\delta}(x)\mu_{\delta\gamma}(y)\rangle_{J^*\ge J_c} \tag{5.70}$$

holds (see [16]). Since duality exchanges fixed and free boundary conditions, we then write the dual of (5.69) as

$$\phi_{f\alpha}\cdot\phi_{\alpha f} = I + c'\,\sigma_\alpha + \cdots\,, \tag{5.71}$$

with c' a new structure constant. For the boundary correlators G_{lurd}, we have simple duality relations like $G_{fff\alpha} = \tilde{G}_{\alpha\alpha\alpha f}$, but also non-trivial ones like

$$G_{f\alpha f\alpha} = a_1\,\tilde{G}_{\alpha f\alpha f} + a_2\,\tilde{G}_{\alpha f\beta f}\,, \tag{5.72}$$

$$G_{f\alpha f\beta} = a_3\,\tilde{G}_{\alpha f\alpha f} + a_4\,\tilde{G}_{\alpha f\beta f}\,, \tag{5.73}$$

where $\alpha \neq \beta$. In order to determine the coefficients $a_1, \ldots, a_4$ we use (5.69) and (5.71) to take the limits $x_1 \to x_2$ and $x_3 \to x_4$ on both sides, take (5.70) into account to equate the coefficients of the two-point functions we are left with, and obtain

$$a_1 = a_3 = 1\,, \qquad a_2 = (q-1)(c'/c)^2\,, \qquad a_4 = -(c'/c)^2\,. \tag{5.74}$$

Since $P_v = 1 - \lim_{q\to 1} Z^{ff}_{\alpha\beta} = 1 - \lim_{q\to 1}\left[a_3 + a_4 \tilde{Z}^{\alpha\beta}_{ff}\right]$, comparison with (5.64) and (5.74) gives $(c'/c)^2 = 1$ at $q = 1$. Putting all together, the combination of partition functions in (5.8) can be written as

$$R = \frac{Z^{ff}_{ff} Z^{ff}_{\alpha\alpha}}{Z^{ff}_{\alpha f} Z^{ff}_{f\alpha}} = \frac{G_{f\alpha f\alpha}}{G_{f\alpha ff}\, G_{fff\alpha}} = \frac{\tilde{G}_{\alpha f\alpha f} + a_2\, \tilde{G}_{\alpha f\beta f}}{\tilde{G}_{\alpha f\alpha\alpha}\, \tilde{G}_{\alpha\alpha\alpha f}} = \frac{\tilde{Z}^{\alpha\alpha}_{\alpha\alpha}\left[\tilde{Z}^{\alpha\alpha}_{ff} + a_2\, \tilde{Z}^{\alpha\beta}_{ff}\right]}{\tilde{Z}^{\alpha\alpha}_{f\alpha}\, \tilde{Z}^{\alpha\alpha}_{\alpha f}}\,, \tag{5.75}$$

with $a_2 = q - 1 + O((q-1)^2)$. Now it is not difficult to use our expressions for the partition functions $\tilde{Z}^{lr}_{ud}$ to check that $\lim_{q\to 1} \partial_q \log R$ gives the r.h.s. of (5.63).

Chapter 6

Density profile of the spanning cluster

In this chapter we determine the density profile of the spanning cluster for a percolation problem defined on a strip above p_c. Our result can be derived as a byproduct of the study of the magnetization profile in the q-color Potts model when boundary conditions generate a phase separation.

6.1 Statement of the problem and final result

Consider a percolation problem defined in the scaling limit for $p > p_c$ on a rectangle of width R and length L. We restrict to configurations such that clusters connected to the left half of the boundary cannot be connected to the right half of the boundary. In the limit $L \to \infty$ and $R \gg \xi$, where ξ is the percolative correlation length, consider the probability $P_s(x)$ that a cluster s spanning between the negative part of the edges of the strip contains the point x of the horizontal axis, see Fig. 6.1. We will show that the following result holds

$$P_s(x,0) = \frac{P}{2}\left[1 - \mathrm{erf}\Big(\sqrt{\frac{2m}{R}}\,x\Big) - \gamma\sqrt{\frac{2}{\pi m R}}\,e^{-2mx^2/R} + \dots\right], \qquad (6.1)$$

where P is the probability that a site belongs to the infinite cluster on the infinite plane, and the parameter m is related to the exponential correlation length above

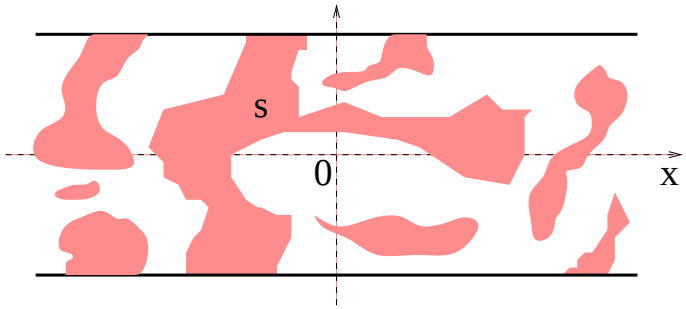

Figure 6.1: For percolation on the strip of width R, consider only the configurations without clusters connecting the part of the edges with $x < 0$ to the part with $x > 0$. Eq. (6.1) gives the probability that a point on the x axis belongs to a cluster s spanning between the negative part of the edges, in the scaling limit above p_c and for $R \gg \xi = 1/2m$.

p_c as $\xi = 1/2m$ (see [18]); the constant γ is not known because as we will describe in the next sections the two-kink form factor of the Potts spin σ_α is available only for real rapidities [18]. The error function in (6.1) is defined by $\mathrm{erf}(x) = \frac{2}{\sqrt{\pi}} \int_0^x d\eta \; \mathrm{e}^{-\eta^2}$.

We will derive (6.1) in a more general context, studying the physics of phase separation in two dimensions.

6.2 Derivation. Phase separation in two dimensions

6.2.1 Introduction

Boundary conditions notoriously play an important role in the theory of phase transitions. For a system of ferromagnetic spins taking discrete values, a pure phase of type a with translation invariant spontaneous magnetization below the critical temperature T_c can be selected fixing all boundary spins to the value a and then sending the boundary to infinity. On the other hand, if the spins are fixed to a value a on the left half of the boundary and to a different value b on the right half, a pattern of phase separation between phases of type a and type b is expected in the large volume limit below T_c, at least away from an interfacial

region anchored to the points of the boundary where boundary conditions change from a to b. The properties of the phase separation and the notion of interface have been extensively studied both in two and three dimensions through rigorous [106], exact [107] and approximate [108] methods. The most advanced analytic results are available in two dimensions, where the exact asymptotic magnetization profile has been obtained for the Ising model [109, 110] exploiting its lattice solvability at any temperature. This result shows in particular that in two dimensions the Ising interface has middle point fluctuations which diverge as the square root of the volume, a property previously proved for low temperatures in [111]. The result for the Ising magnetization profile also admits a simple interpretation in terms of passage probability of the interface through a point [112]. No exact result for the magnetization profile is available in three dimensions.

In the rest of this chapter we use field theory as a general framework for the study of phase separation in the scaling limit below T_c, for any two-dimensional model possessing a discrete set of ordered phases and undergoing a continuous phase transition. For a strip of width R we derive the large R asymptotics for the magnetization profiles along the longitudinal axis in the middle of the strip and show that a generalization of the Ising result holds whenever the surface tension between the phases a and b cannot be decomposed into the sum of smaller surface tensions. The formalism explicitly illustrates the role played by the topological nature of the elementary excitations (domain walls), which for a discrete set of ground states is peculiar of the two-dimensional case. The interpretation in terms of passage probability holds in general, with subsequent terms in the large R expansion accounting for the emergence of an interfacial region with finite width in a way that can be understood through renormalization group considerations.

The trajectories on the plane of the domain wall excitations of the field theory are naturally interpreted as the continuum limit of the boundaries of clusters made of nearest neighbors with the same value of the spin. In the last years the scaling properties of cluster boundaries have been extensively studied at criticality in the framework of Schramm-Loewner evolution (SLE, see e.g. [43] for a review); the application of SLE methods to the off-critical case, on the other hand, is up to now much more limited (see [113, 114]). The renormalization group interpretation of our results below T_c is that the cluster boundary connecting the two boundary

changing points on the edges and the interfacial curve between the two phases coincide as $R \to \infty$, and then have the same Gaussian passage probability density; when R decreases, the interfacial region with finite width emerges via branching of the interface and formation of intermediate clusters. We write down the leading term associated to branching and determine its coefficient for the q-color Potts model.

The rest of the chapter is organized as follows. In the next subsection we introduce the field theoretical formalism and derive the large R results for the magnetization profiles. Section 6.2.3 is then devoted to the interpretation of the results and to the discussion of the interface structure. The specific cases of q-color Potts and an application to percolation are finally discussed in section 6.2.4 where we derive the result (6.1) for the density profile of the spanning cluster.

6.2.2 Field theoretical formalism

Consider a ferromagnetic spin model of two-dimensional classical statistical mechanics in which each spin can take n discrete values that we label by an integer $a = 1, 2, \ldots, n$. To be definite we refer to the case in which the energy of the system is invariant under global transformations of the spins according to a symmetry group; the spontaneous breaking of the symmetry below a critical temperature T_c is responsible for the presence on the infinite plane of n translation invariant pure phases; the phase of type a can be selected starting with the system on a finite domain with boundary spins fixed to the value a, and then removing the boundary to infinity. We denote by Z_a and $\langle \cdots \rangle_a$ the partition function and the statistical averages, respectively, in the phase a.

We consider the scaling limit below T_c, described by a Euclidean field theory defined on the plane with coordinates (x, y); it corresponds to the analytic continuation to imaginary time of a (1+1)-dimensional relativistic field theory with space coordinate x and time coordinate $t = iy$. This theory possesses degenerate vacua $|\Omega_a\rangle$ associated to the pure phases of the system. In 1+1 dimensions the elementary excitations will correspond to stable kink (domain wall) states $|K_{ab}(\theta)\rangle$ which interpolate between different vacua $|\Omega_a\rangle$ and $|\Omega_b\rangle$; the rapidity θ parameterizes the energy and momentum of the kinks as $(e, p) = (m_{ab} \cosh\theta, m_{ab} \sinh\theta)$, m_{ab} being the kink mass. In general, connecting $|\Omega_a\rangle$ and $|\Omega_b\rangle$ requires a multi-

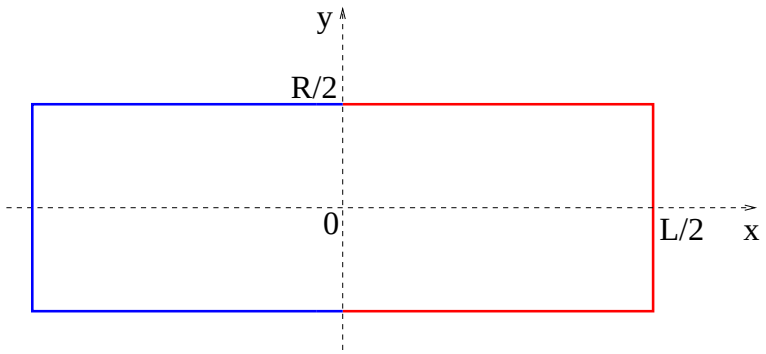

Figure 6.2: The scaling limit below T_c of a ferromagnet is considered on a rectangle with boundary spins fixed to take the value a for $x < 0$ and a different value b for $x > 0$. The case $L \to \infty$ and $R \gg \xi$ is considered throughout the chapter.

kink state $|K_{aa_1}(\theta_1)K_{a_1a_2}(\theta_2)\dots K_{a_{n-1}b}(\theta_n)\rangle$ passing through other vacua; we call adjacent vacua two vacua that can be connected through a single-kink excitation. There can be kinks with different masses connecting two adjacent vacua $|\Omega_a\rangle$ and $|\Omega_b\rangle$; in such a case the notations $|K_{ab}(\theta)\rangle$ and m_{ab} refer to the kink with the lowest mass, which is leading in the large distance limits we will consider.

Consider now the scaling limit on a rectangle (Fig. 6.2) with horizontal sides of length L and vertical sides of length R (the origin of the coordinates is taken in the center of the rectangle), with the following choice of boundary conditions (boundary conditions of type ab): the boundary spins are fixed to a value a for $x < 0$, and to a different value b for $x > 0$. Let us denote by Z_{ab} and $\langle\cdots\rangle_{ab}$ the partition function and the statistical averages for the system with this choice of boundary conditions. We consider the limit $L \to \infty$ and want to study properties of the system as a function of the width R of the resulting infinite strip, focusing on the asymptotic limit in which R is much larger than the correlation length ξ.

Within the field theoretical formalism the boundary condition at time t switching from a to b at a point x_0 is realized by a boundary state that we denote by $|B_{ab}(x_0;t)\rangle$. This state can be expanded over the basis of asymptotic particle states of the relativistic theory. The change of boundary conditions at the point x_0 requires that kink excitations interpolating between $|\Omega_a\rangle$ and $|\Omega_b\rangle$ are

emitted/absorbed at that point. Then, if $|\Omega_a\rangle$ and $|\Omega_b\rangle$ are adjacent vacua, the boundary state has the form

$$|B_{ab}(x_0;t)\rangle = e^{-itH+ix_0P}\left[\int_{-\infty}^{\infty}\frac{d\theta}{2\pi}f_{ab}(\theta)|K_{ab}(\theta)\rangle + \dots\right], \tag{6.2}$$

where H and P are the energy and momentum operators of the (1+1)-dimensional theory, $f_{ab}(\theta)$ is the amplitude[1] for the kink to be emitted at the boundary changing point, and the dots correspond to states with total mass larger than m_{ab}. The partition function we are considering can be written as

$$Z_{ab}(R) = \langle B_{ab}(x_0;iR/2)|B_{ab}(x_0;-iR/2)\rangle = \langle B_{ab}(0;0)|e^{-RH}|B_{ab}(0;0)\rangle \tag{6.3}$$

and, as a consequence of (6.2), has the large R asymptotics

$$Z_{ab}(R) \sim \int_{-\infty}^{\infty}\frac{d\theta}{2\pi}\, e^{-m_{ab}R\cosh\theta}|f_{ab}(\theta)|^2 \sim \frac{|f_{ab}(0)|^2}{\sqrt{2\pi m_{ab}R}}\, e^{-m_{ab}R}. \tag{6.4}$$

The specific interfacial free energy, or surface tension, is given by

$$\Sigma_{ab} = -\lim_{R\to\infty}\frac{1}{R}\,\ln\frac{Z_{ab}(R)}{Z_a(R)}\,, \tag{6.5}$$

where $Z_a(R)$ is the partition function for uniform boundary conditions of type a on the strip. Since the lowest mass state entering the expansion of the boundary state $|B_a(t)\rangle$ for uniform boundary condition is the vacuum $|\Omega_a\rangle$, $Z_a(R)$ tends to $\langle\Omega_a|\Omega_a\rangle = 1$ as $R\to\infty$, so that

$$\Sigma_{ab} = m_{ab}\,. \tag{6.6}$$

If $|\Omega_a\rangle$ and $|\Omega_b\rangle$ are not adjacent vacua the expansion of the boundary state $|B_{ab}(x_0;t)\rangle$ starts with a multi-kink state, and the corresponding surface tension is a sum of surface tensions between adjacent vacua, see [20].

Let us denote by σ a generic component of the spin field, omitting for the time being the index which in general labels the different components. The

[1] We use the normalization $\langle K_{ab}(\theta)|K_{a'b'}(\theta')\rangle = 2\pi\delta_{aa'}\delta_{bb'}\delta(\theta-\theta')$.

magnetization profile along the horizontal axis in the middle of the strip for ab boundary conditions and a and b adjacent phases is

$$\langle\sigma(x,0)\rangle_{ab} = \frac{1}{Z_{ab}}\langle B_{ab}(0;0)|\mathrm{e}^{-HR/2+ixP}\sigma(0,0)\mathrm{e}^{-HR/2-ixP}|B_{ab}(0;0)\rangle \tag{6.7}$$
$$\sim \frac{1}{Z_{ab}}\int \frac{d\theta}{2\pi}\frac{d\theta'}{2\pi} f^*(\theta)f(\theta')\langle K_{ab}(\theta)|\sigma(0,0)|K_{ab}(\theta')\rangle\times$$
$$\times\, e^{m_{ab}[-(\cosh\theta+\cosh\theta')R/2+i(\sinh\theta-\sinh\theta')x]},$$

the last line being the large R limit obtained from (6.2). The matrix element of the spin field it contains is related by the crossing relation

$$\langle K_{ab}(\theta)|\sigma(0,0)|K_{ab}(\theta')\rangle = F^{\sigma}_{aba}(\theta-\theta'+i\pi) + 2\pi\delta(\theta-\theta')\langle\sigma\rangle_a\,, \tag{6.8}$$

to the form factor

$$F^{\sigma}_{aba}(\theta_1-\theta_2) \equiv \langle\Omega_a|\sigma(0,0)|K_{ab}(\theta_1)K_{ba}(\theta_2)\rangle\,, \tag{6.9}$$

where the vacuum expectation value $\langle\sigma\rangle_a$ appearing in the disconnected part is the spontaneous magnetization in the phase a on the infinite plane. When $\theta_1-\theta_2 = i\pi$ the kink and the anti-kink in (6.9) have opposite energy and momentum and can annihilate each other. In 1+1 dimensions these annihilation configurations produce in general simple poles that have been characterized for general k-particle form factors in integrable field theories (see in particular [60]). For $k=2$, however, integrability plays no role in the determination of the residue, which for the case of kink excitations reads [62]

$$\mathrm{Res}_{\theta=i\pi}F^{\sigma}_{aba}(\theta) = i\big[\langle\sigma\rangle_a - \langle\sigma\rangle_b\big]. \tag{6.10}$$

For $R\to\infty$ the integral in (6.7) is dominated by small rapidities and the leading contribution can be written as

$$\langle\sigma(x,0)\rangle_{ab} \sim \langle\sigma\rangle_a + \frac{i}{2\pi}\big[\langle\sigma\rangle_a - \langle\sigma\rangle_b\big]\int_{-\infty}^{\infty} d\theta_-\frac{1}{\theta_-}\,e^{-m_{ab}R\theta_-^2/8+im_{ab}x\theta_-}\,, \tag{6.11}$$

where we used (6.4), (6.8) and (6.10), $\theta_- \equiv \theta-\theta'$, and we integrated over $\theta_+ \equiv \theta+\theta'$. The last integral is regularized moving the pole slightly above the real axis, so that the usual relation $(x-i0)^{-1} = i\pi\delta(x) + \mathrm{p.v.}\,x^{-1}$ finally gives

$$\langle\sigma(x,0)\rangle_{ab} \sim \frac{1}{2}\big[\langle\sigma\rangle_a + \langle\sigma\rangle_b\big] - \frac{1}{2}\big[\langle\sigma\rangle_a - \langle\sigma\rangle_b\big]\mathrm{erf}\Big(\sqrt{\frac{2m_{ab}}{R}}\,x\Big)\,, \tag{6.12}$$

where the principal value of the integral in (6.11) has been expressed in terms of the error function (see e.g. [115]). The same result can be obtained differentiating (6.11) with respect to x in order to get rid of the pole, and then integrating the result of the integral over θ_- with the condition $\langle\sigma(+\infty,0)\rangle_{ab} = \langle\sigma\rangle_b$.

For the Ising model ($\langle\sigma\rangle_a = -\langle\sigma\rangle_b$) the result (6.12) coincides with the scaling limit of that obtained from the lattice in [109, 110]. Even in our more general setting, it shows that for $R \to \infty$ $\langle\sigma(\alpha(m_{ab}R)^\beta/m_{ab},0)\rangle_{ab}$ tends to the pure values $\langle\sigma\rangle_a$ or $\langle\sigma\rangle_b$ for $\beta > 1/2$ and α negative or positive, respectively, and to the average value $(\langle\sigma\rangle_a + \langle\sigma\rangle_b)/2$ for $\beta < 1/2$.

The result (6.12) is produced by the leading term in the small rapidity expansion of the emission amplitude in (6.2) and of the matrix element (6.8). More generally, for the latter we write

$$F^\sigma_{aba}(\theta + i\pi) = \sum_{k=-1}^{\infty} c^{(k)}_{ab}\,\theta^k\,, \tag{6.13}$$

with $c^{(-1)}_{ab}$ given by (6.10). As for the emission amplitude, it satisfies $f_{ab}(\theta) = f_{ba}(-\theta)$ as a consequence of reflection symmetry about the vertical axis. In any model in which a and b play a symmetric role we will have $f_{ab}(\theta) = f_{ba}(\theta)$ and $f_{ab}(\theta) = f_{ab}(0) + O(\theta^2)$. Then it is easy to check that the next contribution to $\langle\sigma(x,0)\rangle_{ab}$ produced by the small rapidity expansion is

$$c^{(0)}_{ab}\sqrt{\frac{2}{\pi m_{ab}R}}\,e^{-2m_{ab}x^2/R}\,. \tag{6.14}$$

Notice that the error function in (6.12) is leading with respect to (6.14) as $R \to \infty$ for $x \sim (m_{ab}R)^\beta/m_{ab}$ with $\beta > 0$; the two terms are of the same order for $\beta = 0$.

6.2.3 Passage probability and interface structure

The results of the previous subsection allow an interpretation based on renormalization group and probabilistic considerations. It is clear that the problem has two length scales: the correlation length ξ, proportional to the inverse of the kink masses, which is the scale of the fluctuations within the pure phases, and the width R of the strip, which sets the scale at which we observe the system with ab boundary conditions. In an expansion around $R/\xi = \infty$ the leading term corresponds to the crudest description of phase separation in which all short distance

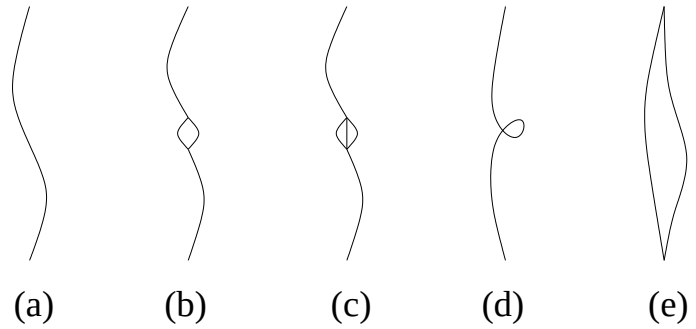

Figure 6.3: Some configurations of the interfacial region. Lines correspond to domain walls between different phases.

features are washed out and one is left with two pure phases sharply separated by a simple curve connecting the two boundary changing points (Fig. 6.3a). Hence, the notion of curvilinear interface naturally arises in this limit and can be formulated directly in the continuum. It is clear, however, that this picture cannot hold true for finite values of R/ξ, and that one needs to switch from the notion of sharp separation and curvilinear interface to that of an interfacial region (or thick interface) with a width which diverges as the correlation length when the critical point is approached: such a divergence simply reflects the fact that phase separation disappears at criticality. Within the large R/ξ expansion the leading deviations from the simple curvilinear picture are expected from effects such as branching and recombination as well as self-intersection of the curve[2] (Fig. 6.3b-d). These effects appear in the expansion through insertions (delta functions) localized on the curve separating the two pure phases.

According to this discussion the large R/ξ expansion for the magnetization at a point x on the axis $y = 0$ when the interface passes through a point u on this axis can be expected to start as

$$\sigma_{ab}(x|u) = \theta(u-x)\langle\sigma\rangle_a + \theta(x-u)\langle\sigma\rangle_b + A^{(0)}_{ab}\delta(x-u) + A^{(1)}_{ab}\delta'(x-u) + \dots , \quad (6.15)$$

[2] At a later stage in the expansion thickness is generated also by multi-kink terms in the boundary state (6.2), which will produce a bundle of thin interfaces rather than just one (Fig. 6.3e). Multi-kink contributions to Z_{ab} are suppressed at large R as e^{-MR}, M being the total mass.

where $\theta(x)$ is the step function equal to 1 for $x > 0$ and zero for $x < 0$, and the prime denotes differentiation. If $p_{ab}(u)du$ is the probability that the curve intersects the axis $y = 0$ in the interval $[u, u + du]$, with $p_{ab}(u) = p_{ab}(-u)$ and $\int_{-\infty}^{\infty} du\; p_{ab}(u) = 1$, then the average magnetization is

$$\begin{aligned}\langle\sigma(x,0)\rangle_{ab} &= \int_{-\infty}^{\infty} du\, p_{ab}(u)\, \sigma_{ab}(x|u) + \dots \\ &= \langle\sigma\rangle_a \int_{x}^{\infty} du\; p_{ab}(u) + \langle\sigma\rangle_b \int_{-\infty}^{x} du\; p_{ab}(u) + A^{(0)}_{ab} p_{ab}(x) \\ &\quad - A^{(1)}_{ab} p'_{ab}(x) + \dots, \end{aligned} \tag{6.16}$$

where the dots in the first line stay for the contribution of multi-kink states. Comparison with (6.12) and (6.14), as it is easily seen, shows correspondence between the two expansions and determines

$$p_{ab}(u) = \sqrt{\frac{2m_{ab}}{\pi R}}\; \mathrm{e}^{-2m_{ab}u^2/R}\,, \tag{6.17}$$

$$A^{(0)}_{ab} = c^{(0)}_{ab}/m_{ab}\,. \tag{6.18}$$

The last as well as additional terms in (6.16) should be compared with those produced in (6.7) by further expansion around $\theta = \theta' = 0$. The Gaussian form of $p_{ab}(u)$ is model independent and of course coincides with the scaling limit of that deduced in [112] for the Ising model[3]. As shown in the previous subsection the integral, non-local terms in (6.16) are entirely due to the pole term in (6.13), which in turn is produced by the non-locality of the kinks with respect to the spin field[4].

[3]The Gaussian probability density (6.17) indicates an effective Brownian behavior of the interface. The convergence of the interface to a Brownian bridge for all subcritical temperatures has been proved in [116] for the Ising model and in [117] for the q-color Potts model. We thank Y. Velenik for bringing these references to our attention.

[4]If we consider the form factor of the energy density ε, the residue at $i\pi$ is given by (6.10) with σ replaced by ε, and vanishes because the expectation value of ε is the same in all stable phases. This reflects the fact that even for a domain wall excitation the energy density is spatially localized (on the wall).

For any lattice configuration there is a cluster (let us call it the left cluster) formed by nearest neighboring spins with value (color) a and whose external perimeter is formed by the left half of the boundary of the strip together with a path connecting the two boundary changing points. This path, whose identification may be ambiguous and require some lattice dependent prescription, becomes a simple curve in the continuum limit. A second curve connecting the two boundary changing points completes the perimeter of the cluster of color b anchored to the right half of the boundary (the right cluster). In general the two curves, which can touch but not intersect, enclose other clusters in between them. Among these intermediate clusters, those adjacent to the left (right) cluster have color different from a (b). The first few terms in (6.15) and (6.16) are compatible with a picture in which a uniform magnetization $\langle\sigma\rangle_a$ ($\langle\sigma\rangle_b$) is assigned to the region enclosed by the perimeter of the left (right) cluster: the two curves become coincident as $R/\xi \to \infty$, with asymptotic passage probability density given by (6.17); the first deviation from this situation as R/ξ decreases is expected to happen via bifurcation and recombination around a cluster of color $c \neq a, b$ (Fig. 6.3b), and to be associated to the term containing $A^{(0)}_{ab}$. We will see in the next subsection that this term is indeed absent in the Ising model, where bifurcation is not allowed[5].

6.2.4 Potts model and percolation

Potts model. The lattice Hamiltonian [23]

$$H_{Potts} = -J \sum_{\langle \mathbf{x_1}, \mathbf{x_2} \rangle} \delta_{s(\mathbf{x_1}), s(\mathbf{x_2})}, \qquad s(\mathbf{x}) = 1, \ldots, q\,, \tag{6.19}$$

is invariant under global permutations of the values of the spins $s(\mathbf{x})$. For $J > 0$ in two dimensions the phase transition is continuous for $q \leq 4$ and above J_c there are q degenerate vacua located at the vertices of a hypertetrahedron in the (q-1)-dimensional order parameter space. Kinks with equal masses run along the edges of the hypertetrahedron and all the vacua are adjacent according to the definition given in section 6.2.2. The results we obtained for the magnetization profile apply to each component $\sigma_c(\mathbf{x}) \equiv \delta_{s(\mathbf{x}),c} - 1/q$, $c = 1, \ldots, q$, of the spin

[5]Splitting into an odd number of paths (Fig. 6.3c), however, is allowed and encoded by subsequent terms in the expansion.

field; taking into account that $\sum_{c=1}^{q}\sigma_c = 0$ and $\langle\sigma_a\rangle_b = \frac{q\delta_{ab}-1}{q-1}\langle\sigma_a\rangle_a$, one obtains

$$\begin{aligned}\langle\sigma_c(x,0)\rangle_{ab} &= \frac{\langle\sigma_a\rangle_a}{2}\left[\frac{q(\delta_{ca}+\delta_{cb})-2}{q-1} - \frac{2q(\delta_{ca}-\delta_{cb})}{q-1}\int_0^x du\, p(u)\right.\\ &+ \left.[2-q(\delta_{ca}+\delta_{cb})]\,\frac{B}{m}\,p(x)\right] + \dots\,, \end{aligned} \tag{6.20}$$

where $p(u)$ is (6.17) with $m_{ab} = m$. Potts field theory is integrable [27] and from the known form factors [62] we obtain

$$B = \frac{1}{2\sqrt{3}},\ \frac{2}{3\sqrt{3}} \tag{6.21}$$

for $q = 3, 4$, respectively. For $c \neq a, b$ the integral term in (6.20) is absent and the x-dependence of the magnetization profile is entirely due to the structure of the interface. The Gaussian term in (6.20) is produced by the leading deviation from the picture of the interface as a simple curve separating the phases a and b, which was argued in the previous subsection to correspond to the appearance of an island of the phase c via bifurcation and recombination of the curve. Bifurcation is not allowed in the Ising model, and indeed the coefficient of $p(x)$ vanishes at $q = 2$, where c necessarily coincides with a or b. Directly at $q = 2$, the same conclusion is obtained from the explicit form $F^{\sigma}_{aba}(\theta) = i\langle\sigma\rangle_a \tanh(\theta/2)$ of the spin form factor, implying that (6.13) contains only the terms with k odd.

Percolation. If we consider the Potts model with boundary conditions of type ab on the strip, the probability $\langle\delta_{s(x,0),a}\rangle_{ab}$ that the spin $s(x,0)$ has color a is given by the probability $P(x,0)$ that it belongs to an FK cluster touching the part of the boundary with $x < 0$ (which has color a), plus $1/q$ times the probability $1-P(x,0)-P(-x,0)$ that it belongs to a bulk FK cluster. This can be rewritten as

$$\langle\sigma_a(x,0)\rangle_{ab} = \frac{q-1}{q}P(x,0) - \frac{1}{q}P(-x,0)\,. \tag{6.22}$$

The FK expansion of Z_{ab} does not contain configurations with clusters connecting the boundary regions with $x < 0$ and $x > 0$; this restriction is inherited by the percolation problem we consider. When the occupation probability p for the sites is above the percolation threshold p_c (this corresponds to our case $J > J_c$ in the

Potts model), even for $R \to \infty$ there is a positive probability of having a spanning cluster which connects the upper and lower parts of the boundary with $x < 0$ (Fig. 6.1). Then the probability $P(x,0)|_{q=1}$ that the site $(x,0)$ is connected to the left part of the boundary is given by the probability $P_s(x,0)$ that it belongs to such spanning cluster plus the probability $P_{ns}(x,0)$ that it belongs to a cluster touching only the upper or lower edge. Since the clusters of the latter type have an average linear extension of order $1/m$, $P_{ns}(x,0)$ vanishes exponentially when $mR \to \infty$. Hence in this limit we have $P_s(x,0) \sim P(x,0)|_{q=1}$, and from (6.20), (6.22) we obtain (6.1) with $P = \lim_{q\to 1} \frac{q}{q-1} \langle \sigma_a \rangle_a$ and $\gamma \equiv \mathrm{Res}_{q=1} B(q)$.

Although not related to percolation, we find interesting to finish this chapter mentioning how the theory of phase separation described above applies to the Ashkin-Teller model. This corresponds to two Ising spins $\sigma_1(\mathbf{x}), \sigma_2(\mathbf{x}) = \pm 1$ on each site interacting as specified by the Hamiltonian

$$H_{AT} = -\sum_{\langle \mathbf{x_1}, \mathbf{x_2} \rangle} \{ J[\sigma_1(\mathbf{x_1})\sigma_1(\mathbf{x_2}) + \sigma_2(\mathbf{x_1})\sigma_2(\mathbf{x_2})] + J_4\, \sigma_1(\mathbf{x_1})\sigma_1(\mathbf{x_2})\sigma_2(\mathbf{x_1})\sigma_2(\mathbf{x_2}) \} \ . \tag{6.23}$$

Each site can be in one of four states (σ_1, σ_2) that we label $a = 1, 2, 3, 4$, corresponding to $(+,+)$, $(+,-)$, $(-,-)$, $(-,+)$, respectively. The model, that we consider for $J > 0$, is well known to possess a line of critical points parameterized by J_4 [39]. In the scaling limit close to this line it renormalizes onto the sine-Gordon field theory (see [118, 50]), where a parameter β^2 plays the role of J_4; $\beta^2 = 4\pi$ describes a free fermionic theory and corresponds to the decoupling point $J_4 = 0$. Below critical temperature the model possesses four degenerate vacua $|\Omega_a\rangle$ and for any value of β^2 there are kinks $|K_{a,a\pm 1 (mod\, 4)}\rangle$ with the same mass m.

For $\beta^2 < 4\pi$ the interaction among these kinks (which correspond to sine-Gordon solitons) is attractive and produces bound states, the lightest of which have mass $m' = 2m \sin \frac{\pi\beta^2}{2(8\pi - \beta^2)}$ and are kinks $|K_{a,a\pm 2 (mod\, 4)}\rangle$. Hence, in this regime any pair of vacua is connected by a single-kink excitation, all the vacua are adjacent and the boundary state $|B_{ab}\rangle$ has in any case the form (6.2). The results of the previous sections apply with surface tensions $\Sigma_{a,a\pm 1 (mod\, 4)} = m$ and $\Sigma_{a,a\pm 2 (mod\, 4)} = m'$; the bifurcation coefficients (6.18) can be obtained from the form factors computed in [118, 50]. For $\beta^2 = 2\pi$ the masses m and m' coincide

and one recovers the $q = 4$ Potts model.

For $\beta^2 \geq 4\pi$ there are no bound states and the vacua with indices differing by two units are not adjacent, with surface tension $\Sigma_{a,a\pm 2(mod\,4)} = 2m$. In this case (6.2) is replaced by

$$|B_{a,a\pm 2}(x_0;t)\rangle = e^{-itH+ix_0P}\left[\sum_{c=a\pm 1}\int \frac{d\theta_1}{2\pi}\frac{d\theta_2}{2\pi}\, f_{a,c,a\pm 2}(\theta_1,\theta_2)\,|K_{ac}(\theta_1)K_{c,a\pm 2}(\theta_2)\rangle + \ldots\right], \tag{6.24}$$

(indices are intended mod 4) and (6.15) has to be replaced by a description in terms of two interfaces (Fig. 6.3e).

Let us conclude this section mentioning that studies of cluster boundaries at criticality can be found in particular in [119, 48] for the Potts model and in [120, 121, 122] for the Ashkin-Teller model; we refer the reader to [123] for results on cluster densities in critical percolation.

Chapter 7

Correlated percolation. Ising clusters and droplets

In this final chapter we will adapt the analysis of chapter 4 for random percolation to the case of the Ising model. The percolative transition of the spin clusters in the Ising model can be mapped into the spontaneous breaking of the permutational symmetry S_q in the q-color dilute Potts model when $q \to 1$. In the scaling limit near the critical temperature in zero magnetic field the dilute Potts field theory is integrable and several universal amplitude ratios can be computed.

7.1 Introduction

The simplest observable one can think of within the lattice modelization of a ferromagnet is the average value of the spin at a given site. On an infinite regular lattice this gives the magnetization per site M, which serves as order parameter of the ferromagnetic transition. It is also natural, however, to look at extended (non-local) objects like the clusters formed by neighboring spins with the same value. Then the probability P that a given site belongs to an infinite cluster provides the order parameter of a percolative phase transition. The relation between the magnetic and percolative transitions within the ferromagnet is far from trivial and has been the subject of many studies [6], first of all for the basic case of the Ising ferromagnet which is also the subject of this chapter.

The coincidence of the two transitions (concerning both the location of the critical point and the critical exponents) was the requirement of the droplet model for ferromagnetism [124]. It is not fulfilled by the ordinary clusters defined above, but is satisfied by special clusters whose mass is suitably reduced as the temperature increases [125]; these particular clusters are then called droplets. On usual lattices in two-dimensions also the ordinary clusters percolate at the Curie temperature T_c at which the magnetic transition takes place [126], although in this case the percolative and magnetic critical exponents do not coincide [127]. As a result, T_c is simultaneously the location of the ferromagnetic transition and of the percolative transition for both clusters and droplets.

A formulation of the problem suitable for theoretical study, for both clusters and droplets, is obtained coupling the Ising spins to auxiliary color variables whose expectation value becomes the percolative order parameter P [25, 128]. In this way also the cluster properties are related to correlation functions of local variables and can be studied using the renormalization group [125] and field theory [129, 130]. In particular, the exact results of two-dimensional conformal field theory [12] allowed the identification of the critical exponents also for clusters [131].

In this respect, it is worth recalling that in recent years the role of non-local observables within spin models has been much emphasized in connection with Schramm-Loewner evolution (SLE) (see e.g. [43, 44] for reviews). Indeed, the latter provides an approach to two-dimensional critical behavior based on the study of conformally invariant random curves which may be thought as cluster boundaries. Some exponents and other critical properties have been derived in this way within an approach alternative to conformal field theory. On the other hand, moving away from the critical point in the SLE framework still appears a difficult task, and very few steps have been done in this sense (see e.g. [113, 114]).

Moving away from criticality within field theory is, on the contrary, very natural and, in many cases, can be done preserving integrability [132]. It was shown in [46] how Ising clusters and droplets near criticality can be described using perturbed conformal field theory and, in particular, how the second order transition that clusters undergo above T_c in an external field becomes integrable in the scaling limit. In this chapter we use the field theoretical setting of [46]

to quantitatively characterize the universal properties of clusters and droplets in their approach to criticality. This is done exploiting integrability to compute universal combinations of critical amplitudes of the main percolative observables, namely the order parameter, the connectivity length, the mean cluster number and the mean cluster size.

We obtain new results for clusters, but also for droplets. This may appear surprising in consideration of the fact that droplets provide the percolative description of the magnetic transition, for which all canonical universal ratios are known exactly [133, 134]. The point is that, while the critical exponents are determined by the singularities of correlation functions at distances much shorter than the correlation length ξ (in the scaling limit $T \to T_c$, where ξ is anyway very large), the amplitude ratios are also sensitive to correlations at larger distances. The spin-spin correlator and the connectivity within finite droplets have the same singular behavior at short distances but, due to the contribution of infinite droplets, differ at larger distances below T_c. As a result, magnetic and percolative exponents coincide, while some amplitude ratios differ.

A similar characterization of cluster properties has been done for the case of random percolation in chapter 4. Of course the important physical difference with respect to that case is that in Ising percolation cluster criticality is determined by the ferromagnetic interaction. The site occupation probability is not an independent parameter to be tuned towards its critical value, as in the random case, but is instead a function of temperature and magnetic field. One visible manifestation of this difference within the formalism arise in the evaluation of correlation functions through the spectral decomposition over intermediate particle states. While in random percolation all degrees of freedom, and then all particles, are auxiliary, in Ising percolation the particles associated to the magnetic degrees of freedom are also part of the game. This leads us to formulate selection rules which identify the particle states actually contributing to the percolative properties. The picture which emerges is that of a sharp separation between states contributing to magnetic correlations and states contributing to cluster connectivity. For the mean cluster number, which is related to the free energy, the presence of the magnetic interaction results into the appearance of logarithmic terms which are absent in the random case. Altogether, our analysis

produces a number of universal field theoretical predictions for both clusters and droplets, and for different directions in parameter space, that will be interesting to compare with lattice estimates when these will become available.

The chapter is organized as follows. In the next section we recall how percolative observables are described in terms of auxiliary color variables before turning to the characterization of their behavior near criticality in section 7.3. Section 7.4 is devoted to the field theory description, while universal amplitude combinations are discussed in section 7.5. Two appendices complete the chapter.

7.2 Fortuin-Kasteleyn representation

We consider the ferromagnetic Ising model defined by the reduced Hamiltonian

$$-\mathcal{H}_{\rm Ising} = \frac{1}{T}\sum_{\langle x,y\rangle}\sigma(x)\sigma(y) + H\sum_x \sigma(x)\,, \tag{7.1}$$

where $\sigma(x) = \pm 1$ is a spin variable located at the site x of an infinite regular lattice $\mathcal{L}$, $T \geq 0$ and H are couplings that we call temperature and magnetic field, respectively, and the first sum is restricted to nearest-neighbor spins.

Correlated percolation in the Ising model can be conveniently studied by coupling Ising spins to auxiliary Potts variables taking the values (colors) $s(x) = 1, \ldots, q$. Replacing Ising spins with lattice gas variables $t(x) = \frac{1}{2}(\sigma(x)+1) = 0, 1$, the resulting model is a ferromagnetic dilute q-color Potts model with Hamiltonian

$$\begin{aligned} -\mathcal{H}_q =& \frac{4}{T}\sum_{<x,y>} t(x)t(y) + \Delta\sum_x t(x) + J\sum_{<x,y>} t(x)t(y)\left(\delta_{s(x),s(y)} - 1\right) + \\ &+ \tilde{h}\sum_x \left(\delta_{s(x),1} - \frac{1}{q}\right) t(x), \end{aligned} \tag{7.2}$$

where $\Delta = 2H - a/T$, with a a lattice-dependent constant, and we allow for the presence of a field $\tilde{h}$ which explicitly breaks the S_q invariance under permutations of the q colors. The Potts spins[1]

$$\sigma_k(x) \equiv \left(\delta_{s(x),k} - \frac{1}{q}\right) t(x), \qquad k = 1, \ldots, q, \tag{7.3}$$

[1]The definition of the Potts spin differs by a factor q from that used in the previous chapters.

effectively live only on the restricted lattice $\mathcal{L}_0$ formed by the sites of $\mathcal{L}$ with positive Ising spin (i.e. with $t(x) = 1$).

The partition function Z_q associated to the Hamiltonian (7.2) admits the following Fortuin-Kasteleyn (FK) representation [25, 128]

$$\begin{aligned} Z_q &= \sum_{\{t(x)\}} \sum_{\{s(x)\}} \mathrm{e}^{-\mathcal{H}_q} \\ &= \sum_{\mathcal{L}_0 \subseteq \mathcal{L}} \mathrm{e}^{-\mathcal{H}_{\mathrm{Ising}}} q^{N_e} \sum_{\mathcal{G}} \Lambda(\mathcal{G}) \prod_c \left[\mathrm{e}^{\tilde{h}\left(1-\frac{1}{q}\right)s_c} + (q-1)\mathrm{e}^{-\tilde{h}\frac{s_c}{q}} \right], \end{aligned} \tag{7.4}$$

where N_e is the number of "empty" sites (i.e. having $t(x) = 0$ and then not belonging to $\mathcal{L}_0$). For any lattice gas configuration $\{t(x)\}$, the sum over the Potts variables $s(x)$ is transformed into a sum over all possible graphs $\mathcal{G}$ obtained drawing bonds between nearest neighbors belonging to $\mathcal{L}_0$. The weight associated to each such a bond is $p = 1 - \mathrm{e}^{-J}$ (bond occupation probability), so that the weight of a graph $\mathcal{G}$ is $\Lambda(\mathcal{G}) = p^{|E(\mathcal{G})|}(1-p)^{|E(\mathcal{L}_0)|-|E(\mathcal{G})|}$, with the same notations of chapter 1. Connected components of $\mathcal{G}$ are called FK clusters and s_c is the number of sites in the c-th cluster[2].

For $\tilde{h} = 0$ the product over clusters in (7.4) reduces to q^{N_c}, $N_c \equiv |C(\mathcal{G})|$ being the number of FK clusters in $\mathcal{G}$. The factor $q^{N_e+N_c}$ disappears in the limit $q \to 1$, so that (7.4) defines a percolative average for FK clusters living on Ising clusters. In particular, the FK clusters become the Ising clusters when $p = 1$, i.e. when $J \to +\infty$. In this section we refer to the general case of FK clusters.

Standard definitions for percolative observables apply. The percolative order parameter P is the probability that the site in the origin belongs to an infinite cluster, namely the average fraction of sites of $\mathcal{L}$ belonging to infinite clusters. The average size of finite clusters containing the origin is

$$S = \frac{1}{N} \langle {\sum_c}' s_c^2 \rangle \,, \tag{7.5}$$

where the primed sum runs over finite clusters only and N is the number of sites in $\mathcal{L}$, which diverges in the thermodynamic limit we are considering. The probability $P_f(x)$ that the origin and x belong to the same finite cluster defines the 'true'

[2]Unconnected sites on $\mathcal{L}_0$ also counts as clusters with $s_c = 1$.

and 'second moment' connectivity lengths ξ_t and $\xi_{2\mathrm{nd}}$ through the relations[3]

$$P_f(x) \sim \mathrm{e}^{-|x|/\xi_t}, \quad |x| \to \infty\,, \tag{7.6}$$

$$\xi_{2\mathrm{nd}}^2 = \frac{\sum_x |x|^2 P_f(x)}{4\sum_x P_f(x)}\,. \tag{7.7}$$

The observables P and S are related to the dilute Potts magnetization and susceptibility, respectively. Indeed the Potts spontaneous magnetization is

$$\langle\sigma_1(x)\rangle = \frac{1}{N}\,\frac{\partial \ln Z_q}{\partial \tilde{h}}\bigg|_{\tilde{h}=0^+} = \lim_{\tilde{h}\to 0^+}\langle\sum_c F(s_c,\tilde{h},q)\rangle, \tag{7.8}$$

where

$$F(s_c,\tilde{h},q) = \left(1-\frac{1}{q}\right)\frac{s_c}{N}\,\frac{\mathrm{e}^{\tilde{h}\left(1-\frac{1}{q}\right)s_c} - \mathrm{e}^{-\frac{\tilde{h}}{q}s_c}}{\mathrm{e}^{\tilde{h}\left(1-\frac{1}{q}\right)s_c} + \mathrm{e}^{-\frac{\tilde{h}}{q}s_c}(q-1)}. \tag{7.9}$$

In the limit $\tilde{h}\to 0^+$, (7.9) vanishes for any finite cluster, so that only infinite clusters contribute to $\sum_c F$ a term $(1-1/q)$ times the fraction of the lattice they occupy; hence we have the relation

$$P = \lim_{q\to 1}\frac{\langle\sigma_1(x)\rangle}{q-1}\,, \tag{7.10}$$

showing that the percolative transition of clusters maps onto the spontaneous breaking of S_q symmetry in the auxiliary Potts variables. The Potts longitudinal susceptibility $\frac{\partial^2 \ln Z_q}{N\partial\tilde{h}^2}\Big|_{\tilde{h}=0^+}$ can be expressed through the spin-spin correlator or differentiating the cluster expansion (7.4); this leads to the relation[4]

$$S = \lim_{q\to 1}\frac{1}{q-1}\sum_x \langle\sigma_1(x)\sigma_1(0)\rangle_c\,. \tag{7.11}$$

It also follows from (7.4) that the mean cluster number per site is given by

$$\begin{aligned}\frac{\langle N_c\rangle}{N} &= \frac{1}{N}\left(\lim_{q\to 1}\partial_q \ln Z_q|_{\tilde{h}=0} - \langle N_e\rangle\right)\\ &= -\,\partial_q f_q|_{q=1} - \frac{1}{2}(1-M)\,,\end{aligned} \tag{7.12}$$

[3] In the previous chapters we denoted $P_f(x)$ as $P_{aa}(x)$.

[4] Throughout the chapter we denote connected correlators attaching a subscript c to the average symbol.

where $f_q = -(1/N) \ln Z_q|_{\tilde{h}=0}$ is the dilute Potts free energy per site and M is the Ising magnetization per site.

We conclude this section observing that (7.10) and (7.11) can also be derived as follows. Take $\tilde{h} = 0^+$ and denote by ν the average fraction of sites belonging to $\mathcal{L}_0$, and by ν_f the fraction of sites belonging to finite clusters. We have

$$\langle t(x) \rangle = \nu = P + \nu_f, \tag{7.13}$$

$$\langle \delta_{s(x),1} t(x) \rangle = P + \frac{1}{q} \nu_f \,, \tag{7.14}$$

where we use the fact that a site has color 1 with probability $1/q$ if it belongs to a finite cluster, and with probability 1 if it belongs to an infinite cluster[5]; equation (7.10) then follows recalling (7.3). Considering instead two sites x and y, we call $P_{\alpha\beta}(x-y)$ the probability that x is of type α and y of type β, with the following specifications: α and β take the value f if the corresponding site belongs to a finite cluster, i if it belongs to an infinite cluster, and e if it does not belong to a cluster (i.e. it is empty); more precisely, P_{ff} is the probability that the two sites belong to different finite clusters, while we call P_f the probability that they belong to the same finite cluster and P_i the probability that they both belong to infinite clusters. Introducing also the probability P_{oo} that the sites both belong to some cluster, we can write the relations

$$P_{oo} + P_{ie} + P_{fe} = \nu, \tag{7.15}$$

$$P_{oo} + 2(P_{ie} + P_{fe}) + P_{ee} = 1, \tag{7.16}$$

$$P_i + 2P_{if} + P_f + P_{ff} = P_{oo}, \tag{7.17}$$

$$P_i + P_{if} + P_{ie} = P. \tag{7.18}$$

These leave four independent two-point probabilities that we choose to be P_i, P_{if}, P_f and P_{ff}. Through them we can express the four independent two-point spin cor-

[5]Infinite clusters contribute only to the first term inside the product in (7.4) for $\tilde{h} \to 0^+$. In turn, only sites with color 1 contribute to this term.

relators in the dilute Potts model as

$$\langle t(x)t(0)\rangle = P_i + 2P_{if} + P_f + P_{ff}, \tag{7.19}$$

$$\langle \delta_{s(x),1} t(x)\ t(0)\rangle = P_i + \left(1+\frac{1}{q}\right) P_{if} + \frac{1}{q}\left(P_f + P_{ff}\right), \tag{7.20}$$

$$\langle \delta_{s(x),1} t(x)\ \delta_{s(0),1} t(0)\rangle = P_i + \frac{2}{q} P_{if} + \frac{1}{q} P_f + \frac{1}{q^2} P_{ff}, \tag{7.21}$$

$$\langle \delta_{s(x),k} t(x)\ \delta_{s(0),k} t(0)\rangle = \frac{1}{q} P_f + \frac{1}{q^2} P_{ff}, \qquad k \neq 1. \tag{7.22}$$

These equations give in particular

$$G(x) \equiv \langle \sigma_1(x)\sigma_1(0)\rangle_c = \left(1-\frac{1}{q}\right)^2 (P_i - P^2) + \frac{1}{q}\left(1-\frac{1}{q}\right) P_f, \tag{7.23}$$

$$\langle \sigma_k(x)\sigma_k(0)\rangle_c = \frac{1}{q^2}[(P_i - P^2) + (q-1)P_f], \qquad k \neq 1, \tag{7.24}$$

and (7.11) follows from the fact that $S = \lim_{q\to 1} \sum_x P_f(x)$.

7.3 Clusters and droplets near criticality

The critical properties of FK clusters within the Ising model are ruled by the renormalization group fixed points of the dilute Potts Hamiltonian (7.2) with $\tilde{h} = 0$ and $q \to 1$. Since the percolative properties do not affect the magnetic ones, we need to be at the magnetic fixed point $(T, H) = (T_c, 0)$ to start with, and are left with the problem of finding fixed points of the coupling J. It was first argued in [125] that for the case $J > 0$ of interest here there are two such fixed points, with a renormalization group pattern shown in Fig. 7.1. The critical properties of the Ising clusters (the FK clusters with $p = 1$, i.e. $J = +\infty$) renormalize onto those of the fixed point with the larger value of J, that we call J^*. This corresponds to the tricritical point of the dilute Potts model with $q \to 1$.

The second fixed point, located at $J = 2/T_c$, follows from the identity [125]

$$-\mathcal{H}_q|_{\tilde{h}=0,\ J=2/T} = \frac{2}{T} \sum_{<x,y>} (\delta_{\nu(x),\nu(y)} - 1) + (\ln q - 2H) \sum_x \delta_{\nu(x),0}, \quad \nu(x) = 0, 1, \ldots, q, \tag{7.25}$$

showing that for $J = 2/T$ the Ising and color variables can be combined into a single $(q+1)$-state Potts variable $\nu(x)$ taking the value 0 on sites with negative

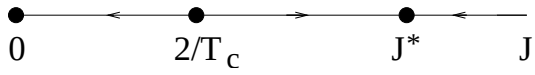

Figure 7.1: Renormalization group flows in the coupling J for the Hamiltonian (7.2) with $q \to 1$, $T = T_c$, $H = 0$. While $J = 0$ is just the Ising magnetic fixed point, $2/T_c$ and J^* are percolation fixed points for Ising droplets and Ising clusters, respectively.

Ising spin, and the values $1, \ldots, q$ on sites with positive Ising spin; for $2H = \ln q$, (7.25) exhibits a S_{q+1} invariance whose spontaneous breaking yields the fixed point at $T = T_c$, $H = 0$, in the limit $q \to 1$. It is natural to associate to the $(q+1)$-color Potts model (7.25) the spin variables

$$\omega_\alpha(x) = \delta_{\nu(x),\alpha} - \frac{1}{q+1}, \qquad \alpha = 0, 1, \ldots, q, \tag{7.26}$$

whose average provides the order parameter of the phase transition. Using $\nu(x) = t(x)s(x)$ and $\sum_{\alpha=0}^{q} \omega_\alpha = \sum_{k=1}^{q} \sigma_k = 0$, it is easy to check that the Ising site variable and the dilute Potts spin (7.3) can be written as

$$t(x) = -\omega_0(x) + \frac{q}{q+1}\,, \tag{7.27}$$

$$\sigma_k(x) = \omega_k(x) + \frac{\omega_0(x)}{q}, \qquad k = 1, \ldots, q\,. \tag{7.28}$$

Denoting $\langle \cdots \rangle_\beta$ the average in the phase where the spontaneous breaking of S_{q+1} permutational symmetry selects the direction β, we have

$$\langle \omega_\alpha \rangle_\beta = [(q+1)\delta_{\alpha\beta} - 1]\frac{M_{q+1}}{q}\,, \tag{7.29}$$

and, using (7.28),

$$\langle \sigma_1 \rangle_\beta = \begin{cases} 0\,, & \beta = 0 \\ \frac{q^2-1}{q^2} M_{q+1}\,, & \beta = 1\,. \end{cases} \tag{7.30}$$

At this point (7.10) implies $P = 0$ in the phase $\beta = 0$, and $P = M$ in the phase $\beta = 1$, where $M = 2M_2$ is the Ising spontaneous magnetization, as implied by (7.27) and (7.29). This amounts to say that there is a first order percolative transition along the segment $T < T_c$, $H = 0$, where the limit $H \to 0^{\mp}$ is described

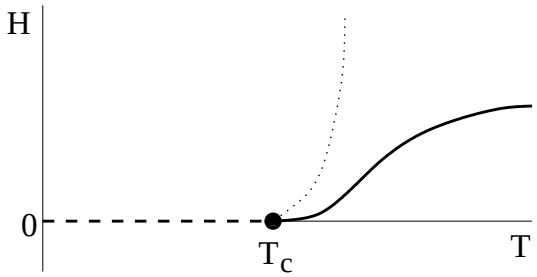

Figure 7.2: Phase diagrams for Ising clusters and droplets in two dimensions. The first order transition (dashed line) is common to clusters and droplets. Above T_c there is a second order transition along the continuous line for clusters, and along the Kertész line (dotted) for droplets.

by the phases $\beta = 0, 1$, respectively, of (7.25) with $q \to 1$. Hence, for $H = 0$, the magnetic and percolative transitions have the same nature and location, and, due to the identity $P = M$ at $H = 0^+$, the same critical exponents. Since these are the requirements of the droplet model [124] aimed at describing the magnetic transition as a percolation transition, the FK clusters with $p = 1 - e^{-2/T}$ are called *droplets*.

In two dimensions also the Ising clusters undergo a first order transition for $H = 0, T < T_c$ [126, 127]. Above T_c they exhibit instead a second order transition going from $(T, H) = (T_c, 0)$ to a non-negative value of H at infinite temperature, where, due to the vanishing of the ferromagnetic interaction, a random percolation fixed point is located. The first and second order transition lines determine a curve in the T-H plane above which $P > 0$ (Fig. 7.2).

Droplets cannot percolate at infinite temperature since they have $p = 0$ there. There is however a second order transition line, the Kertész line [135], going from the Curie point to a value of T at $H = +\infty$, where again a random percolation fixed point is located; $P > 0$ to the left of the Kertész line (Fig. 7.2).

The Curie point $(T, H) = (T_c, 0)$ is a fixed point for both Ising clusters and droplets. We consider the critical behavior of the percolative observables introduced in the previous section when this point is approached both at $H = 0$ and at $T = T_c$. Denoting by g the deviation from criticality, i.e. $|T - T_c|$ in the first

case and $|H|$ in the second, we have for $g \to 0$

$$P = B\, g^{\beta}\,, \tag{7.31}$$

$$S = \Gamma\, g^{-\gamma}\,, \tag{7.32}$$

$$\xi = f\, g^{-\nu}\,, \tag{7.33}$$

$$\left(\frac{\langle N_c\rangle}{N} - \frac{M}{2}\right)_{\rm sing} = \left(\frac{A_{-1}}{2}\ln^2 g - A_0 \ln g + \delta_{A_{-1},0}\, A_1\right) g^{\mu}\,. \tag{7.34}$$

Critical exponents[6] and critical amplitudes depend on the direction along which the critical point is approached. We distinguish the following cases:

(a) $T \to T_c^+$, $H = 0$: we attach a subscript a to amplitudes and exponents. As discussed in the next section, we will consider this limit only for droplets;

(b) $T \to T_c^-$, $H = 0^{\pm}$: we attach a subscript b to amplitudes and exponents and a superscript $\pm$ to the amplitudes. Droplet exponents are the same as in case (a);

(c) $T = T_c$, $H \to 0^{\pm}$: we attach a subscript c to amplitudes and exponents and a superscript $\pm$ to the amplitudes.

The form of (7.34) needs to be explained. Since the approach to criticality of the Ising magnetization M is known (see [134]), the most interesting part of (7.12) is the contribution coming from the dilute Potts free energy f_q. This is the sum of a regular part containing non-negative powers of g, and of a singular part,

$$f_q^{\rm sing}(g) = F_q\, g^{\mu_q}\,, \qquad g \to 0\,, \tag{7.35}$$

that we need to consider in the limit $q \to 1$. If μ_1 happens to coincide with a non-negative integer, the resonance with the regular part is signalled by a pole in the amplitude F_q. The latter can be expanded around $q = 1$ in the form

$$F_q = \sum_{k=-1}^{\infty} a_k \left[\Delta\mu_q\right]^k\,, \tag{7.36}$$

with $\Delta\mu_q \equiv -(\mu_q - \mu_1)$. Evaluation of (7.35) for $q \to 1$ then leads to

$$f_{\rm Ising}^{\rm sing}(g) = (-a_{-1}\ln g + \delta_{a_{-1},0}\, a_0)\, g^{\mu}\,, \qquad \mu \equiv \mu_1\,, \tag{7.37}$$

[6]Notice that for convenience the critical exponent μ has been defined instead of the more conventional notation $2 - \alpha$.

while $\partial_q f_q^{\rm sing}|_{q=1}$ yields (7.34) with

$$A_k = \partial_q \mu_q|_{q=1}\, a_k\,, \qquad k = -1, 0, 1\,. \tag{7.38}$$

When μ is an integer, i.e. when $a_{-1} \neq 0$, the term coming from A_1 in (7.34) and that coming from a_0 in (7.37) contribute to the regular part. Notice that in the case of random percolation[7] $f_1^{\rm sing}(g) = 0$, so that (7.36) starts from $k = 1$ and (7.34) holds with $M = A_{-1} = A_0 = 0$.

7.4 Field theory

As shown in [46], in the *scaling limit* towards the Curie point, each of the two phase diagrams of Fig. 7.2 (one for clusters, one for droplets) can be seen as the $q \to 1$ projection of a phase diagram living in a three-dimensional space with coordinates (g_1, g_2, q), where g_1 and g_2 are couplings which become $\tau \sim T - T_c$ and $h \sim H$, respectively, at $q = 1$. This three-dimensional phase diagram is associated to the field theory with action

$$\mathcal{A} = \mathcal{A}_{\rm CFT} - g_1 \int d^2x\, \phi_1(x) - g_2 \int d^2x\, \phi_2(x)\,, \tag{7.39}$$

where $\mathcal{A}_{\rm CFT}$ is the conformal action describing the pertinent critical line (parameterized by q) within the scaling limit of the dilute Potts model (7.2), and ϕ_1, ϕ_2 are S_q-invariant relevant fields in this conformal theory. Recalling that two-dimensional conformal field theories, see chapter 1, characterized by a central charge

$$c = 1 - \frac{6}{t(t+1)} \tag{7.40}$$

contain scalar primary fields $\varphi_{m,n}$ with scaling dimension

$$X_{m,n} = \frac{[(t+1)m - tn]^2 - 1}{2t(t+1)}\,, \tag{7.41}$$

[7] In random percolation $g = |p - p_c|$ measures the deviation from the critical site occupation probability.

	ν_b	β_b	γ_b	μ_b	ν_c	β_c	γ_c	μ_c
clusters	1	5/96	91/48	2	8/15	1/36	91/90	16/15
droplets	1	1/8	7/4	2	8/15	1/15	14/15	16/15

Table 7.1: Critical exponents for Ising percolation.

the action (7.39) that for $q \to 1$ describes the scaling limit for clusters and droplets is specified as follows [46]

$$\begin{aligned} &\text{clusters:} && \sqrt{q} = 2\sin\frac{\pi(t+2)}{2t}, && \phi_1 = \varphi_{1,3}, \quad \phi_2 = \varphi_{1,2}\,; \\ &\text{droplets:} && \sqrt{q+1} = 2\sin\frac{\pi(t-1)}{2(t+1)}, && \phi_1 = \varphi_{2,1}, \quad \phi_2 = \varphi_{(t+1)/2,(t+1)/2}\,. \end{aligned}$$

In the cluster case $\mathcal{A}_{\rm CFT}$ corresponds to the tricritical line of the dilute q-color Potts model, and ϕ_1, ϕ_2 are the dilution and energy fields along this line. In the droplet case $\mathcal{A}_{\rm CFT}$ corresponds to the critical line of the pure $(q+1)$-state Potts model (7.25), ϕ_1 is the energy field on this line and ϕ_2 the spin field ω_0. In both cases $q = 1$ corresponds to $t = 3$ and, as expected, $c = 1/2$, the central charge of the critical Ising model. The Potts spin has dimension X_s given by $X_{t/2,t/2}$ for clusters [131] and $X_{(t+1)/2,(p+1)/2}$ for droplets. The critical exponents in (7.31)-(7.34) are given by

$$\nu = \frac{1}{2-X}, \qquad \beta = X_s|_{q=1}\nu, \qquad \gamma = 2(1-X_s|_{q=1})\nu, \qquad \mu = 2\nu, \quad (7.42)$$

with $X = 1$ in cases (a) and (b), and $X = 1/8$ in case (c). The exponents are collected in Table 7.1.

The percolative transitions in the scaling Ising model are the $q \to 1$ limit of transitions associated to spontaneous breaking of S_q symmetry in (7.39). For both clusters and droplets, the first order part of the transition corresponds to $g_2 = 0$ and $g_1 < 0$. The second order part corresponds to $g_2 = 0$ and $g_1 > 0$ for clusters, while for droplets it maps onto a renormalization group trajectory with g_1 and g_2 both non-zero [46]. In particular, this implies that the deviation from $H = 0$ of the transition above T_c for clusters is entirely due to corrections to scaling, namely that the behavior associated to the limit (a) for clusters is non-

universal[8] and, in general, is not determined by the scaling theory (7.39). This is why the limit (a) for clusters is excluded in our study of universal amplitude ratios.

7.4.1 Integrability

It is known from [132] that deformations of conformal field theories with $c < 1$ through a single field of type $\varphi_{1,2}$, $\varphi_{2,1}$ or $\varphi_{1,3}$ are integrable. This means that cases (b),(c) for clusters and cases (a),(b) for droplets all are $q \to 1$ limits of integrable cases of (7.39). Integrable field theories are solved in the S-matrix framework [14], and we now recall the solutions for the scaling pure and dilute Potts model.

$\varphi_{2,1}$ and $\varphi_{1,2}$ deformations. Consider a (1+1)-dimensional integrable field theory with spontaneously broken S_Q symmetry [27]. The elementary excitations are kinks $K_{ij}(\theta)$, $i \neq j$, with mass m and energy-momentum $(m\cosh\theta, m\sinh\theta)$, interpolating between pairs of degenerate vacua $|\Omega_i\rangle$, $i = 1, \ldots, Q$. Integrability ensures that any scattering process reduces to a sequence of elastic two-kink collisions of type

$$|K_{ik}(\theta_1)K_{kj}(\theta_2)\rangle = \sum_l S_{ij}^{kl}(\theta_1 - \theta_2)\,|K_{il}(\theta_2)K_{lj}(\theta_1)\rangle\,, \tag{7.43}$$

where "in" ("out") asymptotic states correspond to θ_1 larger (smaller) than θ_2. Permutational symmetry implies that there are only four different two-kink scattering amplitudes $S_{ij}^{kl}(\theta)$: indeed, there are two scattering channels ($i = j$ and $i \neq j$) and in each of them the central vacuum can preserve its color ($l = k$) or change it ($l \neq k$). The minimal solution for these amplitudes, satisfying the constraints of unitarity, crossing symmetry, factorization and bootstrap, was determined in [27] and contains a parameter λ which is related to Q as

$$\sqrt{Q} = 2\sin\frac{\pi\lambda}{3}\,. \tag{7.44}$$

[8] In particular, the second order percolative transition is expected to stay at $H = 0$ for the triangular lattice, while it develops as in Fig. 7.2 for the square lattice (see [46]). As a consequence, the connectivity length for clusters at $T > T_c$, $H = 0$ is infinite in the first case, and finite in the second.

We discussed the solution to the scattering problem in an S_Q invariant field theory in section 2.7. For $Q \in (0,4)$, it corresponds to the $\varphi_{2,1}$ deformation of the Q-state Potts critical line when $\lambda \in (0,3/2)$, and to the $\varphi_{1,2}$ deformation of the Q-state Potts tricritical line when $\lambda \in (3/2,3)$. The critical and tricritical lines meet at $Q=4$ and have central charge (7.40) with

$$\lambda = \begin{cases} \frac{3(t-1)}{2(t+1)}\,, & \text{critical line} \\ \\ \frac{3(t+2)}{2t}\,, & \text{tricritical line}\,. \end{cases} \tag{7.45}$$

The spontaneously broken phase we are discussing corresponds to a specific sign of the coupling g conjugated to the field responsible for the deformation; the unbroken phase corresponds to the other sign and is related to the broken phase by duality.

The full particle spectrum is determined investigating the pole structure of the amplitudes and going through the bootstrap procedure [27, 102]. For our purposes it is enough to know that the two lightest topologically neutral bound states B_j, $j=1,2$, appear for $\lambda > j$ as poles of the kink-antikink amplitudes S_{ii}^{kl}; they have mass $m_j = 2m \sin \frac{j\pi}{2\lambda}$.

Integrability allows in particular the exact determination of the singular part of the free energy per unit area. For the $\varphi_{1,2}$ deformation it reads [136]

$$f^{\text{sing}}(g,t) = -\frac{\sin\left(\frac{\pi t}{3t+6}\right)}{4\sqrt{3}\sin\left(\frac{\pi(2t+2)}{3t+6}\right)}\, m^2\,, \tag{7.46}$$

where the kink mass is related to the coupling g as

$$m = \frac{2^{\frac{t+5}{3t+6}}\sqrt{3}\,\Gamma\left(\frac{1}{3}\right)\Gamma\left(\frac{t}{3t+6}\right)}{\pi\,\Gamma\left(\frac{2t+2}{3t+6}\right)} \left[\frac{\pi^2\, g^2\,\Gamma^2\left(\frac{3t+4}{4t+4}\right)\Gamma\left(\frac{1}{2}+\frac{1}{t+1}\right)}{\Gamma^2\left(\frac{t}{4t+4}\right)\Gamma\left(\frac{1}{2}-\frac{1}{t+1}\right)}\right]^{\frac{t+1}{3t+6}}\,. \tag{7.47}$$

Comparison with (7.35) gives

$$\mu(t) = \frac{4(t+1)}{3(t+2)}\,. \tag{7.48}$$

The corresponding results for the $\varphi_{2,1}$ deformation are obtained through the replacement $t \to -t-1$ into the last three equations [136].

$\varphi_{1,3}$ **deformation.** Consider a S_Q-invariant theory on the first order transition point where the ordered vacua $|\Omega_i\rangle$, $i = 1, \ldots, Q$, are degenerate with the disordered vacuum $|\Omega_0\rangle$. The elementary excitations are kinks K_{0i} with mass m, going from the disordered to the i-th ordered vacuum, together with their antikinks K_{i0}. There are again four different two-kink amplitudes which in the notation (7.43) read S_{00}^{kl}, S_{kl}^{00}, where the cases $k = l$ and $k \neq l$ have to be distinguished. The minimal integrable solution was given in [137] and corresponds to the $\varphi_{1,3}$ deformation of the Q-state Potts tricritical line. In this case the interaction among the kinks does not produce bound states. Again we refer to a specific sign (positive) of the coupling g conjugated to $\varphi_{1,3}$, the other sign corresponding to the massless flow from the tricritical to the critical line.

For the free energy we now have [138, 139]

$$f^{\rm sing}(g,t) = -\frac{\sin^2\frac{\pi t}{2}}{2\sin\pi t}\, m^2\,, \tag{7.49}$$

$$m = \frac{2\,\Gamma\left(\frac{t}{2}\right)}{\sqrt{\pi}\,\Gamma\left(\frac{t+1}{2}\right)}\left[\frac{\pi\, g\,(t-1)(2t-1)}{(1+t)^2}\sqrt{\frac{\Gamma\left(\frac{1}{1+t}\right)\Gamma\left(\frac{1-2t}{1+t}\right)}{\Gamma\left(\frac{t}{1+t}\right)\Gamma\left(\frac{3t}{1+t}\right)}}\right]^{\frac{1+t}{4}}\,, \tag{7.50}$$

$$\mu(t) = \frac{t+1}{2}\,. \tag{7.51}$$

7.4.2 Connectivity

Within our formalism based on factorized scattering among kinks, correlators are expressed as spectral sums

$$\langle\Phi(x)\Phi(0)\rangle_c = \sum_{n=1}^{\infty}\sum_{\gamma_1,\ldots,\gamma_{n-1}}\int_{\theta_1>\ldots>\theta_n}\frac{d\theta_1}{2\pi}\cdots\frac{d\theta_n}{2\pi}|F^{\Phi}_{\alpha\gamma_1\ldots\gamma_{n-1}\beta}(\theta_1,\ldots,\theta_n)|^2 e^{-m|x|\sum_{k=1}^n\cosh\theta_k}, \tag{7.52}$$

where the form factors

$$F^{\Phi}_{\alpha\gamma_1\ldots\gamma_{n-1}\beta}(\theta_1,\ldots,\theta_n) = \langle\Omega_\alpha|\Phi(0)|K_{\alpha\gamma_1}(\theta_1)K_{\gamma_1\gamma_2}(\theta_2)\ldots K_{\gamma_{n-1}\beta}(\theta_n)\rangle \tag{7.53}$$

can be computed exactly relying on the knowledge of the S-matrix (see the form factor equations in Appendix A). The greek vacuum indices in (7.53) take the

color value $k = 1, \ldots, q$, and also the value 0 when $q + 1$ phases coexist; it is understood that adjacent vacuum indices cannot coincide. We included in (7.52) only the states made of elementary kink excitations; it is understood that if there are stable bound states they also contribute to the spectral sum. It is well known that spectral series in integrable field theory converge very rapidly and that truncation of the series to the first (lightest) contribution is sufficient to provide accurate results upon integration in d^2x (see in [18]) the results obtained in this way for random percolation). This is the approximation we are going to adopt also in this chapter.

It follows from (7.23) that the problem of determining the connectivity function $P_f(x)$ reduces to the study of the Potts connected correlator $G(x)$ in the limit $q \to 1$. This correlator vanishes at $q = 1$ (no Potts degrees of freedom), and (7.23) shows that it vanishes linearly in $q - 1$:

$$P_f(x) = \lim_{q \to 1} \frac{G(x)}{q - 1} \,. \tag{7.54}$$

The S-matrix does not force itself the form factors to vanish at $q = 1$; the vanishing of form factors can instead be induced by the color structure of the fields and by their normalization conditions. The constraint $\sum_k \sigma_k = 0$ can induce a linear vanishing of the form factors of σ_1 on some states; the contribution of these states then vanishes quadratically in the spectral decomposition of $G(x)$, and can be ignored for $q \to 1$. This means that the leading (linear) contribution in $q - 1$ to $G(x)$ comes entirely from the sum over color indices in the spectral sum, i.e. from the multiplicity of form factors identified by color symmetry.

Notice that this symmetry can identify form factors of σ_1 only through permutations of the vacuum indices $\gamma_i = 2, \ldots, q$, because color 1 is carried by the field itself[9]. It follows in particular that the states whose vacuum indices take only the values 0 and 1 (i.e. the states which are well defined at $q = 1$ and that, for this reason, we call Ising states) cannot contribute to the multiplicity factor $q - 1$, and then are among those giving a subleading contribution as $q \to 1$. Finally we conclude that the leading contribution to $G(x)$ for $|x| \to \infty$, $q \to 1$, comes from the states with minimal total mass which are not Ising states. It

[9] In the cases we consider the external indices α, β in (7.53) take values 0 or 1.

follows from (7.6) that this minimal total mass coincides with the inverse true connectivity length ξ_t.

We now discuss the correlator $G(x)$, first for clusters and then for droplets, in the cases (a), (b) and (c) defined in the previous section, recalling that these are cases of (7.39) with $q \to 1$: (a) (for droplets only) and (b) correspond to $g_2 = 0$, while (c) corresponds to $g_1 = 0$; the sign of $T - T_c$ and H coincides with that of g_1 and g_2, respectively.

Clusters. In the case (b) we are within the $\phi_{1,3}$ deformation of the Potts tricritical line, with degenerate vacua $|\Omega_\alpha\rangle$, $\alpha = 0, 1, \ldots, q$. For $H = 0^+$, the color symmetry is spontaneously broken and $P = \partial_q \langle \Omega_1 | \sigma_1 | \Omega_1 \rangle|_{q=1} \neq 0$. The form factors entering the spectral sum for $G(x)$ are of type $F^{\sigma_1}_{10k0j\cdots 01}$, and the lightest non-Ising contribution comes from the four-kink term $\sum_{k=2}^q |F^{\sigma_1}_{10k01}|^2 = (q-1)|F^{\sigma_1}_{10201}|^2$. It follows, in particular, that $\xi_t = 1/4m$. For $H = 0^-$ we are in the Potts disordered vacuum and $P = \langle \Omega_0 | \sigma_1 | \Omega_0 \rangle = 0$. $G(x)$ decomposes on the form factors $F^{\sigma_1}_{0k0i\cdots j0}$ and the lightest non-Ising contribution comes from the two-kink term $\sum_{k=2}^q |F^{\sigma_1}_{0k0}|^2 = (q-1)|F^{\sigma_1}_{020}|^2$; $\xi_t = 1/2m$. It is interesting to compare the true connectivity length with the magnetic true correlation length $\hat{\xi}_t$ defined from the decay of the Ising spin-spin correlator,

$$\langle \sigma(x)\sigma(0) \rangle_c \sim \mathrm{e}^{-|x|/\hat{\xi}_t}, \quad |x| \to \infty \,. \tag{7.55}$$

This is now determined by the lightest Ising states in the topologically neutral sector, i.e. $\hat{\xi}_t = 1/2m$ for $H = 0^\pm$.

Case (c) corresponds to the $\varphi_{1,2}$ deformation of the Potts tricritical line. For $H \to 0^+$ we are in the spontaneously broken phase with degenerate vacua $|\Omega_k\rangle$, $k = 1, \ldots, q$, and $P = \partial_q \langle \Omega_1 | \sigma_1 | \Omega_1 \rangle|_{q=1} \neq 0$. It follows from what we said about this deformation and from (7.44) that $q \to 1$ amounts to $\lambda \to 5/2$, so that the theory possesses, in particular, also the stable topologically neutral bound states B_j. However, the states $|B_j\rangle$ are Ising states, and the lightest non-Ising contribution to $G(x)$ comes from the term $\sum_{k=2}^q |F^{\sigma_1}_{1k1}|^2 = (q-1)|F^{\sigma_1}_{121}|^2$, which implies $\xi_t = 1/2m$. For $H \to 0^-$ there is instead a single, disordered vacuum, and the excitations are not kinks. This phase, however, is related to the previous one by duality [62], so that $G(x)$ at $H \to 0^-$ coincides with $\langle \mu_j(x)\mu_j(0) \rangle$ at $H \to 0^+$, where $\mu_j(x)$ is the Potts disorder field which interpolates the kink

K_{1j}. The lightest contribution to $G(x)$ comes then from the single one-kink term $|F_{1j}^{\mu_j}(\theta)|^2$. The latter, however, coincides [62] with $\langle\Omega_1|\sigma_1|\Omega_1\rangle|F_{1j1}^{\sigma_1}(\infty,0)|$, and then is proportional to $q-1$, as required. It also follows that $\xi_t = 1/m$. Concerning the magnetic correlation length, the lightest topologically neutral Ising state is $|B_1\rangle$, so that $\hat{\xi}_t = 1/m_1 = 1/(2m\sin\frac{\pi}{5})$ for $H \to 0^{\pm}$.

Droplets. Case (b) corresponds to the $\varphi_{2,1}$ deformation of the $(q+1)$-state Potts critical line, with S_{q+1} permutational symmetry, degenerate vacua $|\Omega_\alpha\rangle$ and kinks $K_{\alpha\beta}$, $\alpha,\beta = 0,1,\ldots,q$, which are the only particles for $q \leq 2$. For $H = 0^+$ the S_{q+1} symmetry is spontaneously broken in the direction 1, and $\langle\Omega_1|\sigma_1|\Omega_1\rangle$ is given by the second line of (7.30). The lightest non-Ising contribution to $G(x)$ is $\sum_{k=2}^{q}|F_{1k1}^{\sigma_1}|^2 = (q-1)|F_{121}^{\sigma_1}|^2$. For $H = 0^-$ the S_{q+1} symmetry is spontaneously broken in the direction 0, so that the S_q color symmetry is unbroken and $P = \langle\Omega_0|\sigma_1|\Omega_0\rangle = 0$, as in the first line of (7.30). The lightest non-Ising contribution to $G(x)$ is $\sum_{k=2}^{q}|F_{0k0}^{\sigma_1}|^2 = (q-1)|F_{020}^{\sigma_1}|^2$. We have $\xi_t = \hat{\xi}_t = 1/2m$ for $H = 0^{\pm}$.

Case (a) corresponds to the same deformation as case (b), but with the S_{q+1} symmetry unbroken and a single vacuum. Relation (7.28) and use of S_{q+1} invariance give $G(x) = [(q^2-1)/q^2]\langle\omega_0(x)\omega_0(0)\rangle$, which already contains the factor $q-1$. Again duality identifies $\langle\omega_0(x)\omega_0(0)\rangle$ of the unbroken phase with the correlator $\langle\Omega_1|\tilde{\omega}_j(x)\tilde{\omega}_j(0)|\Omega_1\rangle$ of the disorder field computed in the broken phase, which receives its lightest contribution from the one-kink term $|F_{1j}^{\tilde{\omega}_j}|^2$. Notice that, as in case (c) for clusters, this term can be rewritten as $\langle\Omega_1|\omega_1|\Omega_1\rangle|F_{1j1}^{\omega_1}(\infty,0)|$, but this time $\langle\Omega_1|\omega_1|\Omega_1\rangle$ does not vanish for $q \to 1$, because we are in a $(q+1)$-state Potts model, and this agrees with the fact that the necessary $q-1$ factor in $G(x)$ has already been obtained. For the correlation lengths we have $\xi_t = \hat{\xi}_t = 1/m$. Droplet connectivity at $H = 0$ is further discussed in appendix B.

In case (c) the theory is not integrable for $q > 1$, and this eventually does not allow the computation of the form factors. We can however discuss some essential features. We deal with a $(q+1)$-state Potts model in presence of a field ω_0 which explicitly breaks the symmetry down to the S_q color symmetry. We see from the phase diagram of Fig. 7.2 that for $H \to 0^+$ we are inside the region with $P > 0$, where the color symmetry is spontaneously broken, so that there are q degenerate vacua $|\Omega_k\rangle$ and elementary kink excitations K_{ij} interpolating among them. The

lightest non-Ising contribution to $G(x)$ is $\sum_{k=2}^{q} |F_{1k1}^{\sigma_1}|^2 = (q-1)|F_{121}^{\sigma_1}|^2$, which implies $\xi_t = 1/2m$. For $H \to 0^-$ the color symmetry is unbroken and the vacuum is unique, but this time we are not able to use duality to make contact with the broken phase.

7.5 Universal ratios

The connections with integrable field theory discussed in the previous section allows us to compute many of the critical amplitudes defined by (7.31)-(7.34), both for clusters and droplets. The amplitudes are not universal, but universal combinations can be made out of them in which metric factors cancel [75].

As we saw, the amplitudes Γ and f for mean cluster size and connectivity lengths follow from the study of the Potts spin correlator $G(x)$, which determines the connectivity function $P_f(x)$. The known effectiveness of the large $|x|$ approximation, as well as the use of duality, allowed us to reduce the problem to that of the determination of some n-kink form factors of the Potts spin field. We saw that $n = 2$ in most cases, while one case requires $n = 4$. Four-kink form factors of the Potts spin for generic q have not been studied in the literature, and we make no attempt to discuss them here. Concerning the two-kink form factors of the Potts spin field, complete results were obtained in [137] for the $\varphi_{1,3}$ deformation; the $\varphi_{2,1}$ and $\varphi_{1,2}$ deformations are more complicated and only partial results are available [62, 18]. In appendix B we give an approximate form factor solution that we use for the evaluation of some droplets amplitudes at $H = 0$.

The amplitudes B of the percolative order parameter are also related to the Potts spin two-kink form factors. Indeed eq. (7.60) of appendix A with $n = 0$ and $\Phi = \sigma_1$ relates these matrix elements to the vacuum expectation value in (7.10).

The amplitudes A_k entering (7.34) follow from the $t \to 3$ limit of the free energies (7.46), (7.49), through (7.38). Phases coexisting at a first order transition point have the same free energy, as well as phases related by duality. Since $\mu = \mu_1$ is an integer in the case of the $\varphi_{1,3}$ and $\varphi_{2,1}$ deformations, $f^{\rm sing}(g,p)$ has a pole at $t = 3$ (i.e. $a_{-1} \neq 0$, see Table 7.2), in agreement with the discussion at the end of section 7.3. These deformations both give the scaling Ising model with $H = 0$ when $p \to 3$, and the fact that they yield the same coefficients a_{-1} and a_0 is then

Deformation	a_{-1}	a_0	a_1	$\partial_q \mu_q\|_{q=1}$
ϕ_{13}	$-\pi$	$\pi(\gamma + \ln \pi)$	-	$\frac{9}{4\pi\sqrt{3}}$
ϕ_{12}	0	$-1.1977..$	2.7929..	$\frac{6}{25\pi\sqrt{3}}$
ϕ_{21}	$-\pi$	$\pi(\gamma + \ln \pi)$	-	$-\frac{4}{3\pi}$

Table 7.2: Results determining the amplitudes (7.38) for the different integrable directions. γ is the Euler-Mascheroni constant.

expected from (7.37).

The results for the universal combinations of critical amplitudes that we obtain exploiting all these pieces of information are collected in Table 7.3. They include the combinations

$$U \equiv \frac{4B^2 (f^-_{\rm 2nd})^2}{\Gamma^-}\,, \qquad\qquad R \equiv A^-_0 (f^-_{\rm t})^2\,, \tag{7.56}$$

whose universality follows from the scaling relations $2\beta + \gamma = 2\nu = \mu$.

In Table 7.3 the results involving only the amplitudes[10] $f_{\rm t}$, $\hat{f}_{\rm t}$ and A_k are exact. The results which involve the amplitudes $f_{\rm 2nd}$ and Γ, whose evaluation requires the integration of the connectivity function, are instead approximated, with the following exceptions for the droplet case. As shown in appendix B, droplet connectivity is the same for $H = 0^{\pm}$, and this is why we quote that Γ^+_b/Γ^-_b and $f^+_{{\rm 2nd},b}/f^-_{{\rm 2nd},b}$ are exactly equal to 1; moreover, (7.68) determines the droplet connectivity in case (a) in terms of the Ising spin-spin correlator, which is exactly known [133] and gives the exact result for $f_{{\rm 2nd},a}/f_{{\rm t},a}$.

The approximated results are of two types. Those involving the truncation of the spectral series as the only approximation are expected to be very accurate, with an error that, as in other similar computations (see e.g. [18]), is hardly expected to exceed 1%. Those droplet results (signalled by a dagger) which instead also rely on the use of the approximate two-kink form factor (7.76) could have larger errors.

We close this section discussing the issue of the correspondence between magnetic and droplet universal properties at $H = 0^+$. As we saw in section 7.3 there

[10] We denote $\hat{f}_{\rm t}$ the amplitudes of the magnetic correlation length defined by (7.55).

	clusters	droplets
Γ_a/Γ_b^+	non-universal	$40.3^\dagger$
$f_{2\mathrm{nd},a}/f_{\mathrm{t},a}$	"	0.99959..
$f_{\mathrm{t},a}/f_{\mathrm{t},b}^+$	"	2
$f_{\mathrm{t},a}/\hat{f}_{\mathrm{t},a}$	"	1
$A_{k,a}/A_{k,b}^+;\ k=0,-1$	"	1
Γ_b^+/Γ_b^-	-	1
$f_{\mathrm{t},b}^+/f_{\mathrm{t},b}^-$	1/2	1
$f_{2\mathrm{nd},b}^-/f_{\mathrm{t},b}^-$	0.6799	$0.61^\dagger$
$f_{2\mathrm{nd},b}^+/f_{2\mathrm{nd},b}^-$	-	1
$f_{\mathrm{t},b}^+/\hat{f}_{\mathrm{t},b}^\pm$	1/2	1
U_b	24.72	$15.2^\dagger$
$A_{k,b}^+/A_{k,b}^-;\ k=0,-1$	1	1
$A_{0,b}^\pm/A_{-1,b}^\pm$	$-\gamma-\ln\pi=-1.7219..$	$-\gamma-\ln\pi=-1.7219..$
R_b	$\frac{3\sqrt{3}(\gamma+\ln\pi)}{64\pi^2}=0.014165..$	$-\frac{\gamma+\ln\pi}{12\pi^2}=-0.014539..$
$f_{\mathrm{t},c}^+/f_{\mathrm{t},c}^-$	1/2	-
$f_{2\mathrm{nd},c}^-/f_{\mathrm{t},c}^-$	1.002	-
$f_{\mathrm{t},c}^+/\hat{f}_{\mathrm{t},c}^\pm$	$\sin\frac{\pi}{5}=0.58778..$	-
$A_{k,c}^+/A_{k,c}^-;\ k=0,1$	1	-
$A_{0,c}^\pm/A_{1,c}^\pm$	$-0.42883..$	-
R_c	$-3.7624..\times10^{-3}$	-

Table 7.3: Results for amplitude ratios in Ising correlated percolation. Those quoted without decimal digits or followed by dots are exact, the others are computed in the two-kink approximation; the dagger signals the use of the approximate form factor (7.76). Empty cases are due to ignorance of some form factors in integrable cases or, in direction (c) for droplets, to lack of integrability; ratios involving amplitudes for clusters in direction (a) are non-universal. $\gamma=0.5772..$ is the Euler-Mascheroni constant.

is in the case an identification of the order parameters: $P = M$. This is at the origin of the fact that the magnetic correlator $\langle\sigma(x)\sigma(0)\rangle_c$ and the droplet connectivity $P_f(x)$ both diverge as $|x|^{-1/4}$ when $|x|/\xi \to 0$. In turn, this implies that the magnetic susceptibility χ and the mean droplet size S, which are the integrals over x of these two functions, diverge with the same exponent $\gamma = 7/4$ as $T \to T_c$. Equation (7.68) shows that the magnetic correlator actually coincides with $2P_f$ at all distances above T_c; the two functions, however, differ below T_c due to the presence of infinite droplets. It follows that the ratio of droplet size amplitudes above and below T_c does not coincide with the corresponding susceptibility ratio, a fact already pointed out in [140]. Actually, (7.68) implies that the size ratio is larger than the susceptibility ratio. Our computation shows that the difference between the two ratios is not very large: our approximated result for the first, close to 40, has to be compared with the susceptibility result 37.7 [133]. Similar remarks apply to any ratio involving integrated correlations below T_c.

Appendix A

The n-kink form factors (7.53) satisfy functional equations similar to those well known for form factors on non-topological excitations [61, 60]. For $n = 2$ the kink form factor equations where considered in [62]; here we write them for any n:

$$F^{\Phi}_{\ldots\gamma_{i-1}\gamma_i\gamma_{i+1}\ldots}(\ldots,\theta_i,\theta_{i+1},\ldots) = \sum_{\delta} S^{\gamma_i\delta}_{\gamma_{i-1}\gamma_{i+1}}(\theta_i-\theta_{i+1}) F^{\Phi}_{\ldots\gamma_{i-1}\delta\gamma_{i+1}\ldots}(\ldots,\theta_{i+1},\theta_i,\ldots)\,, \tag{7.57}$$

$$-i\,\mathrm{Res}_{\theta_1-\theta_2=iu^a_{KK}} F_{\alpha\gamma_1\gamma_2\ldots}(\theta_1,\theta_2,\ldots) = (1-\delta_{\alpha\gamma_2})\Gamma^K_{KK} F^{\Phi}_{\alpha\gamma_2\ldots}(\theta_a,\theta_3,\ldots) + \delta_{\alpha\gamma_2}\Gamma^B_{KK} F^{\Phi}_{\alpha\alpha\gamma_3\ldots}(\theta_a,\theta_3,\ldots)\,, \tag{7.58}$$

$$F^{\Phi}_{\alpha\beta\gamma_1\ldots\gamma_{n-2}\alpha}(\theta',\theta,\theta_1,\ldots,\theta_{n-2}) = F^{\Phi}_{\beta\gamma_1\ldots\gamma_{n-2}\alpha\beta}(\theta,\theta_1,\ldots,\theta_{n-2},\theta'-2i\pi)\,, \tag{7.59}$$

$$-i\,\mathrm{Res}_{\theta'=\theta+i\pi} F^{\Phi}_{\alpha\beta\gamma_1\ldots\gamma_{n-2}\alpha}(\theta',\theta,\theta_1,\ldots,\theta_{n-2}) = \delta_{\alpha\gamma_1}[F^{\Phi}_{\alpha\gamma_2\ldots\gamma_{n-2}\alpha}(\theta_1,\ldots,\theta_{n-2}) + \tag{7.60}$$

$$-\sum_{\delta_1\ldots\delta_{n-3}} S^{\gamma_1\delta_1}_{\beta\gamma_2}(\theta-\theta_1)\ldots S^{\gamma_{n-3}\delta_{n-3}}_{\delta_{n-4}\gamma_{n-2}}(\theta-\theta_{n-3}) S^{\gamma_{n-2}\beta}_{\delta_{n-3}\alpha}(\theta-\theta_{n-2}) F^{\Phi}_{\beta\delta_1\ldots\delta_{n-3}\beta}(\theta_1,\ldots,\theta_{n-2})]\,.$$

Equation (7.57) immediately follows from the commutation relations (7.43). Equation (7.58) is the statement that the form factor inherits from the S-matrix the bound state poles corresponding to kinks (K) or topologically neutral particles (B); the residue of the scattering amplitudes on these poles determines also the three-particle couplings Γ^a_{KK}.

Equations (7.59) and (7.60), that we wrote for the case of a topologically neutral field Φ, can be derived adapting to the kink case an argument of [60]. Consider the set of rapidities $\theta' \geq \theta > \theta_1 > \ldots > \theta_{n-2}$, and recall that particles ordered with decreasing (increasing) rapidities form an "in" ("out") state. The relations

$$\langle K_{\alpha\beta}(\theta')|\Phi|K_{\beta\gamma_1}(\theta)K_{\gamma_1\gamma_2}(\theta_1)\ldots K_{\gamma_{n-2}\alpha}(\theta_{n-2})\rangle = F^{\Phi}_{\alpha\beta\gamma_1\ldots\gamma_{n-2}\alpha}(\theta'+i\pi,\theta,\theta_1,\ldots,\theta_{n-2}) + 2\pi\delta(\theta'-\theta)\delta_{\alpha\gamma_1}F^{\Phi}_{\alpha\gamma_2\ldots\gamma_{n-2}\alpha}(\theta_1,\ldots,\theta_{n-2})\,, \tag{7.61}$$

$$\langle K_{\alpha\beta}(\theta')|\Phi|K_{\beta\delta_1}(\theta_{n-2})\dots K_{\delta_{n-3}\delta_{n-2}}(\theta_1)K_{\delta_{n-2}\alpha}(\theta)\rangle = F^{\Phi}_{\beta\delta_1\dots\delta_{n-2}\alpha\beta}(\theta_{n-2},\dots,\theta_1,\theta,\theta'-i\pi) + 2\pi\delta(\theta'-\theta)\delta_{\beta\delta_{n-2}}F^{\Phi}_{\beta\delta_1\dots\delta_{n-3}\beta}(\theta_{n-2},\dots,\theta_1)\,, \tag{7.62}$$

are pictorially shown in Fig. 7.3 and correspond to the crossing of the kink with rapidity θ' into an "in" or an "out" state, respectively. The term containing the delta function is a disconnected part associated to kink-antikink annihilation. We can now use (7.43) to reverse the ordering of the kinks with rapidities $\theta_{n-2},\dots,\theta_1,\theta$ in (7.62), with the result

$$\sum_{\varepsilon_1\dots\varepsilon_{n-2}} S^{\delta_{n-2}\varepsilon_{n-2}}_{\delta_{n-3}\alpha}(\theta_{n-2}-\theta)S^{\delta_{n-3}\varepsilon_{n-3}}_{\delta_{n-4}\varepsilon_{n-2}}(\theta_{n-3}-\theta)\dots S^{\delta_1\varepsilon_1}_{\beta\varepsilon_2}(\theta_1-\theta)\times \Big[\langle K_{\alpha\beta}(\theta')|\Phi|K_{\beta\varepsilon_1}(\theta)...K_{\varepsilon_{n-2}\alpha}(\theta_{n-2})\rangle - F^{\Phi}_{\beta\varepsilon_1\dots\varepsilon_{n-2}\alpha\beta}(\theta,\theta_1,...,\theta_{n-2},\theta'-i\pi)\Big] = 2\pi\delta(\theta'-\theta)\delta_{\beta\delta_{n-2}}F^{\Phi}_{\beta\delta_1\dots\delta_{n-3}\beta}(\theta_1,...,\theta_{n-2}). \tag{7.63}$$

The relation (see Fig. 7.3)

$$\sum_{\delta_1\dots\delta_{n-2}} \Big[S^{\sigma_1\delta_1}_{\beta\sigma_2}(\theta-\theta_1)\dots S^{\sigma_{n-3}\delta_{n-3}}_{\delta_{n-4}\sigma_{n-2}}(\theta-\theta_{n-3})S^{\sigma_{n-2}\delta_{n-2}}_{\delta_{n-3}\alpha}(\theta-\theta_{n-2})\times S^{\delta_{n-2}\varepsilon_{n-2}}_{\delta_{n-3}\alpha}(\theta_{n-2}-\theta)S^{\delta_{n-3}\varepsilon_{n-3}}_{\delta_{n-4}\varepsilon_{n-2}}(\theta_{n-3}-\theta)\dots S^{\delta_1\varepsilon_1}_{\beta\varepsilon_2}(\theta_1-\theta)\Big] = \delta^{\varepsilon_1}_{\sigma_1}\dots\delta^{\varepsilon_{n-2}}_{\sigma_{n-2}}\,, \tag{7.64}$$

allows to rewrite (7.63) as

$$\langle K_{\alpha\beta}(\theta')|\Phi|K_{\beta\gamma_1}(\theta)K_{\gamma_1\gamma_2}(\theta_1)...K_{\gamma_{n-2}\alpha}(\theta_{n-2})\rangle = F^{\Phi}_{\beta\gamma_1\dots\gamma_{n-2}\alpha\beta}(\theta,\theta_1,...,\theta_{n-2},\theta'-i\pi)+ 2\pi\delta(\theta'-\theta)\sum_{\delta_1\dots\delta_{n-3}} S^{\gamma_1\delta_1}_{\beta\gamma_2}(\theta-\theta_1)\dots S^{\gamma_{n-2}\beta}_{\delta_{n-3}\alpha}(\theta-\theta_{n-2})F^{\Phi}_{\beta\delta_1\dots\delta_{n-3}\beta}(\theta_1,...,\theta_{n-2}). \tag{7.65}$$

Comparison of (7.61) and (7.65) for $\theta\neq\theta'$ and $\theta=\theta'$ leads to (7.59) and (7.60), respectively.

Appendix B

We saw in section 7.4 that the droplet connectivity in case (b) is related to $G(x)=\langle\Omega_\alpha|\sigma_1(x)\sigma_1(0)|\Omega_\alpha\rangle_c$ in the $(q+1)$-state Potts model, with $\alpha=0,1$ for

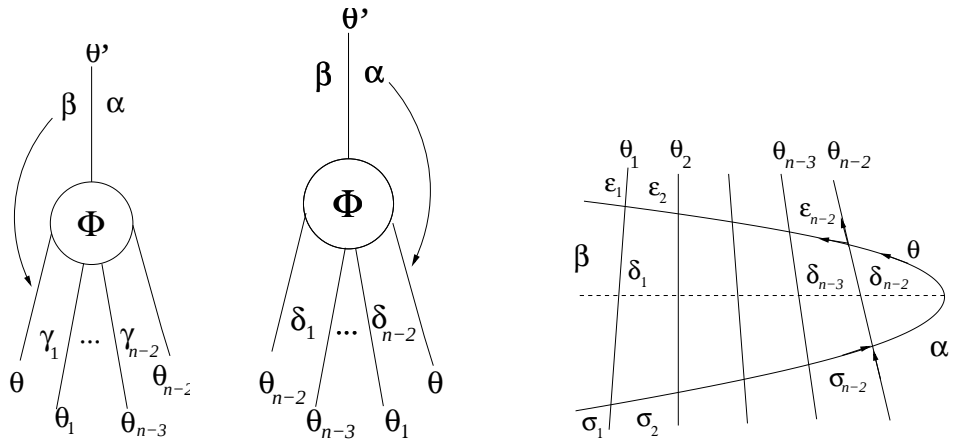

Figure 7.3: Graphical representations of the crossing patterns in (7.61) and (7.62), and of the amplitude product in (7.64).

$H = 0^{\mp}$, respectively. Using (7.28), $\sum_{k=0}^{q} \omega_k = 0$ and permutational symmetry one easily obtains

$$\begin{aligned} G(x) &= \sum_{j,k=2}^{q} \langle \Omega_\alpha | \omega_j(x) \omega_k(0) | \Omega_\alpha \rangle_c + O((q-1)^2) \\ &= (q-1)[\langle \Omega_\alpha | \omega_3(x)\omega_3(0) - \omega_2(x)\omega_3(0) | \Omega_\alpha \rangle_c] + O((q-1)^2)\,, \end{aligned} \tag{7.66}$$

which is the same for the two values of α. On the other hand, (7.24), (7.28) and permutational symmetry give for the connectivity within infinite droplets at $H = 0^+$

$$P_i(x) - P^2 = \lim_{q\to 1} \langle \sigma_{k\neq 1}(x)\sigma_{k\neq 1}(0)\rangle_c = 2 \lim_{q\to 1} \langle \Omega_1 | \omega_0(x)\omega_0(0) + \omega_2(x)\omega_0(0) | \Omega_1 \rangle_c\,. \tag{7.67}$$

Repeating the computation at $H = 0^-$, namely on the vacuum $|\Omega_0\rangle$, gives 0, as expected. Since for $\alpha = 1$ we are free to permute $3 \to 0$ in (7.66), comparison with the last equation together with (7.54) give for the magnetic correlator

$$\langle \sigma(x)\sigma(0)\rangle_c = 2P_f(x) + P_i(x) - P^2, \qquad H = 0^+, \tag{7.68}$$

where we also used $\sigma = -2\omega_0 + O(q-1)$, a consequence of (7.27). Actually, it is easy to see computing $G(x)$ for unbroken S_{q+1} symmetry that (7.68) holds also

for $T > T_c$, where of course $P_i = P = 0$.

Expanding (7.66) over kink states one recovers the result of section 7.4 for the droplet connectivity in case (b), namely

$$P_f(x) = \int\limits_{\theta_1>\theta_2} \frac{d\theta_1}{2\pi}\frac{d\theta_2}{2\pi}|F(\theta_1,\theta_2)|^2 e^{-m|x|(\cosh\theta_1+\cosh\theta_2)} + O(e^{-3m|x|})\,, \tag{7.69}$$

with

$$F = F^{\sigma_1}_{\alpha 2\alpha}|_{q=1} = (F^\omega_1 + F^\omega_3)|_{q=1} \tag{7.70}$$

as a consequence of (7.28) and

$$F^{\omega_\alpha}_{\gamma\beta\gamma} \equiv \delta_{\alpha\gamma}F^\omega_1 + \delta_{\alpha\beta}F^\omega_2 + (1-\delta_{\alpha\gamma})(1-\delta_{\alpha\beta})F^\omega_3\,, \tag{7.71}$$

$$F^\omega_1 + F^\omega_2 + (q-1)F^\omega_3 = 0\,. \tag{7.72}$$

The form factors (7.71) were studied in [62]. For $q+1=2$, $F^\omega_1(\theta_1,\theta_2)$ is simply given by $iM_2\tanh(\theta/2)$, where $M_2 = P/2$ is defined in (7.29) and $\theta = \theta_1 - \theta_2$; $F^\omega_3(\theta_1,\theta_2) \equiv iM_2 f_3(\theta)$ is the solution of the constraints[11]

$$f_3(\theta) = -\frac{\sqrt{2}\sinh\frac{3\theta}{4}}{\sinh\left[\frac{3}{4}\left(\theta - \frac{i\pi}{3}\right)\right]}\tanh\frac{\theta}{2} + \left[\frac{\sqrt{2}\sinh\frac{3\theta}{4}}{\sinh\left[\frac{3}{4}\left(\theta - \frac{i\pi}{3}\right)\right]} - 1\right] f_3(-\theta)\,, \tag{7.73}$$

$$f_3(\theta + 2i\pi) = f_3(-\theta)\,, \tag{7.74}$$

$$\mathrm{Res}_{\theta=i\pi} f_3(\theta) = 0\,, \tag{7.75}$$

with the mildest asymptotic behavior as $\theta \to +\infty$. Here we content ourselves with an approximate solution to this analytic problem. Notice first of all that (7.73) and (7.74) yield in particular $f_3(0) = 0$ and $f_3(+\infty) = -i$; a solution of (7.73) is easily checked to be $-i\tanh\frac{3\theta}{4}\tanh\frac{\theta}{2}$. If we take instead

$$\tilde{f}_3(\theta) = -i\tanh\theta\tanh\frac{\theta}{2}\,, \tag{7.76}$$

we satisfy (7.74) and (7.75) at the price of badly approximating $f_3(\theta)$ near $\theta = 0$, where in any case this function is vanishing and can be expected to give a small contribution to the rapidity integral in the spectral sum. The quality of the approximation is illustrated in Table 7.4.

[11] Equations (7.73), (7.74), (7.75) are the specialization of (7.57), (7.59), (7.60), respectively.

rhs/lhs	θ
0.5	0
$0.763 + 0.150i$	1
$0.933 + 0.061i$	2
$0.983 + 0.017i$	3
$0.996 + 0.004i$	4
$0.999 + 0.001i$	5

Table 7.4: The ratio between the rhs and the lhs of (7.73) with (7.76) in place of f_3, for some values of θ.

Bibliography

[1] S. Broadbent and J. Hammersley, Proceedings of the Cambridge Philosophical Society 53 (1957) 629-645.

[2] B. Bollobas and O. Riordan, Percolation, Cambridge, 2006.

[3] G. Grimmett, Percolation (2nd ed.), Springer, 1999.

[4] C. Itzykson and J. M. Drouffe, Statistical Field Theory vol. I and II, Cambridge, 1989.

[5] J. Cardy, Renormalization and scaling in statistical physics, Cambridge, 1996.

[6] D. Stauffer and A. Aharony, Introduction to percolation theory (2nd ed.), Taylor & Francis, London, 1992.

[7] R. Albert and L. Barabasi, Rev. Mod. Phys. 74 (2002).

[8] P. G. De Gennes, Scaling concepts in polymer physics, Cornell Univ. Press, 1979.

[9] M. Sahimi, Applications of percolation theory, Taylor & Francis, London, 2007.

[10] P. Seiden and L. Schulman, Adv. in Phys. 39 1 (1990).

[11] R. Prange and S. Girving, The Quantum Hall Effect, Springer New York, 1990.

[12] A.A. Belavin, A.M. Polyakov and A.B. Zamolodchikov, Nucl. Phys. B 241 (1984) 333.

[13] P. Di Francesco, P. Mathieu and D. Senechal, Conformal Field Theory, Springer Verlag, 1997.

[14] A.B. Zamolodchikov and Al.B. Zamolodchikov, Ann. Phys. 120 (1979) 253.

[15] G. Mussardo, Statistical Field Theory, Oxford, 2010.

[16] G. Delfino and J. Viti, Nucl. Phys. B 852 (2011) 149-173.

[17] G. Delfino and J. Viti, J. Phys. A: Math. Theor. 44 032001 (2011).

[18] G. Delfino, J. Viti and J. Cardy, J. Phys. A: Math. Theor. 43 152001 (2010)

[19] G. Delfino and J. Viti, J. Phys. A: Math. Theor. 45 032005 (2012).

[20] G. Delfino and J. Viti, submitted to JSTAT, arXiv:1206.4959 [hep-th].

[21] G. Delfino and J. Viti, Nucl. Phys. B 840 (2010) 513-533.

[22] R.B. Potts, Proc. Cambridge Phil. Soc. 48 (1952) 106.

[23] F.Y. Wu, Rev. Mod. Phys. 54 (1982) 235.

[24] W. Werner, Some recent aspects of Random Conformal Invariant Systems, Les Houches Lectures Notes (2005).

[25] P.W. Kasteleyn and C.M. Fortuin, J. Phys. Soc. Jpn. Suppl. 26 (1969) 11; Physica 57 (1972) 536.

[26] G. Grimmet, The Random Cluster Model, arXiv: math/0205237.

[27] L. Chim and A.B. Zamolodchikov, Int. J. Mod. Phys. A 7 (1992) 5317.

[28] V. Guararie, Nucl. Phys. B 410 3 27 (1993) 535-549.

[29] R. Vasseur, J. Jacobsen and H. Saleur, J. Stat. Mech. L07001 (2012).

[30] Al.B. Zamolodchikov, On the three-point function in minimal Liouville gravity, arXiv:hep-th/0505063.

[31] R. Ziff, J.H. Simmons and P. Kleban J. Phys. A 44:065002 (2011).

[32] R. Langlands, C. Pichet, P. Pouliot and Y. Saint-Aubin, J. Stat. Phys. 67 (1992) 553.

[33] J. Cardy, J. Phys. A 25 (1992) L201 [arXiv:hep-th/9111026].

[34] H. Watanabe, S. Yukawa, N. Ito and C.-K. Hu, Phys. Rev. Lett. 93 (2004) 190601.

[35] R. Vasseur and J. Jacobsen, J. Phys. A: Math. Theor. 45 165001 (2012).

[36] A.M. Polyakov, JETP Lett. 12 (1970) 381.

[37] B. Nienhuis, J. Stat. Phys. 34 (1984) 731.

[38] Vl.S. Dotsenko and V.A. Fateev, Nucl. Phys. B 240 (1984) 312.

[39] R.J. Baxter, Exactly Solved Models of Statistical Mechanics, Academic Press, London, 1982.

[40] J. Cardy, Nucl. Phys. B 270 (1986) 186.

[41] A. Cappelli, C. Itzykson and J.B. Zuber, Nucl. Phys. B 280 (1987) 445.

[42] S. Smirnov, C.R. Acad. Sci. Paris, t. 333, Série I (2001) 339.

[43] J. Cardy, Ann. Phys. 318 (2005) 81.

[44] M. Bauer and D. Bernard, Phys. Rep. 432 (2006) 115.

[45] R.G. Priest and T.C. Lubensky, Phys. Rev. B 13 (1976) 4159.

[46] G. Delfino, Nucl. Phys. B 818 (2009) 196 [arXiv:0902.3339 [hep-th]].

[47] N.G. De Bruijn, Asymptotic Methods in Analysis, Dover, New York, 1981; see also http://mathworld.wolfram.com/BellNumber.html.

[48] J. Dubail, J.L. Jacobsen and H. Saleur, J. Phys. A 43 (2010) 482002 [arXiv:1008.1216 [cond-mat]]; J. Stat. Mech. (2010) P12026 [arXiv:1010.1700 [cond-mat]].

[49] A.B. Zamolodchikov and V.A. Fateev, Sov. Phys. JETP 62 (1985) 215.

[50] G. Delfino and P. Grinza, Nucl. Phys. B 682 (2004) 521 [arXiv:hep-th/0309129].

[51] J.M. Drouffe, C. Itzykson and J.B. Zuber, Nucl. Phys. B 147 (1979) 132.

[52] D. Dummit and R. Foote, Abstract Algebra, John Wiley & Sons, 2006.

[53] F.Y. Wu, Phys. Lett. A 228 (1997) 43.

[54] J.L. Jacobsen, Phys. Lett. A 233 (1997) 489.

[55] F.Y. Wu and H.Y. Huang, Phys. Rev. Lett. 78 (1997) 409 [arXiv:cond-mat/9706252].

[56] C. King, J. Stat. Phys. 96 (1999) 1071.

[57] F.Y. Wu, J. Stat. Phys. 52 (1988) 99.

[58] C. Itzykson and J.B. Zuber, Quantum Field Theory, MacGraw-Hill, New-York (1980).

[59] A. B. Zamolodchikov, Adv. Stud. Pure Math. 19 641 (1989).

[60] F. Smirnov, Form Factors in Completely Integrable Quantum Field Theory, World Scientific (1992).

[61] M. Karowski and P. Weisz, Nucl. Phys. B 139 (1978) 445.

[62] G. Delfino and J. Cardy, Nucl. Phys. B 519 551 (1998) [arXiv: hep-th/9712111].

[63] G.Polya and G. Szego, Problems and Theorems in Analysis vol. I, Springer Verlag, Berlin Heidelberg (1998).

[64] The On-Line Encyclopedia of Integer Sequences; http://oeis.org/; A001045.

[65] The On-Line Encyclopedia of Integer Sequences; http://oeis.org/; A006342.

[66] P. Kleban, J.H. Simmons and R.M. Ziff, Phys. Rev. Lett. 97 (2006) 115702 [arXiv:cond-mat/0605120].

[67] J.H. Simmons, P. Kleban and R.M. Ziff, Phys. Rev. E 76 (2007) 041106 [arXiv:0706.4105 [cond-mat]].

[68] Vl.S. Dotsenko and V.A. Fateev, Phys. Lett. B 154 (1985) 291.

[69] J. Teschner, Phys. Lett. B 363 (1995) 63 [ariXiv:hep-th/9507109].

[70] L. Lepori, G.Z. Toth and G. Delfino, J. Stat. Mech. (2009) P11007 [arXiv:0909.2192 [hep-th]].

[71] A. Coniglio and F. Peruggi, J. Phys. A 15 (1982) 1873.

[72] C. Vanderzande, J. Phys. A 25 (1992) L75.

[73] G. Delfino, Nucl. Phys. B 807 (2009) 455 [arXiv:0806.1883 [hep-th]].

[74] M. Caselle, G. Delfino, P. Grinza, O. Jahn and N. Magnoli, J. Stat. Mech. (2006) 0603:P008 [arXiv:hep-th/05011168].

[75] V. Privman, P.C. Hohenberg and A. Aharony, Universal critical-point amplitude relations, in "Phase transitions and critical phenomena", Vol. 14, C. Domb and J.L. Lebowitz eds, Academic Press, New York, 1991.

[76] G. Delfino and G. Niccoli, Nucl. Phys. B 799 (2008) 364 [arXiv:0712.2165 [hep-th]].

[77] S. Lukyanov, Mod. Phys. Lett. A 12 (1997) 2543 [arXiv:hep-th/9703190].

[78] G. Delfino and G. Mussardo, Nucl. Phys. B 516 (1998) 675 [arXiv: hep-th/9709028].

[79] G. Delfino, P. Simonetti and J. Cardy, Phys.Lett. B387 (1996) 327-333.

[80] K. Seaton, J. Phys. A 34 (2001) L759 [arXiv:hep-th/0110282].

[81] C. Domb and C.J. Pearce, J. Phys. A 9 (1976), L137.

[82] A. Aharony and D. Stauffer, J. Phys. A 30 (1997) L301.

[83] M. Corsten, N. Jan and R. Jerrard, Physica A 156 (1989) 781.

[84] I. Jensen and R. Ziff, Phys. Rev. E 74 (2006) 020101(R) [arXiv:cond-mat/0607146].

[85] D. Daboul, A. Aharony and D. Stauffer, J. Phys. A 33 (2000) 1113.

[86] R. Ziff, arXiv:1103.3243.

[87] G. Watts, J. Phys. A 29 (1996) L363.

[88] J. Cardy, Nucl. Phys. B 324 (1989) 581.

[89] J. Cardy, Phys. Rev. Lett. 84 (2000) 3507.

[90] J. Cardy, Lectures on Conformal Invariance and Percolation, arXiv:math-ph/0103018.

[91] L. Berlyand and J. Wehr, J. Phys. A 28 (1995) 7127.

[92] J.-P. Hovi and A. Aharony, Phys. Rev. E 53 (1996) 235.

[93] M. Newman and R. Ziff, Phys. Rev. Lett. 85 (2000) 4104; Phys. Rev. E 64 (2001) 16706.

[94] P. de Oliveira, R. Nóbrega and D. Stauffer, J. Phys. A 37 (2004) 3743.

[95] O.A. Vasilyev, Phys. Rev. E 72 (2005) 036115.

[96] S. Ghoshal and A.B. Zamolodchikov, Int. J. Mod. Phys. A 9 (1994) 3841.

[97] Z. Bajnok, L. Palla and G. Takacs, Nucl. Phys. B 772 (2007) 290.

[98] P. Dorey, M. Pillin, R. Tateo and G. Watts, Nucl. Phys. B 594 (2000) 625.

[99] L. Chim, J. Phys. A: Math Gen. 28 (1995) 7039.

[100] A. Le Clair, G. Mussardo, H. Saleur and S. Skorik, Nucl. Phys. B 453 (1995) 581.

[101] Al. Zamolodchikov, Nucl. Phys. B 342 (1990) 695.

[102] P. Dorey, A. Pocklington and R. Tateo, Nucl. Phys. B 661 (2003) 425.

[103] Z. Bajnok, L. Palla and G. Takacs, Nucl. Phys. B 716 (2005) 519.

[104] G. Pruessner and N.R. Moloney, Phys. Rev. Lett. 95 (2005) 258901.

[105] H. Watanabe and C.-K. Hu, Phys. Rev. Lett. 95 (2005) 258902; Phys. Rev. E 78 (2008) 041131.

[106] G. Gallavotti, Statistical Mechanics: A short treatise, Springer 1999, and references therein.

[107] D.B. Abraham, Surface Structures and Phase Transitions - Exact Results, pp. 1-74 in: C. Domb and J.L. Lebowitz (Eds), Phase Transitions and Critical Phenomena vol. 10, Academic Press, London, 1986, and references therein.

[108] D. Jasnow, ibidem, pp. 269-363, and references therein.

[109] D.B. Abraham and P. Reed, Phys. Rev. Lett. 33 (1974) 377; Commun. Math. Phys. 49 (1976) 35.

[110] D.B. Abraham, Phys. Rev. Lett. 47 (1981) 545.

[111] G. Gallavotti, Commun. Math. Phys. 27 (1972) 103.

[112] D.S. Fisher, M.P.A. Fisher and J.D. Weeks, Phys. Rev. Lett. 48 (1982) 369.

[113] M. Bauer, D. Bernard and L. Cantini, J. Stat. Mech. (2009) P07037.

[114] N. Makarov and S. Smirnov, Off-critical lattice models and massive SLEs, in: P. Exner (Ed.), XVIth International Congress of Mathematical Physics, World Scientific, 2010.

[115] N. Lebedev, Special functions and their applications, Dover 1972.

[116] L. Greenberg and D. Ioffe, Ann. Inst. H. Poincaré Probab. Statist. 41 (2005) 871.

[117] M. Campanino, D. Ioffe and Y. Velenik, Ann. Probab. 36 (2008) 1287.

[118] G. Delfino, Phys. Lett. B 450 (1999) 196.

[119] G. Delfino and P. Grinza, Nucl. Phys. B 682 (2004) 521.

[120] M. Picco and R. Santachiara, Phys. Rev. E 83 (2011) 061124.

[121] M. Caselle, S. Lottini and M.A. Rajabpour, J. Stat. Mech. 1102 (2011) P02039.

[122] Y. Ikhlef and M.A. Rajabpour, J. Stat. Mech. (2012) P01012.

[123] J.J.H. Simmons, P. Kleban, S.M. Flores and R.M. Ziff, J. Phys. A 44 (2011) 385002.

[124] M.E. Fisher, Physics 3 (1967) 255.

[125] A. Coniglio and W. Klein, J. Phys. A 13 (1980) 2775.

[126] A. Coniglio, C. Nappi, F. Peruggi and L. Russo, J. Phys. A 10 (1977) 205.

[127] M.F. Sykes and D.S. Gaunt, J. Phys. A 9 (1976) 2131.

[128] K.K. Murata, J. Phys. A 12 (1979) 81.

[129] A. Coniglio and T.C. Lubensky, J. Phys. A 13 (1980) 1783.

[130] J. Benzoni and J. Cardy, J. Phys. A 17 (1984) 179.

[131] A. Stella and C. Vanderzande, Phys. Rev. Lett. 62 (1989) 1067.

[132] A.B. Zamolodchikov, in Adv. Stud. Pure Math. 19 (1989) 641; Int. J. Mod. Phys. A3 (1988) 743.

[133] T.T. Wu, B.M. McCoy, C.A. Tracy and E. Barouch, Phys. Rev. B 13 (1976) 316.

[134] G. Delfino, J. Phys. A 37 (2004) R45.

[135] J. Kertész, Physica A 161 (1989) 58.

[136] V.A. Fateev, Phys. Lett. B 324 (1994) 45.

[137] G. Delfino, Nucl. Phys. B 554 (1999) 537.

[138] Al.B. Zamolodchikov, Int. J. Mod. Phys. A 10 (1995) 1125.

[139] V. Fateev, S. Lukyanov, A. Zamolodchikov and Al. Zamolodchikov, Nucl. Phys. B 516 (1998) 652.

[140] M. D'Onorio De Meo, D.W. Heermann and K. Binder, J. Stat. Phys. 60 (1990) 585.